

Electronic Thesis and Dissertation Repository

11-13-2018 1:00 PM

Multi-Scale Peripheral Vasculopathy with Metabolic Syndrome

Kent Lemaster

The University of Western Ontario

Supervisor

Jefferson C. Frisbee

The University of Western Ontario

Graduate Program in Medical Biophysics

A thesis submitted in partial fulfillment of the requirements for the degree in Doctor of Philosophy

© Kent Lemaster 2018

Follow this and additional works at: <https://ir.lib.uwo.ca/etd>



Part of the [Medical Biophysics Commons](#)

Recommended Citation

Lemaster, Kent, "Multi-Scale Peripheral Vasculopathy with Metabolic Syndrome" (2018). *Electronic Thesis and Dissertation Repository*. 5835.

<https://ir.lib.uwo.ca/etd/5835>

This Dissertation/Thesis is brought to you for free and open access by Scholarship@Western. It has been accepted for inclusion in Electronic Thesis and Dissertation Repository by an authorized administrator of Scholarship@Western. For more information, please contact wlsadmin@uwo.ca.

Abstract

The combination of cardiovascular and metabolic risk factors including obesity, dyslipidemia, hypertension, and insulin resistance, in combination with a prothrombotic and proinflammatory state, is a condition termed Metabolic Syndrome (METS). Twenty percent of the adult population is afflicted with METS which increases the risk of type-2 diabetes mellitus and cardiovascular disease. Further, the presence of peripheral vascular disease (PVD) is tightly coupled with METS which is a perfusion-demand mismatch of blood supply to active skeletal muscle resulting in painful claudication and a late-stage potential for amputation. The underlying contributors of METS associated micro-vasculopathies in the skeletal muscle, their impact on impaired perfusion, and the potential for reversibility remain unclear. Owing its hyperphagia to leptin signaling resistance, the obese Zucker rat (OZR) is a translationally relevant model for human METS and the associated micro-vasculopathies. The overall purpose of this thesis is to utilize a multi-scale approach, particularly intravital microscopy and isolate vessels, to garner a greater understanding of the observed OZR vasculopathies and to investigate the potential of therapeutic interventions for their reversibility.

Project 1: The purpose was to identify any alterations in postcapillary and collecting venule function in the OZR compared to healthy controls. The OZR presented with impaired dilator reactivity and elevation in thromboxane A₂ constrictor responses for both postcapillary and collecting venules.

Project 2: The purpose was to identify the possible contributors of a disconnect for *in-situ* and *ex-vivo* vascular studies utilizing the OZR model. Using a multi-scale approach, Project 2 provides insight to this disconnect and reveals a heterogenous adrenergic

response in the OZR, giving rise to new potential avenues of study.

Project 3: The purpose was to determine the potential for reversibility or restoration of established PVD using the chronic ingestion of an HMG-CoA inhibitor, atorvastatin, and/or the implementation of regular exercise. Following a seven-week intervention, the intervention groups revealed vascular improvements with the combination group having the greatest capacity for reversibility (in specific indices).

Significance: Therefore, this thesis further advances the understanding of METS associated PVD as well as potential modes for improvement following its establishment.

Keywords

Rodent Model for Metabolic Syndrome, Microvasculopathy, Peripheral Vascular Disease, Venular Function, Skeletal Muscle Blood Flow, Adrenergic Vascular Responses, Reversing Vascular Disease

Co-Authorship Statement

Chapter 2) Lemaster, K. A., Farid, Z., Brock, R. W., Shrader, C. D., Goldman, D., Jackson, D. N., & Frisbee, J. C. (2017). Altered post-capillary and collecting venular reactivity in skeletal muscle with metabolic syndrome. *Journal of Physiology*, 595(15), 5159–5174. <https://doi.org/10.1113/JP274291>

Author Contributions: Conception or design of the work (RWB, DG, DNJ, JCF); acquisition, analysis or interpretation of data for the work (KAL, ZF, RWB, CDS, DG, DNJ, JCF); drafting the work or revising it critically for important intellectual content (KAL, ZF, RWB, CDS, DG, DNJ, JCF). All authors have approved submission of the manuscript.

Chapter 3) Lemaster, K., Jackson, D., Welsh, D. G., Brooks, S. D., Chantler, P. D., & Frisbee, J. C. (2017). Altered distribution of adrenergic constrictor responses contributes to skeletal muscle perfusion abnormalities in metabolic syndrome. *Microcirculation*, 24(2), 7–9. <https://doi.org/10.1111/micc.12349>

Author Contributions: Conception or design of the work (KAL, SDB, PDC, JCF); acquisition, analysis or interpretation of data for the work (all listed authors); drafting the work or revising it critically for important intellectual content (all listed authors).

Chapter 4) Kent A. Lemaster, Stephanie J. Frisbee, Luc Dubois, Nikolaos Tzemos, Fan Wu, Matthew T. Lewis, Robert W. Wiseman, and Jefferson C. Frisbee (2018). Chronic Atorvastatin and Exercise can Partially Reverse Established Skeletal Muscle Microvasculopathy in Metabolic Syndrome. *AJP - Heart and Circulatory Physiology*. Retrieved from 10.1152/ajpheart.00193.2018 [Epub ahead of print]

Author Contributions: Conception or design of the work (KAL, SJF, JCF); acquisition, analysis or interpretation of data for the work (all listed authors); drafting the work or revising it critically for important intellectual content (all listed authors).

Table of Contents

| | |
|--|------|
| Abstract..... | I |
| Co-Authorship Statement..... | III |
| Table of Contents..... | IV |
| Abbreviations..... | VI |
| List of Tables..... | VII |
| List of Figures..... | VIII |
| Chapter 1..... | 1 |
| 1 Introduction and Review of the Literature..... | 1 |
| 1.1 Metabolic Syndrome..... | 1 |
| 1.2 Biophysical Consequences..... | 4 |
| 1.3 Biological Contributors to Biophysical Detriments..... | 9 |
| 1.4 Translational Interventions for PVD: Chronic Exercise and/or HMG-CoA Reductase Inhibitor..... | 15 |
| 1.5 Specific Aims..... | 16 |
| 1.6 Significance..... | 17 |
| 1.7 Literature Cited..... | 17 |
| Chapter 2..... | 28 |
| 2 Altered Postcapillary and Collecting Venular Reactivity in Skeletal Muscle with Metabolic Syndrome..... | 28 |
| 2.1 Abstract..... | 30 |
| 2.2 Introduction..... | 31 |
| 2.3 Materials and Methods..... | 32 |
| 2.4 Results..... | 38 |
| 2.5 Discussion..... | 49 |

| | |
|---|-----|
| 2.6 Literature Cited | 54 |
| Chapter 3 | 59 |
| 3 Altered Distribution of Adrenergic Constrictor Responses Contributes to Skeletal Muscle Perfusion Abnormalities in Metabolic Syndrome | 59 |
| 3.1 Abstract | 60 |
| 3.2 Introduction | 62 |
| 3.3 Materials and Methods | 63 |
| 3.4 Results | 69 |
| 3.5 Discussion | 82 |
| 3.6 Literature Cited | 87 |
| Chapter 4 | 91 |
| 4 Chronic Atorvastatin and Exercise can Partially Reverse Established Skeletal Muscle Microvasculopathy in Metabolic Syndrome | 91 |
| 4.1 Abstract | 92 |
| 4.2 Introduction | 94 |
| 4.3 Materials and Methods | 96 |
| 4.4 Results | 105 |
| 4.5 Discussion | 119 |
| 4.6 Literature Cited | 125 |
| Chapter 5 | 129 |
| 5 Thesis Conclusion | 129 |
| 5.1 Literature Cited | 133 |
| Condensed Curriculum Vitae | 137 |

Abbreviations

ANOVA: analysis of variance
AT: active tone
ATOR: atorvastatin
C_aO₂: arterial oxygen content
C_vO₂: venous oxygen content
CVD: cardiovascular disease
EIA: enzyme immune assay
EXER: exercise
GS-1: Griffonia simplicifolia-1 lectin
HMG-CoA: 3-hydroxy-3-methylglutaryl coenzyme A reductase
ID: internal diameter
IL-10: interleukin 10
IL-1 β : interleukin 1 beta
IL-6: interleukin 6
L-NAME: L-N^G-Nitroarginine methyl ester
MAP: mean arterial pressure
MCP-1: monocyte chemoattractant protein-1
METS: Metabolic syndrome
MTT: maximal twitch tension
MVD: microvessel density
NO: nitric oxide
OZR: obese Zucker rat
PGI₂: Prostacyclin
PHT: phentolamine
PSS: physiological salt solution
PRZ: prazosin
PVD: peripheral vascular disease
Q: muscle blood flow
ROS: reactive oxygen species
T2DM: Type II diabetes mellitus
TEMPOL: 4-hydroxy-2,2,6,6-tetramethylpiperidin-1 -oxyl
TNF- α : tumor necrosis factor-alpha
TxA₂: thromboxane A2
VO₂: oxygen uptake
WT: wall thickness
YOH: Yohimbine

List of Tables

Chapter 2

| | |
|--|----|
| Table 1: Animal numbers, distributions, and condition..... | 43 |
| Table 2: Baseline characteristics..... | 47 |

Chapter 3

| | |
|---|----|
| Table 1: Baseline characteristics..... | 78 |
| Table 2: Baseline hemodynamic characteristics | 79 |
| Table 3: Baseline vascular characteristics | 85 |

Chapter 4

| | |
|------------------------------------|-----------|
| Table 1: Baseline conditions | 114 / 115 |
|------------------------------------|-----------|

List of Figures

Chapter 2

| | |
|---|----|
| Figure 1: Post-capillary venule, <i>in situ</i> cremaster dose response curves | 48 |
| Figure 2: Collecting venules, <i>in situ</i> cremaster dose response curves | 49 |
| Figure 3: Post-capillary venule, <i>in situ</i> cremaster dilator reactivity | 50 |
| Figure 4: Collecting venule, <i>in situ</i> cremaster dilator reactivity..... | 51 |
| Figure 5: Post-capillary venule, <i>in situ</i> cremaster constrictor reactivity | 53 |
| Figure 6: Collecting venule, <i>in situ</i> cremaster constrictor reactivity | 54 |
| Figure 7: <i>In situ</i> cremaster field stimulation | 55 |
| Figure 8: <i>In situ</i> cremaster field stimulation with pre-treatment | 56 |
| Figure 9: Venous production of 6-keto-PGF _{1α} and 11-dehydro-TxB ₂ | 57 |
| Figure 10: Adhesion/rolling leukocytes, <i>in situ</i> | 57 |
| Figure 11: Microvessel densities | 58 |

Chapter 3

| | |
|--|----|
| Figure 1: Whole body, pressor response with phentolamine | 80 |
| Figure 2: Whole body, pressor response with prazosin and yohimbine | 81 |
| Figure 3: Hyperemic response and performance with phentolamine | 82 |
| Figure 4: Hyperemic response and performance with prazosin..... | 83 |
| Figure 5: Hyperemic response and performance with yohimbine | 84 |
| Figure 6: <i>In situ</i> , cremaster constrictor response, proximal arterioles..... | 85 |
| Figure 7: <i>In situ</i> , cremaster dilator response, proximal arterioles..... | 86 |
| Figure 8: Distribution of constrictor responses | 87 |
| Figure 9: <i>In situ</i> , cremaster responses and distribution, distal arterioles | 88 |
| Figure 10: <i>Ex vivo</i> , gracilis arteriole constrictor response | 90 |

Chapter 4

| | |
|---|-----|
| Figure 1: <i>Ex vivo</i> , gracilis arteriole dilator response..... | 116 |
| Figure 2: <i>Ex vivo</i> , gracilis arteriole dilator response in low PO ₂ | 117 |
| Figure 3: <i>Ex vivo</i> , gracilis arteriole constrictor response | 117 |
| Figure 4: <i>In situ</i> , cremaster arteriole dilator response..... | 119 |
| Figure 5: <i>In situ</i> , cremaster arterioles constrictor response | 120 |
| Figure 6: <i>Ex vivo</i> , gracilis arterioles, passive mechanics | 121 |
| Figure 7: Microvessel density | 122 |
| Figure 8: <i>In situ</i> , perfusion heterogeneity | 123 |
| Figure 9: Bioavailability of signaling molecules | 124 |
| Figure 10: <i>In situ</i> , vascular response to contraction | 125 |
| Figure 11: <i>In situ</i> , gastrocnemius tracer washout | 126 |
| Figure 12: <i>In situ</i> , gastrocnemius washout data..... | 127 |

Chapter 1

1 Introduction and Review of the Literature

Metabolic Syndrome (METS) is a myriad of cardiovascular disease and metabolic disease risk factors including obesity, dyslipidemia, hypertension, and insulin resistance/impaired glycemic control tightly coupled with the presence of prothrombotic and proinflammatory physiological states (Frisbee & Delp, 2006). The Adult Treatment Panel III defines individuals with METS as having 3 of the following 5 criteria: abdominal obesity (waist circumference: men >102 cm and women >88 cm), elevated triglycerides (≥ 1.7 mmol/L), reduced HDL cholesterol (men <1.04 mmol/L and female <1.30 mmol/L), elevated blood pressure ($\geq 130/\geq 85$ mmHg), and elevated fasting glucose (≥ 6.1 mmol/L).

1.1 Metabolic Syndrome

One in five adults between the ages of 18-79 are afflicted with METS (Riediger & Clara, 2011) which increases the risk of chronic diseases such as type II diabetes mellitus (T2DM) and cardiovascular disease (CVD) by approximately 5-fold and 2.6-fold, respectively (Grundy et al., 2002; Lakka, 2002). CVD is defined by The American Heart Association as the presentation of poor heart function and/or inadequate blood supply to tissues/organ systems (AHA, 2017) and T2DM is a metabolic disease characterized by insulin resistance and impaired glycemic utilization for energy thereby starving working cells (ADA, 2015). Further, the resulting hyperglycemia may cause detrimental injuries to the eyes, heart, kidneys, and nerves (ADA, 2015). The World Health Organization reports CVD as the world's leading cause of death and T2DM is ranked 7th (WHO, 2018). More specifically, CVD and T2DM remain significant contributors to Canadian mortality rates, accounting for a combined 17% of all health care costs and 43% of all deaths in Canada (MetSC, 2018; Heron, 2007). While METS may serve as a critical precursor for these chronic diseases, detrimental changes to peripheral vascular circulation, both structurally and functionally, are observed in parallel to the onset and progression of METS (Alberti et al., 2009; Chantler & Frisbee, 2015).

A critical consequence of METS on the peripheral vasculature includes the reduction of blood supply and perfusion to working skeletal muscle (McClatchey et al., 2017). Healthy, active muscles produce vasoactive, metabolic byproducts which promote increases in blood flow and perfusion to meet the increased metabolic demand of the working muscle. This physiological process is termed hyperemic response. Both human and animal models have revealed a decreased hyperemic response, despite similar muscle phenotypes, with METS compared to healthy controls (Jacqueline et al., 2016; Guarini et al., 2016). Further supported by both *in-vivo* and *ex-vivo* studies, the blunted hyperemic responses observed with METS and inflammation is a result of pathophysiological alterations in vessel dilation and constriction, vascular densities, and structural compositions (both atherogenic and non-atherogenic changes) all which will be covered with greater detail in subsequent sections (Butcher et al., 2013; Frisbee et al., 2009). Taken together, this supply/demand mismatching and its associated symptoms is known as peripheral vascular disease (PVD).

Pathophysiological alterations to the skeletal muscle may result in PVD which is independently associated with increases in CVD morbidity and mortality (Paraskevas et al. 2010) and that risk is further augmented when coupled with METS (Katsiki et al., 2013; Wassink et al., 2018; Czel & Tefan, 2006). The National Health and Nutrition Examination Survey reported 38.4% of adults with METS, over the age of 40, were diagnosed with PVD (Sumner et al., 2012). Individuals afflicted with PVD may experience leg muscle fatigue, cramps, and pain during bouts of physical activity and, in the more extreme cases of vascular insufficiency when supply/demand mismatching occurs at rest, ulceration or gangrene of the feet may occur with a potential for limb amputation (Abdulhannan et al., 2012). Without revascularization, patients with vascular insufficiency will have a 19% risk of amputation within the first 6 months of initial treatment and 23% risk at one year (Marston et al., 2006).

The Obese Zucker Rat as a Translational Model for Metabolic Syndrome

All of the material presented thus far has mainly been emphasized on epidemiological observations. While technology and public health records enable us to

non-invasively evaluate the broader outcomes of metabolic syndrome in humans, more invasive measures using animal models are essential to further investigate the vasculopathologies with greater control and detail. Most human studies introduce confounding variables such as genetic variations between patients. Albeit, these confounding variables may exist in animal models, but the ability to manipulate, measure, and control for their presence and/or severity is more feasible in utilizing this animal model.

The obese Zucker rat (OZR; fa/fa) is a translationally relevant model for examining metabolic syndrome. When co-expressed, the autosomal recessive mutation, fa, located on chromosome 5 causes a coding error for the leptin receptor gene, thereby producing an amino acid substitution on the leptin receptors and reducing leptin binding to the cerebral cell surface receptors in the choroid plexus and lateral ventricles of the brain (Yarnell et al., 1997; Kurtz, Morris, & Pershadsingh, 1989). Leptin is a key regulating hormone for energy consumption. Produced by the adipose tissue in proportion to fat storage, leptin is released into the circulatory system and interacts with the brain's leptin receptors to signal for a decrease in consumption and an increase in energy expenditure (Halaas et al., 1995). As such, the OZR exhibits an impaired satiety reflex resulting in chronic hyperphagia which leads to the onset of excess body fat as early as 3-4 weeks of life and, by week 14, approximately 40%-50% of the rat's total body weight is adipose tissue while healthy controls from the same litter are measured at approximately 20% (Artinano & Castro, 2009; Cleary et al., 1980). This rapid onset and progression of obesity is paralleled by increases in insulin resistance, dyslipidemia, hyperglycemia, and hypertension (Kurtz, Morris, & Pershadsingh, 1989).

Both humans with METS and the OZR experience similar systemic pathologies as well as prolonged periods of hypertriglyceridemia and insulin resistance prior to the overt development of type II diabetes mellitus (Frisbee & Delp, 2006). Further, the OZR demonstrates clinically relevant mild to moderate hypertension, which is comparable to the severity observed in humans with METS (Johnson et al., 2006) as well as a proinflammatory and prothrombotic state (Vaziri et al., 2005; Frisbee & Delp, 2006). Therefore, when considering the consistent parameters and the similar progression of

those parameters to that of the human conditions, the OZR represents an ideal translational model for garnering a greater understanding of METS.

1.2 Biophysical Consequences

Although the cardiovascular system is essential for physiological functions such as oxygen and nutrient delivery to the body's tissues, thermoregulation, combating diseases, and the clearance of metabolites and carbon dioxide from tissues, its most basic description includes that of a fluid (i.e. blood) transport system. As such, blood flow can be described using Ohm's Law for fluids where flow (Q) is equal to the change in driving pressure (P) generated by the heart divided by the resistance (R).

$$Q = \Delta P / R$$

Further, blood flow in a single vessel of the cardiovascular system can be determined via Poiseuille's Law where the change in pressure across the vessel is multiplied by radius (r) then divided by the vessels length (l) and blood viscosity (η).

$$R = 8\eta l / \pi r^4 \quad Q = (\Delta P \pi r^4) / 8\eta l$$

Due to radius being heavily weighted in the context of fluid/blood resistance, a 50% decrease in lumen diameter will yield a 16-fold increase in resistance. Therefore, radius is a key determinant for fluid resistance and flow in the vasculature.

In the dynamic cardiovascular system, vessel radii, mainly at the arteriolar level, is regulated via both intrinsic and extrinsic signals. Extrinsic systems such as metabolic signals, circulating hormones, and the sympathetic nervous innervation provide external regulatory signaling to the vasculature based on the needs of the supplied tissues. Intrinsic mechanisms such as myogenic control and shear stress further regulate vessel diameter based on intraluminal pressure and shear rate of blood against the lumen walls of the vessel, respectively. The range of vasodilator/constrictive responses may vary depending on the level of vasculature being interrogated such as the arteries, arterioles and their sub-units (Al-Khazraji et al. 2015; Chilian et al., 1989). However, the general

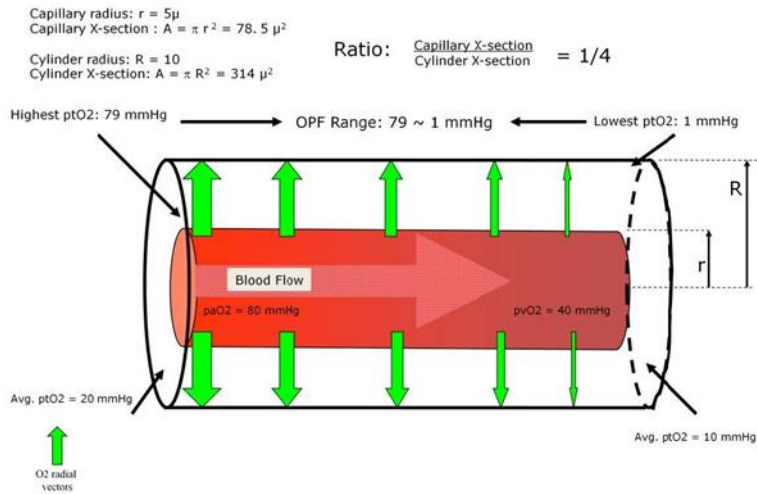
premise of these vascular controllers is to regulate vessel radii via vasoconstriction and vasodilation, dependent on the metabolic needs of perfused tissues.

In the presence of obesity, dyslipidemia, and impaired glycemic control, the vascular dilator and constrictor responses in the skeletal muscle are altered to favor that of a decrease in vessel radius at rest and in response to both extrinsic and intrinsic controllers compared to healthy controls. In accordance with Ohm's Law for Fluids and Poiseuille's Law, a system which favors a vasoconstrictive state, thereby decreasing radii and increasing resistance, will result in a proportional increase in blood pressure and/or a decrease in flow. This insufficiency in blood supply to tissues during higher metabolic demand can contribute to myocardial infarctions, stroke, and intermittent claudication with a potential to result in limb amputation. Biological contributors to these biophysical consequences involved in decreased vessel radii compared to healthy controls will be further defined in subsequent sections. Additionally, insulin resistance and the resulting hyperinsulinemia (Wu et al., 2000) can exert hypertrophic effects on vascular smooth muscle cells (i.e. vessel proliferation) and promote atherogenic monocyte adhesion and infiltration (Yeh, 2004). These pathologies can decrease vessel radii (Hutcheson et al., 2014; Cersosimo et al., 2014) as well as cause decreases in vessel wall deformation (Chantler & Frisbee, 2015) thereby further limiting skeletal muscle perfusion (Fossum et al., 1998).

While temporal regulatory dysfunction of the arterioles is a key contributor toward increases in blood flow resistance in the skeletal muscle vasculature of those with METS, there are detrimental spatial alterations as well. The Frisbee lab reported significant reductions in microvessel densities (i.e. vascular rarefaction) within the gastrocnemius muscle of OZR compared to healthy controls (Frisbee, 2003) and reductions in vessel density have been shown to exert the largest effect on tissue oxygen levels (Greene et al., 1992). As such, tissues of high metabolic demand, but reduced densities may result in reduced oxygen levels which could limit the metabolic activity and performance of that tissue (Greene et al., 1992). Optimal capillary-to-tissue (cylinder) density ratio for sufficient oxygen diffusion across tissues can be described using the Krogh Cylinder Model (Krogh, 1919) with respect to the partial pressure

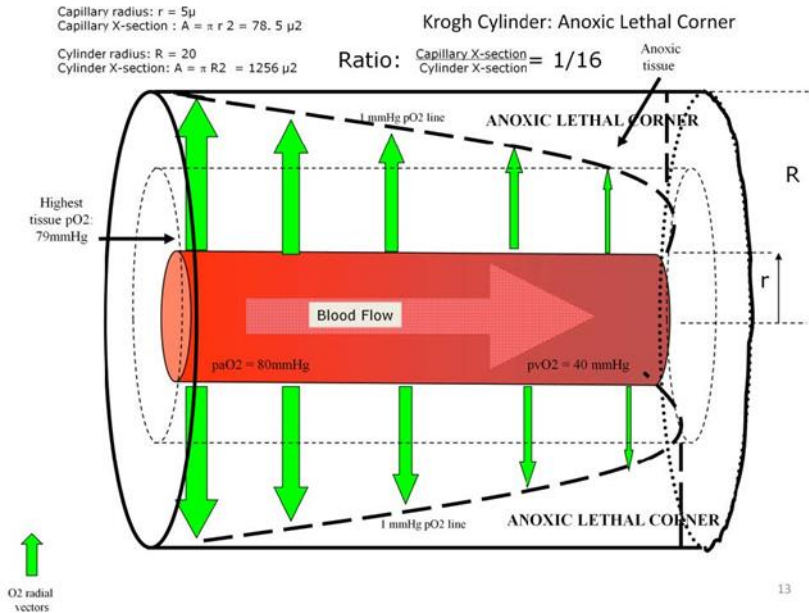
gradient of O₂ (Fig. 1-A). In this model, decreases in capillary density, in the absence of compensatory alterations in tissue density, can shift this optimal ratio and create areas of hypoxia as the cylinder becomes too large for the diffusion of O₂ across tissue (Fig. 1-B).

Figure 1-A: Krogh Cylinder Model describing optimal capillary/tissue ratio and O₂ diffusion to surrounding tissue



(Graphic retrieved from PerfusionTheory.com; link in 1.7)

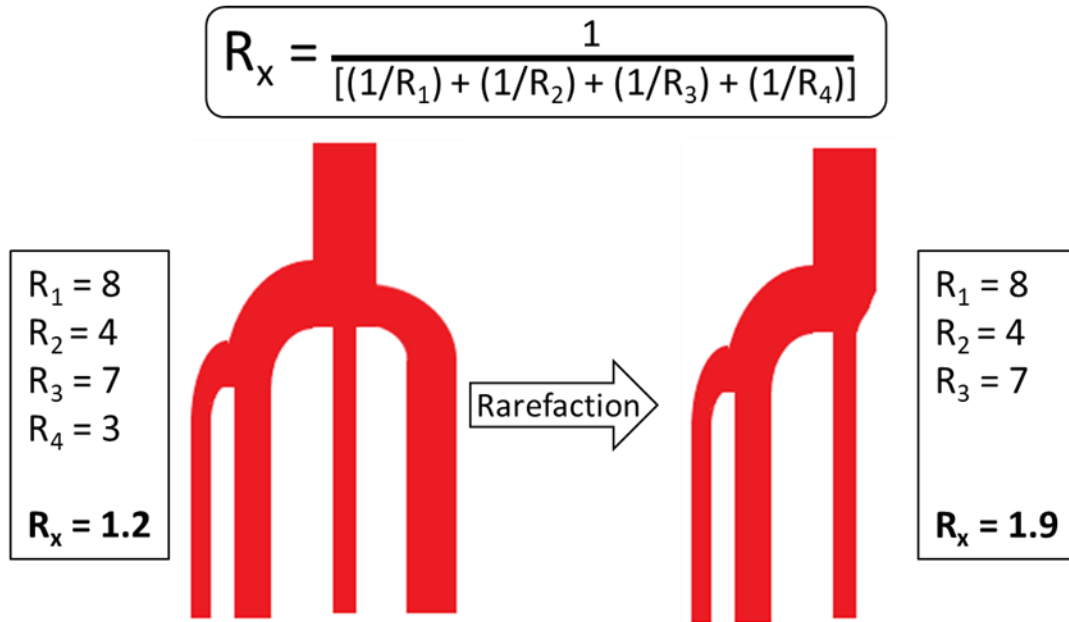
Figure 1-B: Krogh Cylinder Model describing suboptimal capillary/tissue ratios and resulting areas of hypoxia



(Graphic retrieved from PerfusionTheory.com; link in 1.7)

In addition to implications on gas and nutrient delivery/clearance to the perfused tissue, rarefaction can promote increases in overall network resistance (Greene et al., 1989). Figure 2 describes the decrease in the overall resistance (arbitrary numbers) for vessels oriented in parallel to an overall value lower than that of any single vessel within the network and how that overall resistance will increase if one of the parallel vessels is removed, if other variables remain constant. Therefore, vessels in parallel decrease the overall network resistance and reducing the number of vessels in parallel will increase the overall resistance of a network. In the context of METS, fifteen-week-old OZR have a 20-25% reduction in microvessel density (Frisbee, 2003) which can promote both increases in network resistance and decreases in oxygen delivery thereby contributing to reduced blood flow and oxygenation of working skeletal muscles.

Figure 2: Example of increases in network resistance with decreases in parallel vessels (arbitrary units).



Metabolic syndrome is associated with various biophysical consequences such as shifted lumen diameters in response to pharmacological and/or muscle stimulation which favors a more vasoconstrictive state compared to healthy controls. Coupled with structural changes and rarefaction, there is a multitude of factors that increase vascular resistance and decrease muscle perfusion thereby contributing to the high prevalence of PVD with METS. Although most of microcirculatory research interrogates the arterial side, previous studies show the earliest changes in vascular dysfunction can be observed on the venular side of skeletal muscle networks with an emphasis on retrograde rarefaction from the venules to the arterioles (Frisbee et al., 2014). Some of the contributing pathologies of these biophysical consequences are covered in the following sections, with respect to the context of this dissertation.

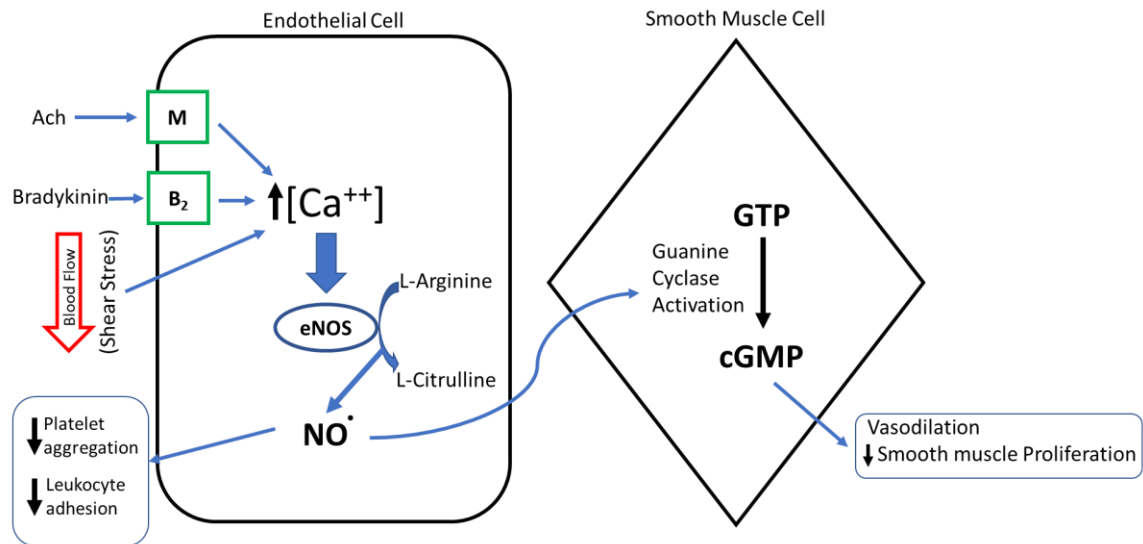
1.3 Biological Contributors to Biophysical Detriments

While biophysical detriments associated with METS contribute to the obstruction and reduction of blood flow to perfused skeletal muscles, the cause of these detriments are rooted in the biological pathologies linked with obesity, impaired glycemic control, and dyslipidemia. This dissertation will explore some of those pathologies and their contributions to increases in vascular resistance on both the arteriole side and the venular side of the microcirculation in the OZR. Further, we will explore interventional and treatment strategies for reversing these pathological contributors with the primary goals of decreasing vascular resistance, increasing tissue perfusion, and increasing microvascular density.

Endothelial nitric oxide

Endothelial dysfunction is a key vascular consequence of METS and chronic inflammation, by which there is a decrease in nitric oxide (NO) bioavailability compared to healthy controls under both resting and stimulated conditions. In short, NO is an essential molecule which signals for vascular smooth muscle relaxation/dilation which is produced in the endothelium and can be stimulated via acetylcholine, bradykinin, and/or the shear stress created by blood flow against the endothelial wall which up regulates intracellular calcium release to activate the NO synthesizing enzyme, endothelial nitric oxide synthase (eNOS; Fig. 3). Following this, eNOS converts L-arginine to L-citrulline and synthesizes NO which diffuses out of the endothelial cell to the neighboring vascular smooth muscle to dephosphorylate guanine triphosphate to elicit vasodilation and prevent smooth muscle proliferation/remodeling thereby promoting decreases in vascular resistance and vessel stiffening, respectively. However, the reduced NO bioavailability associated with METS can shift the vasculature to a more vasoconstrictive state, thus increasing vascular resistance which is a key contributor to elevated blood pressure and hypertension. Furthermore, clot formation and leukocyte recruitment are both inhibited by NO (Hossain et al., 2012), therefore the decrease in NO bioavailability with METS can contribute to the observed prothrombotic and proinflammatory state.

Figure 3: Endothelial nitric oxide production



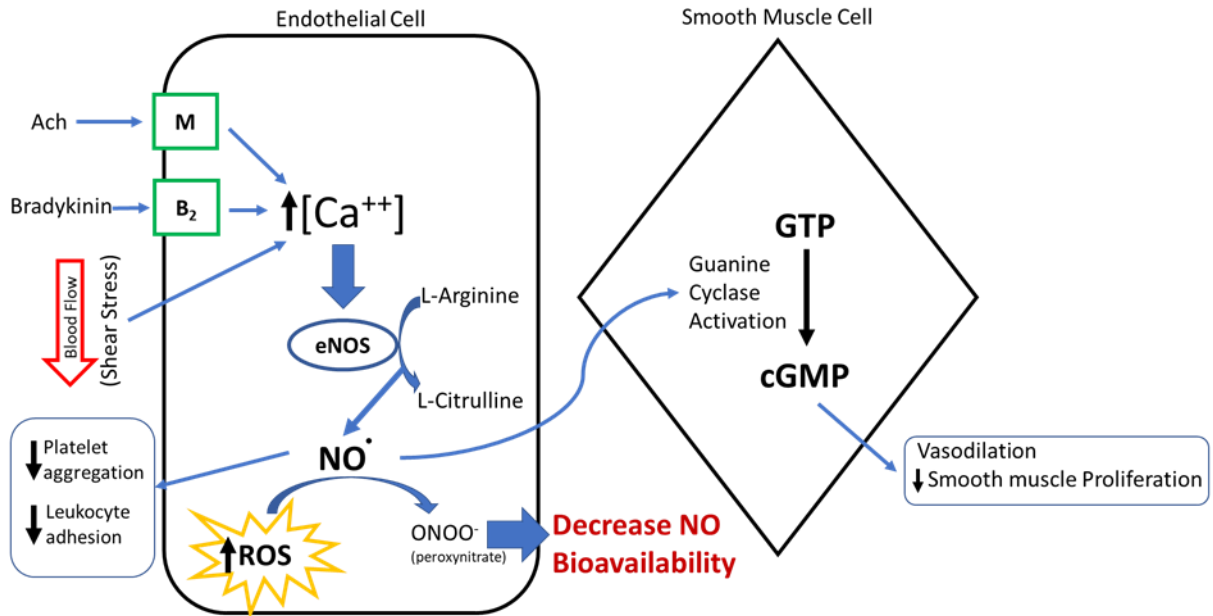
Proinflammation and oxidative stress

While the presence of a proinflammatory state are reliably associated with METS (Ford, 2003), they are not typically considered inclusion criteria for the clinical diagnosis of METS. However, both human and animal models with metabolic syndrome risk factors consistently report evidence of elevated markers including, but not limited to tumor necrosis factor- α (TNF- α), interleukin-6 (IL-6), and c-reactive protein (CRP), all of which can be attributed to excess fat stores (Goodwill, 2008; Ford, 2003; Erdembileg et al., 2015; Bickel et al., 2002). TNF- α cytokines can impact endothelial function (Singer and Granger, 2007), increase reactive oxygen species (ROS) production (Agharazii et al., 2015), alter glucose metabolism of the skeletal muscle via the inhibition of insulin receptor tyrosine kinase (Hotamisligil et al., 1996), promote smooth muscle cell proliferation, and increase monocyte cell adhesion and infiltration (Yeh, 2004). IL-6 is a key regulator for CRP production which is a clinical marker of inflammation that serves as an early predictor for cardiovascular disease, including asymptomatic patients (Ridker et al., 2002). Elevated CRP mediated activity can directly inhibit nitric oxide (NO)

production via inhibition of eNOS and endothelial dysfunction (Jialal, 2009) and contribute to the elevated levels of ROS production associated with a pro-inflammatory state (Prasad, 2004; Singer and Granger, 2007).

ROS is a chemically reactive byproduct of oxidative metabolism which is essential for cell signaling, immune response, as well as non-pathological apoptosis and contain one or more oxygen atoms and unpaired electrons. The highly reactive superoxide anion ($O_2^{\cdot-}$) is the initial ROS produced by mitochondrial metabolism which is normally and rapidly transformed into H_2O_2 and then to water via the antioxidant enzymes superoxide dismutase (SOD) and catalase/glutathione peroxidase, respectively. However, oxidative stress, or elevations in ROS production beyond that of endogenous antioxidant systems, can result in the alteration of essential cellular proteins and increases in proteolytic susceptibility (Davies et al., 1986). There are a multitude of studies connecting oxidative stress with observed vasculopathies associated with impaired glycemic control and insulin resistance, cardiovascular diseases, and a multitude of other diseases (Agharazii et al., 2015; Frisbee & Delp, 2006; Davies et al., 1986). A key consequence of excess ROS in the context of vascular function is its reactivity with endothelial derived NO to form elevated levels of peroxynitrate, which can uncouple eNOS, thus decreasing both the production and the bioavailability of NO (Fig 4; Goodwill and Frisbee, 2012).

Figure 4: Superoxide pathways

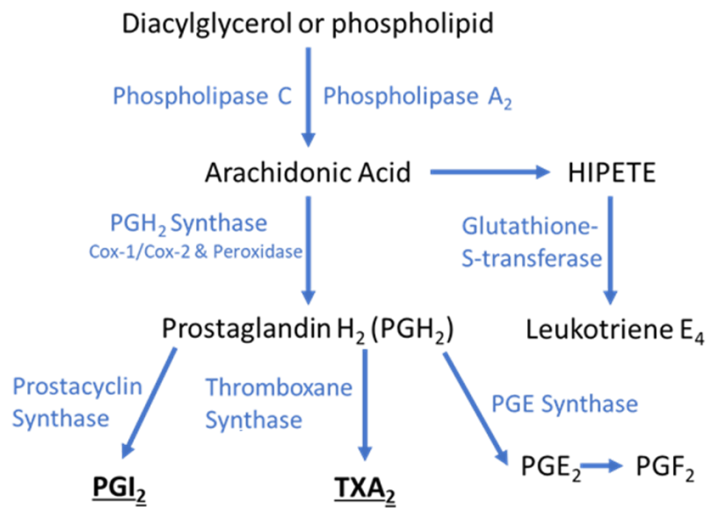


Additionally, vascular necrosis/rarefaction can be linked to increased oxidative stress as NO is essential for the structural maintenance of the vasculature and angiogenesis (Cooke and Losordo, 2002). Decreases in vascular density may lead to increases in hypoxia which can further exacerbate ROS production and contribute to a self-perpetuating pathology (Chandel et al., 1998). Taken together, ROS production is a self-propagating phenomenon which is detrimental to normal cellular function. In the context of this dissertation, 4-hydroxy-2,2,6,6-tetramethylpiperidin-1-oxyl (TEMPOL), a free radical scavenger and superoxide mimetic, is used to measure the contribution of ROS on the blunted dilatory response of the OZR vasculature compared to healthy controls.

An additional consequence includes a ratio shift in prostacyclin (PGI₂) and thromboxane (TxA₂) production attributed mainly to oxidative stress (Goodwill et al, 2008), dyslipidemia, and the oxidization of low density lipoproteins (Palinski et al. 1989; Pfister & Campbell, 1996). PGI₂ and TxA₂ are two well known, vasoactive end products of arachidonic acid (AA) metabolism by cyclooxygenase to prostaglandin endoperoxide H₂ (Figure 5: AA metabolism). PGI₂ and TxA₂ are known to elicit opposite actions on

coagulation and vasodilatory/vasoconstrictive response. PGI₂ is recognized more so as the homeostatic product of AA metabolism as it promotes vasodilation and has anti-coagulant properties, whereas TxA₂ is a potent vasoconstrictor which promotes red blood cell and platelet aggregation and is more so observed at the sight of acute injuries or in pathophysiological conditions.

Figure 5: Arachidonic acid metabolism cascade



In the presence of insulin resistance there is a shift in arachidonic acid metabolism which favors TxA₂ production (Hishinuma, 2001) which has been attributed to the inactivation of prostacyclin synthase via interaction with the elevated levels of peroxynitrite (Davis & Zou, 2005). Further, it has been suggested impaired glycemic control may promote protein kinase C activity with ensuing increases in the inducible isoform, cyclooxygenase-2, activity to produce elevated TxA₂ production in circulating leukocytes (Nusing et al., 1993). This shift promotes a more vasoconstrictive state of the vessels at rest and in response to the TxA₂ mimetic U46619 (Goodwill, 2008) thereby decreasing the lumen size and contributing to increases in vascular resistance. Additionally, the coagulative actions of TxA₂ promotes the prothrombic state observed with METS risk factors which increases the risk of clot/thrombotic formations and associated diseases and detrimental cardiovascular events such as stroke and heart attack.

Adrenergic Control

The altered vasodilatory signaling and reactivity observed with METS and models of METS is well established. Previous studies have also demonstrated the decrease in skeletal muscle lumen diameter in the OZR can be further credited to an elevated constrictor response to sympathetic nervous system (SNS) innervation compared to healthy controls (Stepp & Frisbee, 2002). The SNS elicits vasoconstriction via the release neuronal signals and the interaction with their respective receptors (R) which includes the following: nor-adrenaline (α 1-R & α 2-R; adrenergic), adenosine triphosphate (P2X1-R; purinergic), and neuropeptide Y (Y1-R; peptidergic). Vascular responses to these signals within the arteriole microcirculation experience heterogeneous distribution where proximal arterioles are largely under adrenergic control and the distal arterioles are more so under purinergic and/or peptidergic control (Anderson & Faber, 1991; Al-Khazraji et al. 2015).

It has been suggested the decreases in hyperemic response to occlusion and the more vasoconstricted state observed in OZR may be attributed to the augmentation of α 1-adrenergic response, validated by the rescuing effects of adrenergic blockers such as prazosin and phentolamine (Frisbee, 2006). This dissertation will examine the α -adrenergic response observed using a multi-scale (*in-situ*, *in-vivo*, and *ex-vivo*) approach at various levels of microcirculation (feed arteries, arterioles, terminal/precapillary arteries) to garner a greater understanding of the variability observed when using single point interrogations at a single level of the vasculature. While the majority of previous research in the context of microcirculation and blood flow resistance has focused on the interrogation of arteries and resistance arterioles, we also examine the effects of α -adrenergic mediation of venule diameters to identify potential contributors to the overall increase in vascular resistance observed in METS and METS models.

1.4 Translational Interventions for PVD: Chronic Exercise and/or HMG-CoA Reductase Inhibitor

An existing clinical and translational disparity in animal models with METS associated PVD is that many of the employed interventions are relevant for blunting the severity of vasculopathies of the developing PVD. However, from a clinical stance, this may not serve as the most relevant model as many patients seek medical assistance due to claudication or pain in their extremities when performing physical activity, meaning PVD is already well established. Therefore, animal studies which employ early interventions, prior to the establishment of PVD, are not translationally relevant for humans presenting with established PVD. In the context of this dissertation, we employ interventions following the establishment of PVD which includes regular, physical activity/exercise and/or the chronic ingestion of the HMG-CoA inhibitor, atorvastatin.

Chronic Exercise

It is well established that regular exercise can improve obesity, insulin resistance, and dyslipidemia in both humans and animals (Moller & Kaufman, 2005; Becker-Zimmermann et al., 1982). Additionally, exercise has been shown to improve vascular densities in skeletal muscle, both trained/locomotive muscles (Frisbee, 2006) and non-trained/systemic muscles (Qui et al., 2018), and improves NO bioavailability (Machado et al., 2016). NO bioavailability plays a critical role in angiogenic incompetence and rarefaction (Machado et al., 2016; Ungvari et al., 2018) and this dependency has been suggested to be the major underlying mechanism of microvascular rarefaction in METS (Frisbee, 2005).

A multitude of previous studies indicate improvements in NO bioavailability via increases in eNOS expression and activity for both healthy controls (Parker et al., 2011) and disease states (Orr et al., 2009; Fiuza-Luces et al., 2018). A potential contributor to this upregulation may be in adaptation to the regular increases of exercise induced shear stress from blood flow, a potent stimulus for NO production and vasodilation (Fleming and Busse, 2003). Improvements in NO bioavailability are paralleled by decreases in ROS generation and improvements in antioxidant systems (Kojda & Hambrecht, 2005).

Potential mechanisms include increases in superoxide dismutase, catalase, and peroxidase (Berzosa et al., 2011) as well as decreases in the NADPH oxidase production of ROS (Rush et al., 2003). Taken together, these exercise-induced improvements can result in increases of NO bioavailability in METS models thereby promoting angiogenesis to combat rarefaction and improve many of the other previously listed pathologies associated with impaired NO bioavailability.

HMG-CoA Inhibition

Clinically, the inhibition of liver enzyme 3-hydroxy-3-methylglutaryl coenzyme A reductase (HMG-CoA) is commonly used in an effort to reduce circulating cholesterol levels, thus the target for cholesterol lowering drugs such as the HMG-CoA reductase inhibitor, atorvastatin (ATOR). However, statins also have pleiotropic effects and are therefore increasingly used for reasons beyond lowering cholesterol levels, including anti-inflammation (Fujita et al., 2007). Although the mechanisms are unclear, statins are associated with improvements in inflammatory markers and endothelial cell function which result in better outcomes of inflammation-linked vascular diseases (Haslinger-Löffler, 2008). More specifically, ATOR has been reported to decrease the expression of the previously mentioned inflammatory cytokines (IL-6 and TNF- α), decrease CRP, and improve defense systems against reactive oxygen species (Rabkin et al., 2013; Sodha et al., 2015) thus improving the previously mentioned, associated detriments observed with established PVD.

1.5 Specific Aims

1. To determine alterations for post-capillary venular structure/function in OZR and the extent this contributes to elevated network resistance and impaired mass transport/exchange. These experiments employ intravital imaging of in situ skeletal muscle with specific physiological and pharmacological challenges to determine venular hemodynamic and vasomotor diameter responses in METS.
2. To determine the role of adrenergic signaling and its interaction with altered endothelial function on resistance in pre-capillary, arteriolar networks of OZR and how it

may contribute to skeletal muscle perfusion. These experiments employ *in vivo*, *in situ*, and *ex vivo* conditions to interrogate interactions between adrenergic responses and their influence on vessel diameters.

3. To determine the potential for reversibility of OZR microvasculopathies using exercise and atorvastatin. These experiments employ intravital microscopy of *in situ* skeletal muscle and the study of *ex vivo* arterioles to determine alterations in vessel diameter control, blood flow distribution, and bulk perfusion within arteriolar networks.

1.6 Significance

METS and PVD continue to burden the health of afflicted individuals via decreases in quality of life and increases in both morbidity and mortality. Further, these burdens extend to higher healthcare spending. Although strides have been made to understand these diseases, many of the underlying mechanisms remain unclear. Therefore, this dissertation seeks to further advance the understanding of METS associated PVD and explore potential modes for improvement following its establishment.

1.7 Literature Cited

- 1) Abdulhannan, P., Russell, D. A., & Homer-Vanniasinkam, S. (2012). Peripheral arterial disease: A literature review. *British Medical Bulletin*, 104(1), 21–39.
- 2) ADA: American Diabetes Association. (2015) <http://www.diabetes.org/diabetes-basics/type-2/facts-about-type-2.html>
- 3) AHA: The American Heart Association. (2017) <https://www.heart.org/en/health-topics/consumer-healthcare/what-is-cardiovascular-disease>
- 4) Agharazii, M., St-Louis, R., Gautier-Bastien, A., Ung, R. V., Mokas, S., Larivière, R., & Richard, D. E. (2015). Inflammatory cytokines and reactive oxygen species as mediators of chronic kidney disease-related vascular calcification. *American Journal of Hypertension*, 28(6), 746–755.
- 5) Alberti, K. G. M. M., Eckel, R. H., Grundy, S. M., Zimmet, P. Z., Cleeman, J. I., Donato, K. A., ... Smith, S. C. (2009). Harmonizing the metabolic syndrome: A joint

- interim statement of the international diabetes federation task force on epidemiology and prevention; National heart, lung, and blood institute; American heart association; World heart federation; International atherosclerosis society; And international association for the study of obesity. *Circulation*, 120(16), 1640–1645.
- 6) Aleixandre De Artiñano, A., & Miguel Castro, M. (2009). Experimental rat models to study the metabolic syndrome. *British Journal of Nutrition*, 102(9), 1246–1253.
 - 7) Al-Khazraji, B. K., Saleem, A., Goldman, D., & Jackson, D. N. (2015). From one generation to the next: A comprehensive account of sympathetic receptor control in branching arteriolar trees. *Journal of Physiology*, 593(14), 3093–3108.
 - 8) Anderson, K. M., & Faber, J. E. (1991). Differential sensitivity of arteriolar alpha 1- and alpha 2-adrenoceptor constriction to metabolic inhibition during rat skeletal muscle contraction. *Circulation Research*, 69(1), 174–184.
 - 9) Becker-Zimmerman, K., Berger, M., Berchtold, P., Gries, F. A., Herberg, L., & Schwenen, M. (1982). Treadmill Training Improves Intravenous Glucose Tolerance and Insulin Sensitivity in Fatty Zucker Rats. *Diabetologia*, (22), 468–474.
 - 10) Beilby, J. (2004). Definition of metabolic syndrome: report of the National Heart, Lung, and Blood Institute/American Heart Association conference on scientific issues related to definition. *The Clininal Biochemist Reviews*, 25(August 2004), 195–198.
 - 11) Berzosa, C., Cebrián, I., Fuentes-Broto, L., Gómez-Trullén, E., Piedrafita, E., Martínez-Ballarín, E., ... García, J. J. (2011). Acute Exercise Increases Plasma Total Antioxidant Status and Antioxidant Enzyme Activities in Untrained Men. *Journal of Biomedicine and Biotechnology*, 2011, 1–7.
 - 12) Bickel, C., Rupprecht, H. J., Blankenberg, S., Espinola-Klein, C., Schlitt, A., Rippin, G., ... Meyer, J. ürge. (2002). Relation of markers of inflammation (C-reactive protein, fibrinogen, von Willebrand factor, and leukocyte count) and statin therapy to long-term mortality in patients with angiographically proven coronary artery disease. *The American Journal of Cardiology*, 89(8), 901–908.
 - 13) Butcher, J. T., Goodwill, A. G., Stanley, S. C., & Frisbee, J. C. (2013). Blunted temporal activity of microvascular perfusion heterogeneity in metabolic syndrome: a new attractor for peripheral vascular disease? *American Journal of Physiology-Heart and Circulatory Physiology*, 304(4), H547–H558.

- 14) Cersosimo, E., Xu, X., Upala, S., Triplitt, C., & Musi, N. (2014). Acute insulin resistance stimulates and insulin sensitization attenuates vascular smooth muscle cell migration and proliferation. *Physiological Reports*, 2(8).
- 15) Chandel, N. S., Maltepe, E., Goldwasser, E., Mathieu, C. E., Simon, M. C., & Schumacker, P. T. (1998). Mitochondrial reactive oxygen species trigger hypoxia-induced transcription. *Proceedings of the National Academy of Sciences of the United States of America*, 95(20), 11715–11720.
- 16) Chantler, P. D., & Frisbee, J. C. (2015). Arterial Function in Cardio-Metabolic Diseases: From the Microcirculation to the Large Conduits. *Progress in Cardiovascular Diseases*, 57(5), 489–496.
- 17) Chilian, W. M., Layne, S. M., Eastham, C. L., & Marcus, M. L. (1989). Heterogenous Microvascular Coronary α -Adrenergic Vasoconstriction. *Circulation Research*, 64, 376.
- 18) Cleary, M. P., Vasselli, J. R., & Greenwood, M. R. (1980). Development of obesity in Zucker obese (fafa) rat in absence of hyperphagia. *The American Journal of Physiology*, 238, E284–E292.
- 19) Cooke, J. P., & Losordo, D. W. (2000). Nitric oxide and angiogenesis. *Journal of Neuro-Oncology*, 50(1–2), 139–148.
- 20) Czel, S. T. A. (2006). Adult Treatment Panel III 2001 but Not International Diabetes Federation 2005 Criteria of the Metabolic Syndrome Predict. *Diabetes Care*, 29(4), 901–907.
- 21) Davis, B., & Zou, M. H. (2005). CD40 ligand-dependent tyrosine nitration of prostacyclin synthase in vivo. *Circulation*, 112(14), 2184–2192.
- 22) Davies, K. J., Lin, S. W., & Pacifici, R. E. (1987). Protein damage and degradation by oxygen radicals. IV. Degradation of denatured protein. *Journal of Biological Chemistry*, 262(20), 9914–9920.
- 23) Erdembileg, A., Mirsoian, A., Enkhmaa, B., Zhang, W., Beckett, L. A., Murphy, W. J., & Berglund, L. F. (2015). Attenuated age-impact on systemic inflammatory markers in the presence of a metabolic burden. *PLoS ONE*, 10(3), 1–14.

- 24) Fiuza-Luces, C., Santos-Lozano, A., Joyner, M., Carrera-Bastos, P., Picazo, O., Zugaza, J. L., ... Lucia, A. (2018). Exercise benefits in cardiovascular disease: beyond attenuation of traditional risk factors. *Nature Reviews Cardiology*.
- 25) Fleming, I., & Busse, R. (2003). Molecular mechanisms involved in the regulation of the endothelial nitric oxide synthase. *Am J Physiol Regul Integr Comp Physiol*, 284, R1–R12.
- 26) Ford, E. S. (2003). The metabolic syndrome and C-reactive protein, fibrinogen, and leukocyte count: Findings from the Third National Health and Nutrition Examination Survey. *Atherosclerosis*, 168(2), 351–358.
- 27) Fossum, E., Høieggen, A., Moan, A., Rostrup, M., Nordby, G., & Kjeldsen, S. E. (1998). Relationship Between Insulin Sensitivity and Maximal Forearm Blood Flow in Young Men. *Hypertension*, 32, 838–843.
- 28) Frisbee, J. C. (2003). Remodeling of the skeletal muscle microcirculation increases resistance to perfusion in obese Zucker rats Remodeling of the skeletal muscle microcirculation increases resistance to perfusion in obese Zucker rats, 53226 (March 2003), 104–111.
- 29) Frisbee, J. C. (2004). Enhanced arteriolar alpha-adrenergic constriction impairs dilator responses and skeletal muscle perfusion in obese Zucker rats. *Journal of Applied Physiology (Bethesda, Md.: 1985)*, 97(2), 764–772.
- 30) Frisbee, J. C. (2005). Reduced nitric oxide bioavailability contributes to skeletal muscle microvessel rarefaction in the metabolic syndrome. *American Journal of Physiology-Regulatory, Integrative and Comparative Physiology*, 289(2), R307–R316.
- 31) Frisbee, J. C. (2006). Vascular adrenergic tone and structural narrowing constrain reactive hyperemia in skeletal muscle of obese Zucker rats. *American Journal of Physiology. Heart and Circulatory Physiology*, 290(5), H2066-74.
- 32) Frisbee, J. C., & Delp, M. D. (2006). Vascular function in the metabolic syndrome and the effects on skeletal muscle perfusion: lessons from the obese Zucker rat. *The Biochemical Society*, 42, 145–161.
- 33) Frisbee JC, Goodwill AG, Frisbee SJ, Butcher JT, Brock RW, Olfert IM, DeVallance ER & Chantler PD (2014). Distinct temporal phases of microvascular rarefaction in

- skeletal muscle of obese Zucker rats. *Am J Physiol Heart Circ Physiol* 307(12), H1714-H1728.
- 34) Frisbee, J. C., Hollander, J. M., Brock, R. W., Yu, H.-G., & Boegehold, M. A. (2009). Integration of skeletal muscle resistance arteriolar reactivity for perfusion responses in the metabolic syndrome. *American Journal of Physiology - Regulatory, Integrative and Comparative Physiology*, 296(6), R1771–R1782.
- 35) Frisbee, J. C., Samora, J. B., Peterson, J., & Bryner, R. (2006). Exercise training blunts microvascular rarefaction in the metabolic syndrome. *AJP: Heart and Circulatory Physiology*, 291(5), H2483–H2492.
- 36) Fujita, M., Morimoto, T., Ikemoto, M., Takeda, M., Ikai, A., & Miwa, K. (2007). Dose-dependency in pleiotropic effects of atorvastatin. *The International Journal of Angiology : Official Publication of the International College of Angiology, Inc*, 16(3), 89–91.
- 37) Goodwill, A. G., & Frisbee, J. C. (2012). Oxidant stress and skeletal muscle microvasculopathy in the metabolic syndrome. *Vascular Pharmacology*, 57(5–6), 150–159.
- 38) Goodwill, AG. Stapleton, PA. James, ME. d’Audffret, AC. and Frisbee, J. (2008). Increased vascular thromboxane generation impairs dilation of skeletal muscle arterioles of obese Zucker rats with reduced oxygen tension. *Mircocirculation*, 15(7), 621–631.
- 39) Greene, A. S., Tonellato, P. J., Lui, J., Lombard, J. H., & Cowley, A. W. (1989). Microvascular rarefaction and tissue vascular resistance in hypertension. *The American Journal of Physiology*, 256(1 Pt 2), H126-31.
- 40) Greene, A S., Tonellato, P. J., Zhang, Z., Lombard, J. H., & Cowley, a W. (1992). Effect of microvascular rarefaction on tissue oxygen delivery in hypertension. *Am J Physiol Heart Circ Physiol*, 262(5), H1486-93.
- 41) Grundy, S. M., Cleeman, J. I., Daniels, S. R., Donato, K. A., Eckel, R. H., Franklin, B. A., ... Costa, F. (2002). Diagnosis and Management of the Metabolic Syndrome: An American Heart Association/National Heart, Lung, and Blood Institute Scientific Statement. *Critical Pathways in Cardiology: A Journal of Evidence-Based Medicine*, 1(1), 1–2.

- 42) Guarini, G., Kiyooka, T., Ohanyan, V., Pung, Y. F., Marzilli, M., Chen, Y. R., ... Chilian, W. M. (2016). Impaired coronary metabolic dilation in the metabolic syndrome is linked to mitochondrial dysfunction and mitochondrial DNA damage. *Basic Res Cardiol*.A, 111(3), 29.
- 43) Halaas, J. L., Gajiwala, K. S., Maffei, M., Cohen, S. L., Chait, T., Rabinowitz, D., ... Friedman, J. M. (1995). Weight-Reducing Effects of the Plasma Protein Encoded by the Obese Gene Published by: American Association for the Advancement of Science Stable URL: <http://www.jstor.org/stable/2887669>.
- 44) Haslinger-Löffler, B. (2008). Multiple effects of HMG-CoA reductase inhibitors (statins) besides their lipid-lowering function. *Kidney International*, 74(5), 553–555.
- 45) Heron, M. (2012). Deaths: leading causes for 2004. *National Vital Statistics Reports*, 60(6), 1–94.
- 46) Hishinuma, T., Tsukamoto, H., Suzuki, K., & Mizugaki, M. (2001). Relationship between thromboxane/prostacyclin ratio and diabetic vascular complications. *Prostaglandins Leukotrienes and Essential Fatty Acids*, 65(4), 191–196.
- 47) Hossain, M., Qadri, S. M., & Liu, L. (2012). Inhibition of nitric oxide synthesis enhances leukocyte rolling and adhesion in human microvasculature. *Journal of Inflammation*, 9(1), 28.
- 48) Hotamisligil, G. S., Peraldi, P., Budavari, A., Ellis, R., Morris, F., Hotamisligil, G. S., ... Spiegelmant, B. M. (2018). IRS-1-Mediated Inhibition of Insulin Receptor Tyrosine Kinase Activity in TNF- α -and Obesity-Induced Insulin Resistance. *Science (New York, N.Y.)*, 271(5249), 665–668.
- 49) Hutcheson, R., Chaplin, J., Hutcheson, B., Borthwick, F., Proctor, S., Gebb, S., ... Rocic, P. (2014). miR-21 normalizes vascular smooth muscle proliferation and improves coronary collateral growth in metabolic syndrome. *The FASEB Journal*, 28(9), 4088–4099.
- 50) Jacqueline, L. K., Morgan, B. J., & Schrage, W. G. (2016). Peripheral Blood Flow Regulation in Human Obesity and Metabolic Syndrome. *Exerc Sport Sci Rev*, 44(3), 116–122.

- 51) Jialal I., Verma S., and Devaraj S. (2009). Inhibition of Endothelial Nitric Oxide Synthase by C-Reactive Protein: Clinical Relevance. *Clin Chem.*, 55(2), 206–208.
- 52) Johnson, F. K., Johnson, R. a, Durante, W., Jackson, K. E., Stevenson, B. K., & Peyton, K. J. (2006). Metabolic syndrome increases endogenous carbon monoxide production to promote hypertension and endothelial dysfunction in obese Zucker rats. *American Journal of Physiology. Regulatory, Integrative and Comparative Physiology*, 290(3), R601–R608.
- 53) Katsiki, N., Athyros, V., Karagiannis, A., & Mikhailidis, D. (2014). Metabolic Syndrome and Non-Cardiac Vascular Diseases: An Update from Human Studies. *Current Pharmaceutical Design*, 20(31), 4944–4952.
- 54) Kojda, G., & Hambrecht, R. (2005). Molecular mechanisms of vascular adaptations to exercise. Physical activity as an effective antioxidant therapy? *Cardiovascular Research*, 67(2), 187–197.
- 55) Krogh, A. (1919). THE NUMBER AND DISTRIBUTION OF CAPILLARIES IN MUSCLES WITH CALCULATIONS OF THE OXYGEN PRESSURE HEAD NECESSARY FOR SUPPLYING THE TISSUE. *The Journal of Physiology*, 52(6), 409–415.
- 56) Kurtz, T. W., Morris, R. C., & Pershadsingh, K. (1989). The Zucker fatty rat as a model of obesity and hypertension. *Hypertension*, 13, 896–901.
- 57) Lakka, H.-M. (2002). The Metabolic Syndrome and Total and Cardiovascular Disease Mortality in Middle-aged Men. *Jama*, 288(21), 2709.
- 58) Machado MV, Martins RL, Borges J, Antunes BR, Estado V, Vieira AB, Tibiriçá E. (2016). Exercise Training Reverses Structural Microvascular Rarefaction and Improves Endothelium-Dependent Microvascular Reactivity in Rats with Diabetes. *Metab Syndr Relat Disord*. 14(6):298-304.
- 59) Marston, W. A., Davies, S. W., Armstrong, B., Farber, M. A., Mendes, R. C., Fulton, J. J., & Keagy, B. A. (2006). Natural history of limbs with arterial insufficiency and chronic ulceration treated without revascularization. *Journal of Vascular Surgery*, 44(1), 108–115.

- 60) McClatchey, P. M., Wu, F., Olfert, M., Ellis, C. G., Goldman, D., Reusch, J. E. B., & Frisbee, J. C. (2017). Impaired Tissue Oxygenation in Metabolic Syndrome Requires Increased Microvascular Perfusion Heterogeneity. *J Cardiovasc Transl Res*, 10(1), 69–81.
- 61) MetSC - Metabolic Syndrome Canada (2018). Metabolic syndrome is a health crisis hiding in plain sight. Retrieved from <https://www.metabolicsyndromecanada.ca/about-metabolic-syndrome>
- 62) Moller, D. E., & Kaufman, K. D. (2005). Metabolic Syndrome: A Clinical and Molecular Perspective. *Annual Review of Medicine*, 56(1), 45–62.
- 63) NUSING, R., GOERIG, M., HABENICHT, A. J. R., & ULLRICH, V. (1993). Selective eicosanoid formation during HL-60 macrophage differentiation: Regulation of thromboxane synthase. *European Journal of Biochemistry*, 212(2), 371–376.
- 64) Orr, J. S., Dengo, A. L., Rivero, J. M., & Davy, K. P. (2009). Arterial destiffening with atorvastatin in overweight and obese middle-aged and older adults. *Hypertension*, 54(4), 763–768.
- 65) Parker, B. A., Capizzi, J. A., Augeri, A. L., Grimaldi, A. S., White, C. M., & Thompson, P. D. (2011). Atorvastatin Increases Exercise Leg Blood Flow in Healthy Adults. *Atherosclerosis*, 219(1), 1–23.
- 66) Palinski, W., Rosenfeld, M. E., Ylä-Herttuala, S., Gurtner, G. C., Socher, S. S., Butler, S. W., ... Witztum, J. L. (1989). Low density lipoprotein undergoes oxidative modification in vivo. *Proceedings of the National Academy of Sciences of the United States of America*, 86(4), 1372–1376.
- 67) Paraskevas, K. I., Kotsikoris, I., Koupidis, S. A., Giannoukas, A. D., & Mikhailidis, D. P. (2010). Editorial: Ankle-brachial index: A marker of both peripheral arterial disease and systemic atherosclerosis as well as a predictor of vascular events. *Angiology*, 61(6), 521–523.
- 68) Perfusiontheory.com/oxygen-pressure-field-theory/session-1-understanding-the-oxygen-pressure-field-using-the-krogh-cylinder-model/9/. Graphic.

- 69) Pfister SL, Campbell WB. (1996). Contribution of arachidonic acid metabolites to reduced norepinephrine induced contractions in hypercholesterolemic rabbit aortas. *J Cardiovasc Pharmacol*, 28:784–91.
- 70) Prasad, K. (2004). C-reactive protein increases oxygen radical generation by neutrophils. *J Cardiovasc Pharmacol Ther*, 9(3), 203–209. Retrieved from 04.11.30 Prasad
- 71) Qiu, F., Liu, X., Zhang, Y., Wu, Y., Xiao, D., & Shi, L. (2018). Aerobic exercise enhanced endothelium-dependent vasorelaxation in mesenteric arteries in spontaneously hypertensive rats: the role of melatonin. *Hypertension Research*.
- 72) Rabkin, S. W., Langer, A., Ur, E., Calciu, C. D., & Leiter, L. A. (2013). Inflammatory biomarkers CRP, MCP-1, serum amyloid alpha and interleukin-18 in patients with HTN and dyslipidemia: Impact of diabetes mellitus on metabolic syndrome and the effect of statin therapy. *Hypertension Research*, 36(6), 550–558.
- 73) Ridker PM., Rifai N., Rose L., Buring JE., and Cook NR. COMPARISON OF C-REACTIVE PROTEIN AND LOW-DENSITY LIPOPROTEIN CHOLESTEROL LEVELS IN THE PREDICTION OF FIRST CARDIOVASCULAR EVENTS. (2002). *The New England Journal of Medicine*, 347(20), 1557–1565.
- 74) Riediger, N. D., & Clara, I. (2011). Prevalence of metabolic syndrome in the Canadian adult population. *CMAJ : Canadian Medical Association Journal*, 183(15), E1127-34.
- 75) Rush, J. W. E., Turk, J. R., & Laughlin, M. H. (2003). Exercise training regulates SOD-1 and oxidative stress in porcine aortic endothelium. *American Journal of Physiology-Heart and Circulatory Physiology*, 284(4), H1378–H1387.
- 76) Sandoo, A., Veldhuijzen van Zanten, J. J. C. S., Metsios, G. S., Carroll, D., & Kitas, G. D. (2010). The Endothelium and Its Role in Regulating Vascular Tone. *The Open Cardiovascular Medicine Journal*, 4(1), 302–312.
- 77) Singer G. and Granger DN. (2007). Inflammatory responses underlying the microvascular dysfunction associated with obesity and insulin resistance. *Microcirculation*, 2007;14 (4–5): 375–387

- 78) Sodha, N. R., & Sellke, F. W. (2015). The effect of statins on perioperative inflammation in cardiac and thoracic surgery. *Journal of Thoracic and Cardiovascular Surgery*, 149(6), 1495–1501.
- 79) Statistics Canada. Table: 13-10-0451-01. Health indicators, annual estimates, 2003 – 2014. Retrieved from <https://www150.statcan.gc.ca/t1/tbl1/en/tv.action?pid=1310045101>
- 80) Stepp, D. W., & Frisbee, J. C. (2002). Augmented adrenergic vasoconstriction in hypertensive diabetic obese Zucker rats. *American Journal of Physiology. Heart and Circulatory Physiology*, 282(3), H816-20.
- 81) Sumner, A. D., Khalil, Y. K., & Reed, J. F. (2012). The Relationship of Peripheral Arterial Disease and Metabolic Syndrome Prevalence in Asymptomatic US Adults 40 Years and Older: Results From the National Health and Nutrition Examination Survey (1999-2004). *The Journal of Clinical Hypertension*, 14(3), 144–148.
- 82) Suzuki, T., Hirata, K., Elkind, M. S. V, Jin, Z., Rundek, T., Miyake, Y., Homma, S. (2008). Metabolic syndrome, endothelial dysfunction, and risk of cardiovascular events: the Northern Manhattan Study (NOMAS). *American Heart Journal*, 156(2), 405–10.
- 83) Ungvari, Z., Tarantini, S., Kiss, T., Wren, J. D., Giles, C. B., Griffin, C. T., ... Csiszar, A. (2018). Endothelial dysfunction and angiogenesis impairment in the ageing vasculature. *Nature Reviews Cardiology*, 1–11.
- 84) Vaziri, N. D., Xu, Z. G., Shahkarami, A., Huang, K. T., Rodríguez-Iturbe, B., & Natarajan, R. (2005). Role of AT-1 receptor in regulation of vascular MCP-1, IL-6, PAI-1, MAP kinase, and matrix expressions in obesity. *Kidney International*, 68(6), 2787–2793.
- 85) Wassink, A. M. J., Van Der Graaf, Y., Olijhoek, J. K., & Visseren, F. L. J. (2008). Metabolic syndrome and the risk of new vascular events and all-cause mortality in patients with coronary artery disease, cerebrovascular disease, peripheral arterial disease or abdominal aortic aneurysm. *European Heart Journal*, 29(2), 213–223.
- 86) WHO – World Health Organization (2018). *Global Health Estimates 2016: Deaths by Cause, Age, Sex by Country and by Region, 2000-2016*. Geneva, World Health

Organization. Retrieved from <http://www.who.int/news-room/fact-sheets/detail/the-top-10-causes-of-death>

- 87) Wu, S. Q., Hopfner, R. L., McNeill, J. R., Wilson, T. W., & Gopalakrishnan, V. (2000). Altered paracrine effect of endothelin in blood vessels of the hyperinsulinemic, insulin resistant obese Zucker rat. *Cardiovascular Research*, 45(4), 994–1000.
- 88) Yeh, E. T. H. (2004). CRP as a Mediator of Disease. *Circulation*, 109(21_suppl_1), II-11-II-14. <https://doi.org/10.1161/01.CIR.0000129507.12719.80>

Chapter 2

2 Altered Postcapillary and Collecting Venular Reactivity in Skeletal Muscle with Metabolic Syndrome

Kent A. Lemaster¹, Zahra Farid¹, Robert W. Brock², Carl D. Shrader³,

Daniel Goldman¹, Dwayne N. Jackson¹, Jefferson C. Frisbee¹

Department of Medical Biophysics, Transdisciplinary Program in Vascular Health,
Schulich School of Medicine and Dentistry, University of Western Ontario, London,
Ontario¹

Departments of Physiology and Pharmacology² and Family Medicine³, West Virginia
University HSC, Morgantown, WV

Running Head: venular function, skeletal muscle perfusion, rodent models of obesity

Send Correspondence to:

Jefferson C. Frisbee, Ph.D.
Department of Medical Biophysics; MSB 407
Schulich School of Medicine & Dentistry
Western University
London, Ontario, Canada, N6A 5C1
Phone: (519) 661-2111 x86552
Email: jfrisbee@uwo.ca

KEY POINTS:

- With the development of the metabolic syndrome, both post-capillary and collecting venular dilator reactivity within the skeletal muscle of obese Zucker rats (OZR) is impaired.
- The impaired dilator reactivity in OZR reflects a loss in venular nitric oxide and PGI₂ bioavailability, associated with the chronic elevation in oxidant stress.
- Additionally, with the impaired dilator responses, a modest increase in adrenergic constriction, combined with an elevated thromboxane A₂ production may contribute to impaired functional dilator and hyperemic responses at the venular level.
- The shift in skeletal muscle venular function with development of the metabolic syndrome on issues such as aggregate microvascular perfusion resistance, mass transport and exchange within with capillary networks, and fluid handling across the microcirculation are compelling avenues for future investigation.

2.1 Abstract

While research into vascular outcomes of the metabolic syndrome has focused on arterial/arteriolar and capillary levels, investigation into venular function and how this impacts responses has received little attention. Using the in situ cremaster muscle of obese Zucker rats (OZR; with leans (LZR) as controls), we determined indices of venular function. At ~17 weeks of age, skeletal muscle post-capillary venular density was reduced by ~20% in LZR vs. OZR, although there was no evidence of remodeling of the venular wall. Venular tone at ~25 μm (post-capillary) and ~75 μm (collecting) diameter was elevated in OZR vs. LZR. Venular dilation to acetylcholine was blunted in OZR vs. LZR due to increased oxidant stress-based loss of nitric oxide bioavailability (post-capillary) and increased $\alpha 1$ - (and $\alpha 2$ -) mediated constrictor tone (collecting). Venular constrictor responses in OZR were comparable to LZR for most stimuli, although constriction to $\alpha 1$ adrenoceptor stimulation was elevated. In response to field stimulation of the cremaster muscle (0.5, 1, 3 Hz), venular dilator and hyperemic responses to lower frequencies were blunted in OZR, but responses at 3 Hz were similar between strains. Venous production of TxA₂ was higher in OZR than LZR and significantly higher than PGI₂ production in either following arachidonic acid challenge. These results suggest that multi-faceted alterations to skeletal muscle venular function in OZR may contribute to alterations in upstream capillary pressure profiles and the trans-capillary exchange of solutes and water under conditions of metabolic syndrome.

Key words: venous function, microcirculation, metabolic syndrome, skeletal muscle blood flow

Abbreviations: DPEP IV, dipeptidyl peptidase-4; GS-1, griffonia simplicifolia 1; L-NAME, N ω -Nitro-L-arginine methyl ester hydrochloride; LZR, lean Zucker rat; OZR, obese Zucker rat; PGI₂, prostacyclin; TEMPOL, 4-hydroxy-2,2,6,6-tetramethylpiperidin-1-oxyl; TxA₂, thromboxane A₂

2.2 Introduction

It is well established that the growing incidence and prevalence of the metabolic syndrome presents a consistent threat to aggregate public health cardiovascular outcomes across many societies and developed economies (Mameli et al., 2017; Tune et al., 2017; Vassalo et al., 2016). This syndrome is broadly defined as the combined presentation of obesity, impaired glycemic control, atherogenic dyslipidemia and hypertension, with the additional contributing conditions of pro-oxidant, pro-thrombotic and pro-inflammatory phenotypes (American Heart Association, 2017; Vassalo et al., 2016). While this condition is present in a growing number of afflicted persons worldwide, its influence on morbidity and mortality (Global Burden of Metabolic Risk Factors for Chronic Diseases Collaboration, 2014), as well as the economic costs that must be borne by society (Shamsedden et al., 2011; Trasande and Elbel, 2012), mandate the detailed investigation into this multi-pathology state.

While enormous investment has been made in understanding the impact of the metabolic syndrome on arterial/arteriolar and capillary function (Goodwill et al., 2012, Lemaster et al., 2017, Tune et al. 2017), dedicated study of venular function has been limited and has largely focused on leukocyte-endothelial cell interactions as well as inflammatory and pro-thrombotic processes (Estate et al., 2017; Iba et al., 2012; Scallan et al., 2015). Although these are important aspects of altered venular function, our understanding of venous tone regulation and its potential contribution to integrated microvascular function through the transition from health to disease is far from complete. Population health studies, using the retinal microcirculation as a “window” into altered venular function, suggest that the control of venular diameter and venular network structure can be significantly altered with metabolic disease (Lammert et al., 2012; Wong et al., 2004; Zhao et al., 2012). However, there has been a limited attempt at investigating these relationships in relevant animal models.

The obese Zucker rat (OZR; *fa/fa*) represents a translationally-relevant model to study the metabolic syndrome, as cardiovascular disease in this model tracks well with cardiovascular (dys)function in afflicted humans. OZR develop the metabolic syndrome due to chronic hyperphagia based in leptin resistance, and rapidly develop all of the

systemic phenotypes listed above to comparable levels of severity to that commonly identified in human subjects. Also similar to the health outcomes in humans, OZR exhibiting the metabolic syndrome suffer from a progressive vasculopathy that ultimately develops into overt peripheral vascular disease (Frisbee and Delp, 2006), albeit one without the development of significant atherosclerotic lesions. While there has been extensive interrogation of the impact of metabolic syndrome on the arterial side of the microcirculation in OZR and in comparable models (Tune et al., 2017), there has been less effort devoted to understanding the potential for altered venular function under these conditions and the potential impact on integrated microvascular function.

The purpose of the present study was to begin to understand how the function of in situ post-capillary and collecting venules from obese Zucker rats manifesting the full metabolic syndrome can be impacted as a result of the multi-pathology state. To assess this, we used an array of physiological and pharmacological challenges to understand how function is altered at these two levels within the venular networks. The present study tested the hypothesis that post-capillary and collecting venular function in the in situ skeletal muscle of OZR is altered in a manner that can increase venular blood flow resistance and negatively impact function within the capillary networks.

2.3 Materials and Methods

Ethical Approval: All procedures in the present study had received prior review and approval by the Institutional Animal Care and Use Committee. All animal use procedures, including anesthesia and euthanasia, conform to standards established by the UK/European Union legislation (set out in ASPA Schedule 1 in the UK and in Annex IV in the European Directive 2010/63/EU), the Canadian Council for Animal Care and the United States Department of Agriculture. All details of animal use are provided in the subsequent paragraphs.

Animals: Male lean (LZR, Harlan/Envigo) and obese Zucker rats (OZR, Harlan/Envigo) were acquired at 6-7 weeks of age, and after one week of acclimation, were aged to ~17 weeks of age. All animals were fed standard chow and tap water *ad libitum* for all experiments. On the experiment day, after an 8 hour fast, rats were anesthetized with

injections of sodium pentobarbital ($50 \text{ mg}\cdot\text{kg}^{-1}$ i.p.), and all rats received tracheal intubation to facilitate maintenance of a patent airway. In all rats a carotid artery and an external jugular vein were cannulated for determination of arterial pressure and for intravenous infusion of additional substances as necessary (e.g., anesthesia, heparin, etc.). Any animal in which mean arterial pressure was found to be below 85 mmHg ($<5\%$ in both LZR and OZR), or where it had decreased by more than 15% from that following equilibration (without any pharmacological intervention; $\sim 5\%$ in LZR, $\sim 10\%$ in OZR) was not used in the present study. Blood samples were drawn from the venous cannula for determination of glucose and insulin concentrations (Millipore, Billerica, MA) as well as cholesterol/triglyceride levels (Wako Diagnostics, Richmond, VA), and nitrotyrosine (Oxis International, Foster City, CA). Blood gases were determined using a Corning RapidLab 248 Blood Gas Analyzer (Siemens Medical Solutions, Malvern, PA). Unless otherwise noted, all drugs and chemicals were purchased from Sigma-Aldrich (St. Louis, MO). Adequate depth of anesthesia was confirmed at ~ 15 minute intervals by monitoring ventilation patterns and noting an absence of whisker movement, startle and toe-pinch withdrawal reflexes. Additional anesthetic was introduced in $10 \text{ mg}\cdot\text{kg}^{-1}$ increments, as needed, through the jugular vein cannula. After all experiments, the anesthetized rat was euthanized with an intravenous overdose of sodium pentobarbital ($>200 \text{ mg}\cdot\text{kg}^{-1}$) followed by a bilateral pneumothoracotomy and physical removal of the heart. Due to the lasting effects of some of the pharmacological interventions and the inherent difficulties in reversing them, not all observations could be gathered from every animal. As a result, in specific experiment groups, the actual number of animals used can exceed the number of specific observations. This was done in order to preserve quality and experiment rigor. For clarity, total animal numbers used for the present study, and their distribution across the experimental groups, are summarized in Table 1.

Table 1. Animal numbers, experimental group distributions and condition observation numbers within groups for the present study. All other experiment data came from *ex vivo* tissue analyses recovered from within these animal groups. Please see text for details.

| | LZR | | OZR | |
|----------------------------|-----------|--------------|-----------|--------------|
| | Animals | Observations | Animals | Observations |
| Experiment Group 1 | 6 | 6 | 8 | 8 |
| Experiment Group 2 | 12 | 6 | 12 | 6 |
| Experiment Group 3 | 12 | 6 | 12 | 6 |
| Experiment Group 4 | 6 | 6 | 8 | 8 |
| Experiment Group 5 | 5 | 5 | 5 | 5 |
| Total Animal Number | 41 | --- | 45 | --- |

Preparation of In Situ Cremaster Muscle: In each rat, the left cremaster muscle was prepared for television microscopy (Butcher *et al.*, 2013). After completion of the preparation, the cremaster muscle was superfused with PSS, equilibrated with a gas mixture containing 5% CO₂ and 95% N₂, and maintained at 35°C as it flowed over the muscle. The ionic composition of the PSS was as follows (mM): NaCl 119.0, KCl 4.7, CaCl₂ 1.6, NaH₂PO₄ 1.18, MgSO₄ 1.17, and NaHCO₃ 24.0. Venular diameter was determined with an on-screen video micrometer. After an initial post-surgical equilibration period of 30 minutes, venules of two sizes, ~75 μm diameter; (“collecting”) and ~25 μm diameter (“post-capillary”) were selected for investigation in a clearly visible region of the muscle. Venules selected for study had walls that were clearly visible, a brisk flow velocity, and active tone, as indicated by the occurrence of significant dilation in response to topical application of 10⁻⁵ M adenosine. All venules studied were located in a region of the muscle that was away from any incision. In all experiments, at the conclusion of all procedures, 10⁻³ M adenosine and 10⁻³ M sodium nitroprusside were added to the superfusate to determine maximal diameter of the monitored venules.

Experiments Group 1: These experiments were designed to determine fundamental cremaster muscle venular responses to pharmacological stimuli between LZR and OZR. Following an equilibration period, the responses of selected venules within the cremaster muscle of LZR and OZR were assessed in response to increasing concentrations of acetylcholine (10^{-10} – 10^{-6} M), phenylephrine (α_1 adrenoreceptor agonist; 10^{-10} – 10^{-6} M), clonidine (α_2 adrenoreceptor agonist, 10^{-10} – 10^{-6} M), angiotensin II (vasoconstrictor peptide, 10^{-10} – 10^{-6} M), endothelin (vasoconstrictor peptide, 10^{-10} – 10^{-6} M) or acetylcholine (endothelium-dependent dilator, 10^{-10} – 10^{-6} M).

Experiments Group 2: These experiments determined basic signaling mechanisms that can contribute to the alterations in dilator reactivity to acetylcholine and the constrictor reactivity to phenylephrine determined between LZR and OZR in Group 1. For these experiments, following the determination of baseline responses to acetylcholine and phenylephrine (as above), the cremaster muscle was treated with L-NAME (nitric oxide synthase inhibitor; 10^{-4} M), indomethacin (cyclooxygenase inhibitor; 10^{-5} M), TEMPOL (cell-permeable antioxidant; 10^{-4} M) or SQ-29548 (PGH₂/TxA₂ receptor antagonist, 10^{-5} M). As in our previous studies (Butcher *et al.*, 2013; Frisbee *et al.*, 2014), to exert maximum effectiveness, each inhibitor was applied for at least 45 minutes prior to evaluation of venular reactivity.

In a subset of animals from Experiment Groups 1 and 2, the cremaster muscle of LZR (n=10) and OZR (n=10) was treated with prazosin (α_1 adrenoreceptor blocker, 10^{-5} M), yohimbine (α_2 adrenoreceptor blocker, 10^{-5} M), or both and constrictor responses to norepinephrine (10^{-10} – 10^{-6} M) were determined to assess any differences in receptor contribution between the strains.

Experiments Group 3: These experiments determined basic signaling mechanisms that contribute to acetylcholine-induced dilation or phenylephrine-induced constriction of cremaster muscle venules of LZR and OZR following pretreatment with 10^{-4} M TEMPOL. Following incubation with the antioxidant, venular responses to increasing concentrations of acetylcholine and phenylephrine were assessed under the new “control” conditions, and following treatment of the muscle with L-NAME, indomethacin, or SQ-29548, as described above.

Experiment Group 4: These experiments determined the responses of *in situ* cremaster muscle venules of LZR and OZR in response to increased metabolic demand. Contraction of the cremaster muscle was evoked by three minutes of electrical field stimulation at 0.5, 1 or 3 Hz (400 ms duration, 60 Hz within train, 7V; Grass SD 48). At the conclusion of the muscle contraction period, venular diameter and center-line erythrocyte velocity (optical Doppler velocimeter, Texas A&M University, College Station, TX) were determined and used for the calculation of hyperemic responses (see below).

Experiment Group 5: These experiments determined the degree of leukocyte adhesion and rolling on the post-capillary venular endothelium between LZR and OZR. In a separate cohort of LZR and OZR, the *in situ* extensor digitorum longus muscle was prepared as described previously (Frisbee *et al.*, 2014; Tysl and Budreau, 1991). Following preparation of the muscle for imaging, 10 random high magnification fields of view (Plan-Neo 20x/0.5 and 40x/0.75; Zeiss) were recorded using a high-speed cooled digital imaging system (Axiocam HSm; Zeiss) for later analyses. Animals received a bolus injection of rhodamine 6G (0.3 mg/kg; Sigma) to permit visualization of leukocytes. Rhodamine 6G-labeled vascular cells were visualized by epi-illumination at 510-560 nm, using a 590-nm emission filter. The number of rolling and adherent leukocytes in venules was expressed as cells/mm² of endothelial surface, calculated from the diameter and length of the venular segment. Leukocytes were considered adherent if they remained stationary for a 30 second observation period. Leukocytes were considered rolling if their velocity was less than 250 $\mu\text{m}/\text{sec}$ (Zeintl *et al.*, 1989).

Histological Determination of Microvessel Density: From LZR and OZR that were selected from each of the above groups, the gastrocnemius muscle from the left leg was removed, rinsed in PSS and fixed in 0.25% formalin. Muscles were embedded in paraffin and cut into 5 μm cross sections. Sections were incubated with *Griffonia simplicifolia* I lectin (GS-1) and dipeptidylpeptidase IV (DPEP IV), for subsequent determination of microvessel density. GS-1 is a general stain that labels all microvessels <20 μm in diameter (Greene *et al.*, 1990) and DPEP IV preferentially stains venular ends of capillaries (Mrázková *et al.*, 1986). Labeled microvessel density was determined using fluorescent (for GS-1) or light microscopy (for DPEP IV) as described previously (Frisbee *et al.*, 2014).

Determination of Vascular Metabolites of Arachidonic Acid: Vascular production of 6-keto-prostaglandin F_{1α}(6-keto-PGF_{1α}; the stable breakdown product of PGI₂; Liu *et al.*, 1997; Nies 1986), and 11-dehydro-thromboxane B₂ (11-dehydro-TxB₂; the stable plasma breakdown product of TxA₂; Catella *et al.*, 1986) in response to challenge with arachidonic acid (10⁻⁶ M) was assessed using pooled conduit veins (e.g., femoral, saphenous) from LZR and OZR. Pooled vessels from each animal were incubated in microcentrifuge tubes in 1 ml of physiological salt solution for 30 minutes under control conditions (21% O₂ with the arachidonic acid challenge). After this time, the superfusate was removed, stored in a new microcentrifuge tube and frozen in liquid N₂, while a new aliquot of PSS with arachidonic acid was added to the vessels for the subsequent 30 minutes. After the second 30 minute period, this PSS was transferred to a fresh tube, frozen in liquid N₂ and stored at -80°C. Metabolite release by the vessels was determined using commercially available EIA kits for 6-keto-PGF_{1α} and 11-dehydro-TxB₂ (Cayman).

Data and Statistical Analyses: Blood flow in venular segments within in situ cremaster muscle of LZR and OZR was calculated as:

$$Q = (V \times 1.6^{-1})(\pi r^2)(0.001)$$

where Q represents venular perfusion (nl•s⁻¹), V represents the measured red cell velocity from the optical Doppler velocimeter (mm•s⁻¹; with V/1.6 representing an estimated average velocity assuming a parabolic flow profile; Baker and Wayland, 1974), and r represents venular radius (μm; Davis, 1987).

All data are presented as mean±SD. Statistically significant differences in measured and calculated parameters between LZR and OZR in the present study were determined using repeated measures analysis of variance (RM-ANOVA), where agonist concentration or muscle stimulation frequency were used as the repeated measures. Statistically significant differences in arachidonic acid metabolite production, leukocyte adhesion/rolling and measures of microvessel density between LZR and OZR were assessed using standard ANOVA or Student's t-test, as appropriate. Student-Newman-Keuls post hoc test was used when appropriate and p<0.05 was taken to reflect statistical significance.

2.4 Results

At ~17 weeks, OZR exhibited all aspects of the metabolic syndrome, being obese as compared to age-matched LZR, with impaired glycemic control, dyslipidemia in both cholesterol and triglyceride levels, with a moderate level of hypertension (Table 2). In addition, OZR exhibited both a chronic level of oxidant stress within the vasculature as well as a chronic state of inflammation. Within the *in situ* cremaster muscle, venular diameters under untreated conditions demonstrated a modest reduction in diameter in OZR as compared to LZR, and there was no difference in venular diameter under passive conditions. When taken together, however, calculated active tone of *in situ* venules for OZR in the post-capillary level, but not in the collecting venules, was elevated as compared to that for LZR.

Table 2. Baseline characteristics (mean±SD) of ~17 week old LZR and OZR used in the present study. * p<0.05 versus LZR.

| | LZR | OZR |
|---|---------|----------|
| Mass (g) | 358±59 | 679±71* |
| MAP (mmHg) | 98±21 | 129±35* |
| [Glucose] _{plasma} (mg/dl) | 105±49 | 164±65* |
| [Insulin] _{plasma} (ng/ml) | 1.4±1.1 | 7.6±6.0* |
| [Cholesterol] _{plasma} (mg/dl) | 84±38 | 132±65* |
| [Triglycerides] _{plasma} (mg/dl) | 91±53 | 361±118* |
| [Nitrotyrosine] _{plasma} (ng/ml) | 11±16 | 44±36* |
| [TNF-α] _{plasma} (pg/ml) | 2.1±1.6 | 7.4±4.7* |
| [MCP-1] _{plasma} (pg/ml) | 32±27 | 94±47* |
| Post-Capillary Venules | | |
| Resting Diameter (μm) | 21±11 | 19±12 |
| Maximum/Passive Diameter (μm) | 36±16 | 37±18 |
| Active Tone (%) | 40±17 | 49±17* |
| Collecting Venules | | |
| Resting Diameter (μm) | 66±17 | 62±18 |
| Maximum/Passive Diameter (μm) | 105±21 | 107±24 |
| Active Tone (%) | 37±16 | 42±18 |

Figure 1 summarizes post-capillary venular dilator responses (to acetylcholine, Panel A) or constrictor responses (to endothelin, Panel B; angiotensin II, Panel C; clonidine, Panel D; or phenylephrine, Panel E). In response to increasing concentrations of acetylcholine, dilator responses of both distal and proximal venules of OZR were attenuated as compared to responses in LZR. Venules from OZR and LZR all demonstrated a robust constriction in response to increasing concentrations of endothelin, angiotensin II and clonidine (Panels B-D), although there were no demonstrable differences in these responses between strains. However, venular constrictor responses to increasing concentrations of the α_1 adrenoceptor agonist phenylephrine were significantly increased in OZR over the mid-range of the agonist challenge (Panel E).

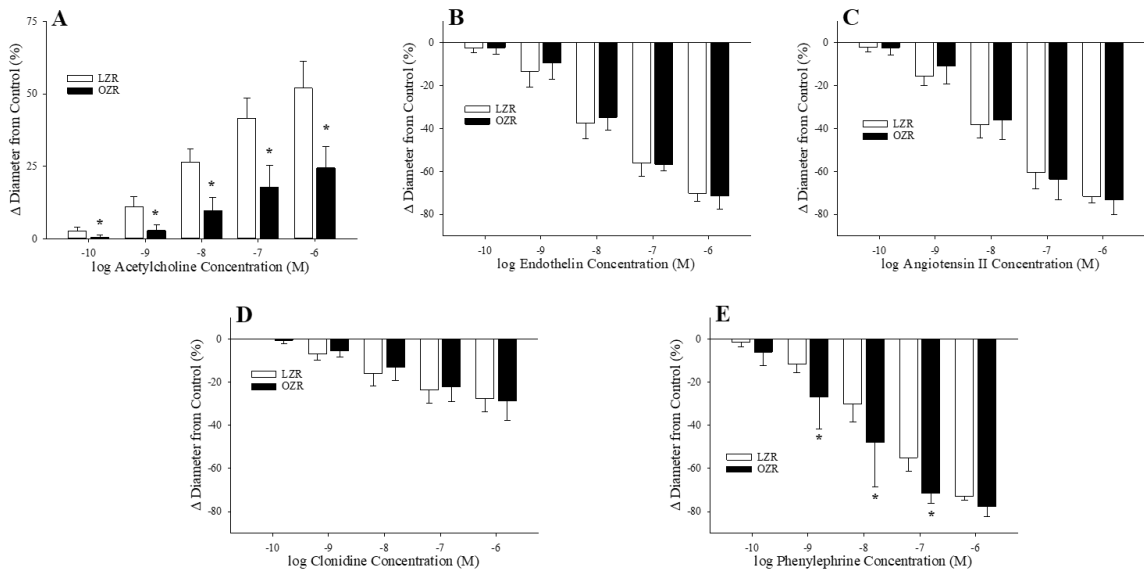


Figure 1. Data describing the reactivity of post-capillary venules within *in situ* cremaster muscle of LZR and OZR in response to increasing concentrations of acetylcholine (Panel A), endothelin (Panel B), angiotensin II (Panel C), clonidine (Panel D) and phenylephrine (Panel E). Data are presented as the mean \pm SD change in venular inner diameter, expressed as a percentage of the initial resting state ($\sim 25 \mu\text{m}$). * represents $p < 0.05$ versus responses from LZR at that agonist concentration. Results and determination of statistically significant difference represent $n=6$ observations from 6 animals in LZR; $n=8$ observations from 8 animals in OZR.

Data describing the reactivity of collecting venules within the *in situ* cremaster muscle of LZR and OZR are presented in Figure 2. As with the smaller venules, dilator responses of larger collecting venules to acetylcholine were attenuated in OZR as compared to responses in LZR (Panel A), while responses to increasing concentrations of endothelin (Panel B) and angiotensin II (Panel C) were comparable. However, while venular constrictor responses to

phenylephrine were enhanced in OZR as compared to LZR (Panel D), responses to clonidine (Panel E) were also increased versus those in LZR.

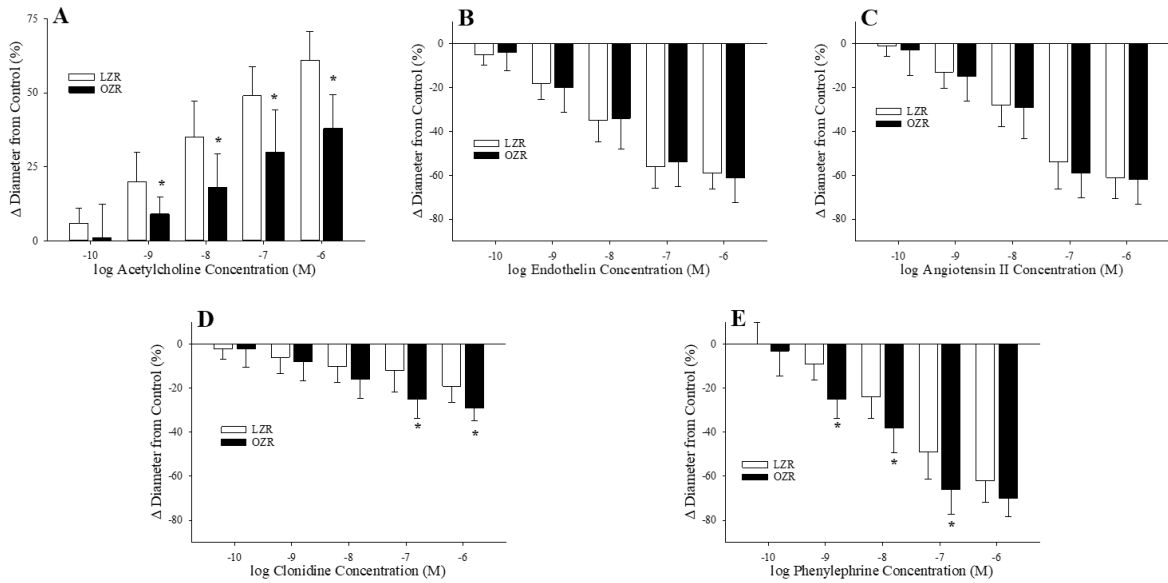


Figure 2. Data describing the reactivity of collecting venules within *in situ* cremaster muscle of LZR and OZR in response to increasing concentrations of acetylcholine (Panel A), endothelin (Panel B), angiotensin II (Panel C), clonidine (Panel D) and phenylephrine (Panel E). Data are presented as the mean \pm SD change in venular inner diameter, expressed as a percentage of the initial resting state ($\sim 70 \mu\text{m}$). * represents $p < 0.05$ versus responses from LZR at that agonist concentration. Results and determination of statistically significant difference represent $n=6$ observations from 6 animals in LZR; $n=8$ observations from 8 animals in OZR.

Figure 3 presents the mechanistic contributors to the venular dilation to acetylcholine in post-capillary venules of LZR (Panels A and C) and OZR (Panels B and D). In LZR, dilator responses of venules to increasing concentrations of acetylcholine were largely nitric oxide-dependent, as treatment with L-NAME significantly attenuated responses (Panel A). While there was a contribution from cyclooxygenase products to this response, it was less substantial than that for nitric oxide. In OZR, the attenuated venular dilation to acetylcholine was abolished following treatment of the cremaster muscle with L-NAME, but only minimally impacted as a result of treatment with indomethacin. However, incubation of the tissue with TEMPOL resulted in a more robust dilation to increasing concentrations of acetylcholine (Panel B). If the cremaster muscle of LZR or OZR was incubated with TEMPOL prior to challenge with increasing concentrations of acetylcholine, these relationships were not fundamentally altered in venules of LZR (Panel C). However, the improvement in the acetylcholine-induced venular dilation in OZR was abolished by L-NAME, unaffected by

indomethacin, and mildly improved by blockade of $\text{PGH}_2/\text{TxA}_2$ receptors with SQ-29548 (Panel D).

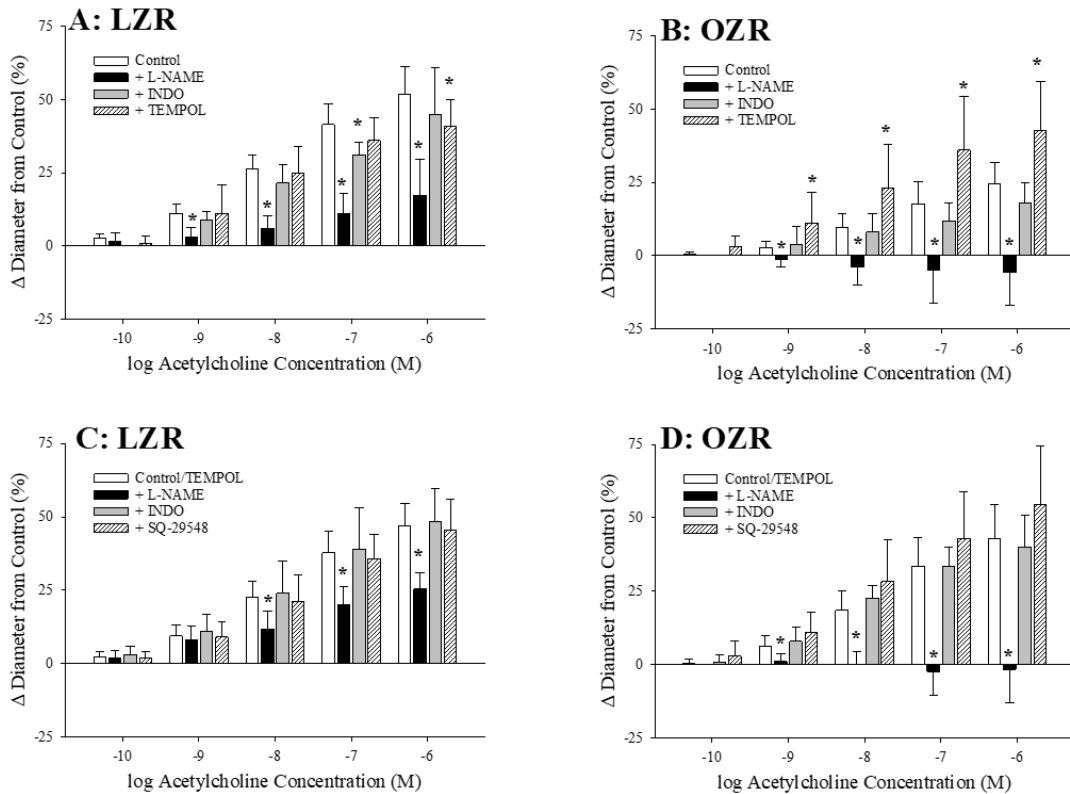


Figure 3. The dilator reactivity of post-capillary venules within *in situ* cremaster muscle of LZR and OZR in response to increasing concentrations of acetylcholine (Panels A and B, respectively). Data are presented for venular reactivity under untreated control conditions, and following pre-treatment of the cremaster muscle with L-NAME, indomethacin (INDO) or TEMPOL. For Panels A and B, results represent n=6 observations from 12 animals in LZR; n=6 observations from 12 animals in OZR. Also presented are data describing the reactivity of post-capillary venules following pre-treatment with TEMPOL in LZR and OZR (Panels C and D, respectively), where the cremaster muscle was subsequently treated with L-NAME, indomethacin (INDO) or SQ-29548 to assess the contributions of nitric oxide, cyclooxygenase products or $\text{PGH}_2/\text{TxA}_2$ to reactivity. Data are presented as the mean \pm SD change in venular inner diameter, expressed as a percentage of the initial resting state ($\sim 25 \mu\text{m}$). * represents $p < 0.05$ versus responses from LZR at that agonist concentration. For Panels C and D, results represent n=6 observations from 12 animals in LZR; n=6 observations from 12 animals in OZR. All statistical analyses were done on the number of observations within the group, not the number of animals within the group. Please see text and Table 1 for details.

The relationships between acetylcholine-induced dilation (with or without pre-treatment with TEMPOL) and its basic mechanistic contributors were consistent in the larger collecting venules within *in situ* cremaster muscle of LZR and OZR with some exceptions (Figure 4, Panels A-D). In post-capillary venules from LZR and OZR rats and in collecting venules from OZR, indomethacin did not have a demonstrable impact on dilator responses to acetylcholine, but significantly attenuated collecting venular dilation in LZR. Further,

the indomethacin-sensitive component of the collecting venular dilation to acetylcholine was absent in OZR and in LZR and OZR pre-treated with TEMPOL.

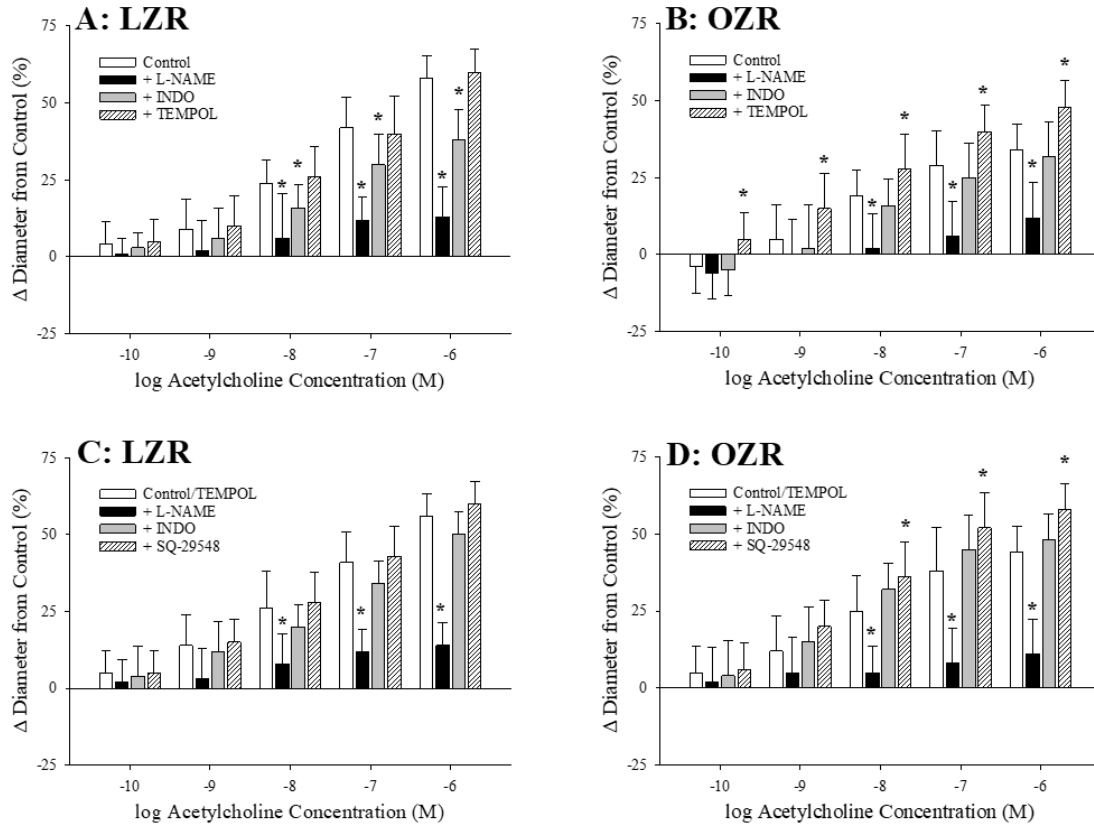


Figure 4. The dilator reactivity of collecting venules within *in situ* cremaster muscle of LZR and OZR in response to increasing concentrations of acetylcholine (Panels A and B, respectively). Data are presented for venular reactivity under untreated control conditions, and following pre-treatment of the cremaster muscle with L-NAME, indomethacin (INDO) or TEMPOL. For Panels A and B, results represent n=6 observations from 12 animals in LZR; n=6 observations from 12 animals in OZR. Also presented are data describing the reactivity of collecting venules following pre-treatment with TEMPOL to normalize responses in OZR (Panels C and D, respectively), where the cremaster muscle was subsequently treated with L-NAME, indomethacin (INDO) or SQ-29548 to assess the contributions of nitric oxide, cyclooxygenase products or PGH₂/TxA₂ to reactivity. Data are presented as the mean±SD change in venular inner diameter, expressed as a percentage of the initial resting state (~ 70 μm). * represents p<0.05 versus responses from LZR at that agonist concentration. For Panels C and D, results represent n=6 observations from 12 animals in LZR; n=6 observations from 12 animals in OZR. All statistical analyses were done on the number of observations within the group, not the number of animals within the group. Please see text and Table 1 for details.

Using prazosin (α_1 adrenergic receptor blocker) and yohimbine (α_2 adrenergic receptor blocker), alone and in combination, the constrictor responses of post-capillary and collecting venules within cremaster muscle of LZR and OZR in response to increasing concentrations of norepinephrine were demonstrated to be almost entirely α_1 -receptor-dependent in postcapillary venules and predominantly α_1 -receptor dependent (with a smaller contribution from α_2 adrenergic receptors) in collecting venules in both strains (data not

shown). Data describing the interaction of altered endothelial function and the venular constriction to increasing concentration of norepinephrine are summarized in Figure 5. In the immediate post-capillary venules, treatment of the cremaster muscle with L-NAME increased constrictor responses to norepinephrine in LZR (Panel A), but was without effect in OZR (Panel B). While treatment with indomethacin was largely without effect in either strain, treatment of the muscle with TEMPOL had only a minor effect on venular responses in LZR, but attenuated the constrictor response in OZR venules. Following pre-treatment of the cremaster muscle with TEMPOL in LZR, responses to increasing concentrations of norepinephrine and the impact of L-NAME, indomethacin and SQ-29548 were similar to that determined under untreated conditions (Panel C). In contrast, pre-treatment of the cremaster muscle of OZR with TEMPOL (moderating the severity of the norepinephrine-induced constriction), shifted venular reactivity such that constrictor responses were increased following treatment with L-NAME, were unaffected by indomethacin, but were reduced following additional treatment with SQ-29548 (Panel D). Comparable to the responses to acetylcholine challenge, these relationships between norepinephrine-induced venular constriction (with or without pre-treatment with TEMPOL) and its basic contributors were similar in the collecting venules within *in situ* cremaster muscle of LZR and OZR (Figure 6, Panels A-D).

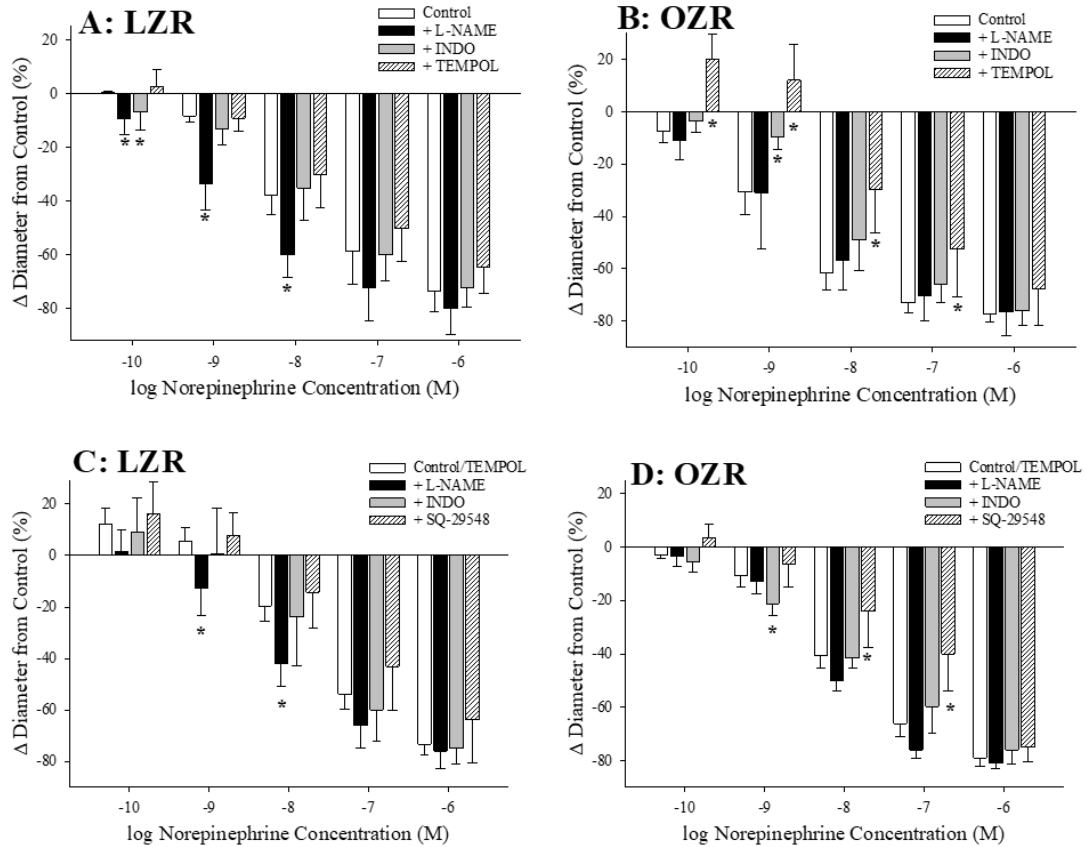


Figure 5. The constrictor reactivity of post-capillary venules within *in situ* cremaster muscle of LZR and OZR in response to increasing concentrations of norepinephrine (Panels A and B, respectively). Data are presented for venular reactivity under untreated control conditions, and following pre-treatment of the cremaster muscle with L-NAME, indomethacin (INDO) or TEMPOL. For Panels A and B, results represent n=6 observations from 12 animals in LZR; n=6 observations from 12 animals in OZR. Also presented are data describing the reactivity of post-capillary venules following pre-treatment with TEMPOL (Panels C and D, respectively), where the cremaster muscle was subsequently treated with L-NAME, indomethacin (INDO) or SQ-29548 to assess the contributions of nitric oxide, cyclooxygenase products or PGH₂/TxA₂ to reactivity. Data are presented as the mean (\pm SD) change in venular inner diameter, expressed as a percentage of the initial resting state ($\sim 25 \mu\text{m}$). * represents $p < 0.05$ versus responses from LZR at that agonist concentration. For Panels C and D, results represent n=6 observations from 12 animals in LZR; n=6 observations from 12 animals in OZR. All statistical analyses were done on the number of observations within the group, not the number of animals within the group. Please see text and Table 1 for details.

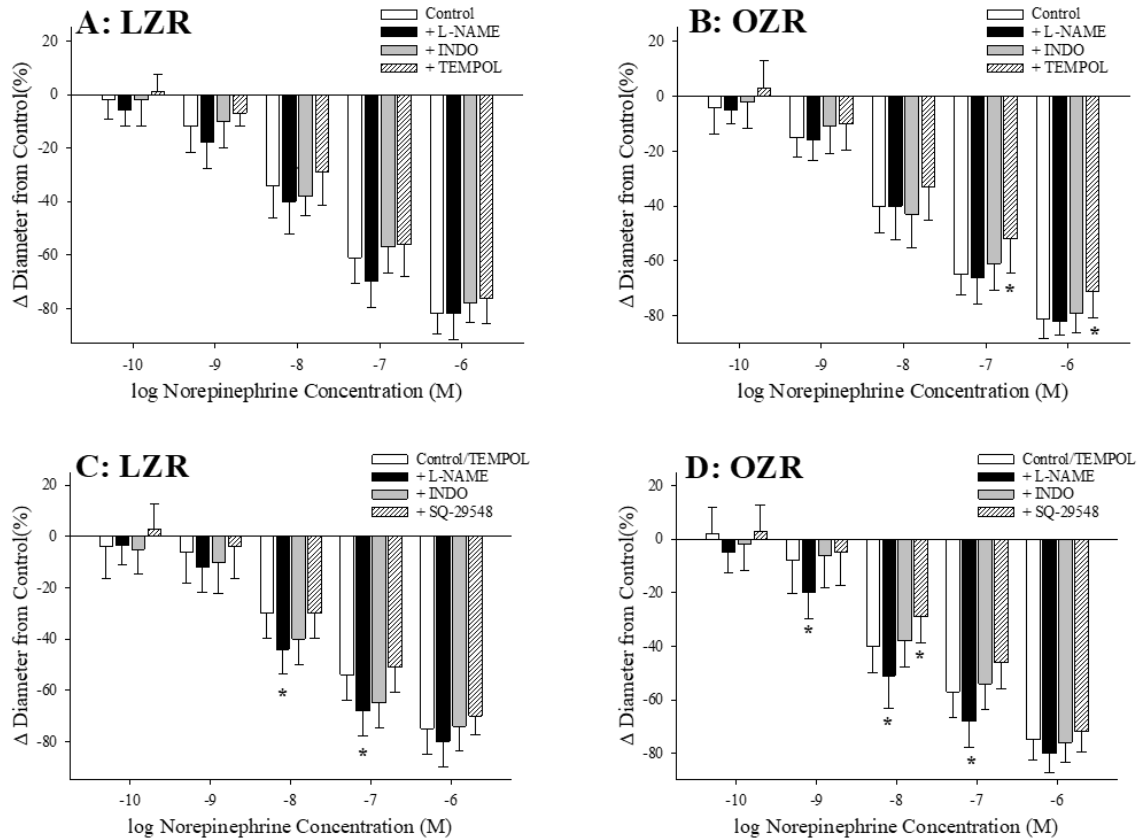


Figure 6. The constrictor reactivity of collecting venules within *in situ* cremaster muscle of LZR and OZR in response to increasing concentrations of norepinephrine (Panels A and B, respectively). Data are presented for venular reactivity under untreated control conditions, and following pre-treatment of the cremaster muscle with L-NAME, indomethacin (INDO) or TEMPOL. For Panels A and B, results represent n=6 observations from 12 animals in LZR; n=6 observations from 12 animals in OZR. Also presented are data describing the reactivity of collecting venules following pre-treatment with TEMPOL (Panels C and D, respectively), where the cremaster muscle was subsequently treated with L-NAME, indomethacin (INDO) or SQ-29548 to assess the contributions of nitric oxide, cyclooxygenase products or PGH₂/TxA₂ to reactivity. Data are presented as the mean (\pm SD) change in venular inner diameter, expressed as a percentage of the initial resting state ($\sim 70 \mu\text{m}$). * represents $p < 0.05$ versus responses from LZR at that agonist concentration. For Panels C and D, results represent n=6 observations from 12 animals in LZR; n=6 observations from 12 animals in OZR. All statistical analyses were done on the number of observations within the group, not the number of animals within the group. Please see text and Table 1 for details.

In response to field stimulation of the *in situ* cremaster muscle of LZR and OZR at increasing metabolic demand, the dilator and perfusion responses of post-capillary and collecting venules are summarized in Figure 7. In response to increasing metabolic demand, the dilator responses of post-capillary (Panel A) and collecting (Panel B) cremaster muscle venules was attenuated at the low (0.5 Hz) and moderate (1.0 Hz) contraction frequencies, but was similar at the high (2.0 Hz) contraction frequency. Perfusion responses followed a similar pattern, exhibiting a restrained hyperemic response at the lower two contraction frequencies in both post-capillary (Panel C) and collecting (Panel D) venules, that was not present at the high contraction frequency.

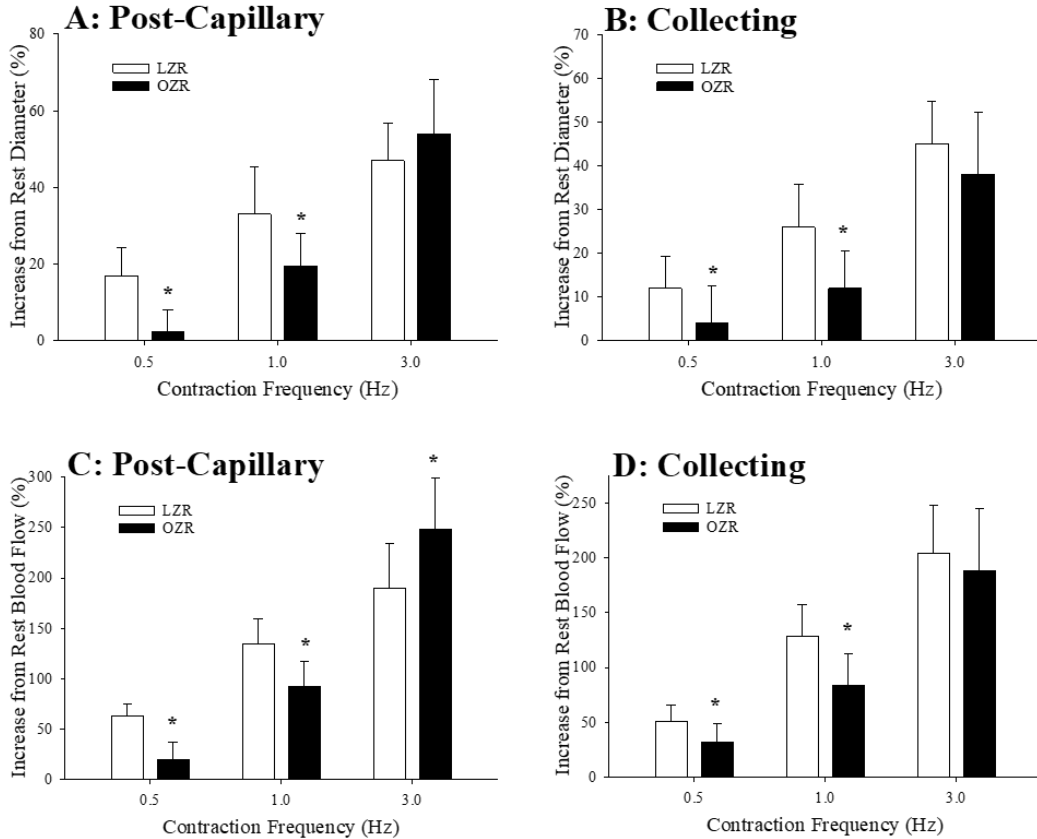


Figure 7. The responses of venules within *in situ* cremaster muscle of LZR and OZR in response to increasing metabolic demand, imposed via field stimulation across the muscle. Dilator responses to elevated metabolic demand are presented for post-capillary and collecting venules in Panels A and B, respectively; while functional hyperemic responses are presented in Panels C and D, respectively. Data (mean±SD) are presented for venular responses, expressed as a percentage of values at the initial resting state. * represents $p < 0.05$ versus responses from LZR at that stimulation frequency. Results represent $n=6$ observations from 6 animals in LZR; $n=8$ observations from 8 animals in OZR. All statistical analyses were done on the number of observations within the group, not the number of animals within the group. Please see text and Table 1 for details.

Pre-treatment of the cremaster muscle with TEMPOL moderated this difference in metabolism-induced venular dilation in the post-capillary venules of OZR, but had no significant effect on the dilator responses to muscle contraction in the larger collecting venules (Figure 8, Panels A and B). A similar impact was determined on blood flow responses, where hyperemia was improved in both venular diameter ranges, although responses in the larger venules failed to achieve statistical significance (Panels C and D). In contrast, pre-treatment of the cremaster muscle with phentolamine (α_1/α_2 adrenoreceptor blocker) had minimal impact on contraction-induced dilation or perfusion in post-capillary venules (Panels A and C), although both the dilator and hyperemic responses were improved in the larger collecting venules (Panels B and D).

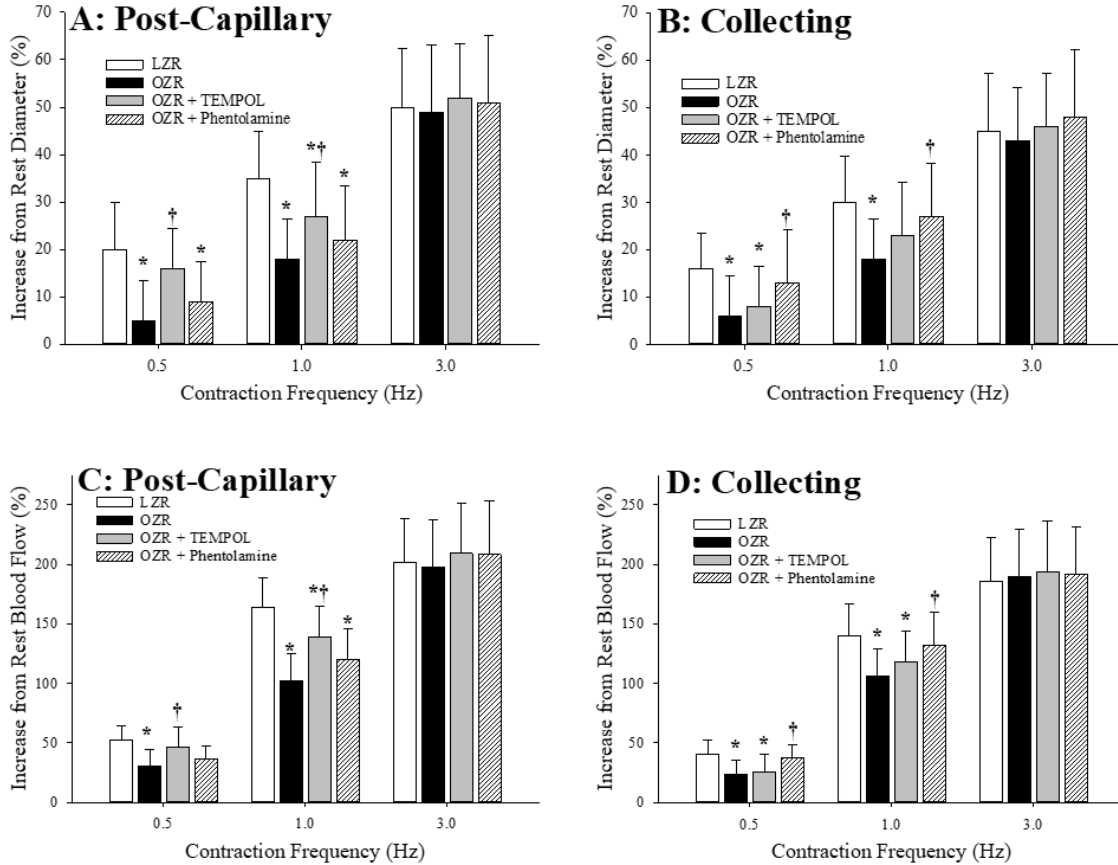


Figure 8. The responses of venules within *in situ* cremaster muscle of LZR and OZR in response to increasing metabolic demand, imposed via field stimulation across the muscle. Dilator responses to elevated metabolic demand are presented for post-capillary and collecting venules in Panels A and B, respectively; while functional hyperemic responses are presented in Panels C and D, respectively. Data (mean±SD) are presented under control conditions for each strain, and following pre-treatment of the cremaster muscle (from OZR only) with TEMPOL or phentolamine. All data are expressed as a percentage of values at the initial resting state. * represents $p < 0.05$ versus responses from LZR at that stimulation frequency. Results represent $n=6$ observations from 6 animals in LZR; $n=8$ observations from 8 animals in OZR. All statistical analyses were done on the number of observations within the group, not the number of animals within the group. Please see text and Table 1 for details.

The venous production of PGI_2 and TxA_2 in response to challenge with arachidonic acid is summarized in Figure 9. Venous PGI_2 production, estimated from the levels of 6-keto- $\text{PGF}_{1\alpha}$, was reduced in OZR as compared to levels in LZR under control conditions (Panel A). Pre-treatment of the pooled veins with TEMPOL had no effect on responses in LZR, but resulted in an increase in the production of PGI_2 in OZR. In contrast, venous production of TxA_2 , estimated from the levels of 11-dehydro- TxB_2 , was elevated in OZR vs. LZR under control conditions (Panel B), but was reduced toward levels determine in LZR following pre-treatment of veins with TEMPOL. Venous production of either PGI_2 or TxA_2 was abolished following treatment of the vessels with indomethacin.

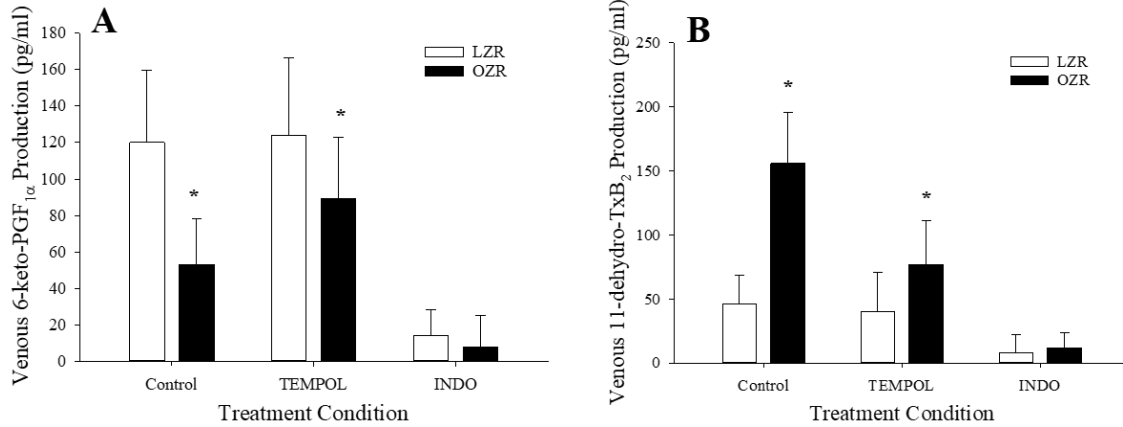


Figure 9. Venous production of 6-keto-PGF_{1α} (from PGI₂; Panel A) and 11-dehydro-TxB₂ (from TxA₂; Panel B) following challenge with arachidonic acid in pooled vessels from LZR and OZR. Data (mean±SD) are presented under control conditions for each strain, and following pre-treatment of the pooled vessels with either TEMPOL or indomethacin (INDO). * represents p<0.05 versus responses from LZR within the treatment group. Results represent n=6 observations from 6 animals in LZR; n=6 observations from 6 animals in OZR. All tissues for these *ex vivo* experiments were taken from animals within Experimental Groups 1 and 2. Please see text for details.

Data describing the adhesion and rolling of leukocytes in the post-capillary venules of the *in situ* extensor digitorum longus muscle of LZR and OZR are summarized in Figure 10. For both adhesion of leukocytes and rolling of adherent cells, responses were increased in the networks of OZR as compared to that for LZR.

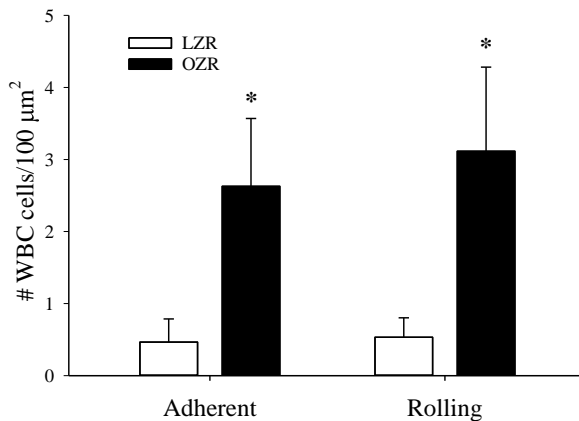


Figure 10. Data describing the adhesion and rolling of leukocytes in the post-capillary venules of *in situ* extensor digitorum longus muscle of LZR and OZR. Rhodamine 6G-labeled vascular cells were visualized by epi-illumination and the number of rolling and adherent leukocytes in venules was expressed as number of cells/are of endothelial surface, calculated from the diameter and length of the venular segment. * represents p<0.05 vs. LZR. Results represent n=5 observations from 5 animals in LZR; n=5 observations from 5 animals in OZR. Please see text for details.

Figure 11 presents data describing microvessel and post-capillary venular density within skeletal muscle of OZR and LZR. In both cases, microvascular and post-capillary venular density were significantly reduced in OZR as compared to levels in age-matched LZR.

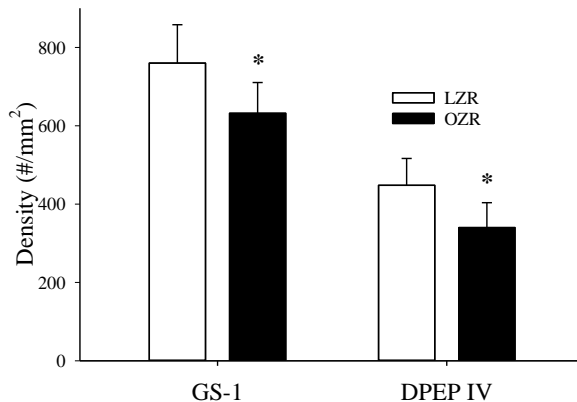


Figure 11. The change in skeletal muscle microvessel density in LZR and OZR. Results are presented following tissue staining with *Griffonia simplicifolia* 1 lectin (GS-1 lectin; for general microvessel density) or dipeptidylpeptidase IV (DPEP IV; for the post-capillary venular ends of capillaries). Data are presented as mean \pm SD, n=8 for both strains of rats. * represents p<0.05 vs. LZR. Results represent n=8 observations from 8 animals in LZR; n=8 observations from 8 animals in OZR. All tissues for these *ex vivo* experiments were taken from animals within Experimental Groups 1 and 2. Please see text for details.

2.5 Discussion

To date, studies elucidating the impact of the metabolic syndrome on vascular regulation have focused on arterial/arteriolar control. However, the arterial/arteriolar dysregulation observed in the metabolic syndrome are (at least partially) a result of a pro-oxidant, pro-inflammatory and pro-thrombotic environment, conditions which are known to also impact the venular/venous side of the circulation. In an effort to provide a foundation from which more targeted investigation can be directed, the present study investigated the impact of the metabolic syndrome on skeletal muscle venular function at two levels (post-capillary and collecting venules). Further, it was recently suggested that the pro-inflammatory and pro-oxidant conditions observed in post-capillary venules may be the initiating site for microvascular rarefaction that is commonly associated with chronic metabolic disease (Clough, 2015; Frisbee *et al.*, 2014; Gilbert, 2013) and that fluid handling across the

microcirculation may be altered by chronic impairments to glycemic control (Huxley and Scallan, 2011; Scallan *et al.*, 2015).

In the present study, impaired acetylcholine-induced venular dilation in OZR appeared to be a result of elevated oxidative stress on venular nitric oxide bioavailability, as treatment of the cremaster muscle with the antioxidant TEMPOL partially restored venular function to that determined in LZR. While this is consistent with data determined in multiple organs (Tune *et al.*, 2017) and across arterial/arteriolar levels (Goodwill and Frisbee, 2012), these data are critical for our understanding of both capillary handling of erythrocytes as well as fluid exchange across the microcirculation. Interestingly, there appears to be a role for an increased arachidonic acid-induced production of TxA₂ in the loss of normal endothelium-dependent dilator reactivity, which is likely associated with the chronic pro-inflammatory condition observed in OZR. While this increase in TxA₂ can have multiple effects, including impacting leukocyte adhesion (Morris *et al.*, 2009; Tole *et al.*, 2010; Totani *et al.*, 2012) and venular reactivity and responses, this also may represent a mechanism for modifying fluid filtration/absorption across the capillary networks under settings of chronic metabolic disease (Huxley and Scallan, 2011; Scallan *et al.*, 2015) as well as contributing to the genesis of the microvessel rarefaction discussed above (Frisbee *et al.*, 2014).

Similar to arteries and arterioles, the sympathetic nervous system is a major regulator of venous and venular tone, with sympathetic nerve fibers directly innervating α_1 and α_2 adrenoreceptors on vascular smooth muscle cells (Mellander and Lewis, 1963; Tabrizchi and Pang, 1992; van Brummelen *et al.*, 1986). However, in contrast to arterioles, increased sympathetic nerve activity to small veins and venules results in a reduction in vascular compliance, thus altering venous volume (capacitance) with comparatively less impact on systemic resistance (Rothe, 1983). Although outside of the scope of the present study, recent work has also demonstrated that a neuropeptide Y (NPY) -induced constriction of veins in humans suggest that, in addition to α_1 - and α_2 -adrenoreceptor mediated control, sympathetic activity can modify venous or venular tone through NPY Y1 receptor activation (Luu *et al.*, 1992; Pongor *et al.*, 2010).

The results from the present study suggest that venular reactivity to adrenergic stimuli was elevated in OZR vs. LZR, with this effect being predominantly mediated via the α_1 adrenoreceptor, but with an apparent role for the α_2 adrenoreceptor as well in the larger collecting venules. While there appeared to be a contribution to this effect mediated via the impaired endothelial function, it was not clear that these contributions, whether mediated via a loss of nitric oxide bioavailability or an increase in venular levels of TxA₂ were significant contributors to the altered tone regulation. However, it was clear this represented an alteration to adrenergic signaling itself, and not a broad-spectrum shift in venular constrictor reactivity at either the post-capillary or collecting venular level of the microcirculation.

The alterations to venular reactivity between LZR and OZR take on additional significance when evaluated in response to metabolic challenge. Increasing metabolic demand, instigated via electrical field stimulation of the cremaster muscle at increasing frequency (McKay *et al.*, 1998; Saito *et al.*, 1994), resulted in a functional dilator and hyperemic response in OZR that was restrained in comparison to that determined in LZR, with the exception of the highest frequency of stimulation (3 Hz; where responses between LZR and OZR venules were comparable).

Previous work by Hester's group has implicated the venular release of prostacyclin (PGI₂), as a contributing mechanism to the dilation of the adjacent arterioles that perfuse the capillary network under conditions of elevated metabolic demand in skeletal muscle (Hester and Hammer, 2002; McKay *et al.*, 1998; Saito *et al.*, 1994). Further, it has also been established that, under conditions of high oxidant stress and inflammation, the production of PGI₂ can be shifted to TxA₂ (Zou, 2007), and that there is an increased arterial (Butcher *et al.*, 2013; Goodwill *et al.*, 2008; Xiang *et al.*, 2006) and venous (above) production of TxA₂ in OZR manifesting the metabolic syndrome. Speculatively, it may be that the negative impact of vascular production of TxA₂ on muscle perfusion that has been demonstrated previously may partially be of venular origin, impacting not only its own reactivity, but also the caliber of adjacent resistance arterioles leading into the microcirculation and contributing to the loss in overall system flexibility and adaptive potential to imposed challenges (Frisbee *et al.*, 2016; Hester and Hammer, 2002). This speculation requires further investigation.

As has been well established, the venular circulation is a low pressure “collecting network” for the output of the high pressure “distribution network” of arteriolar perfusion through the capillaries. While the increased adrenergic reactivity and impaired endothelial function can serve to increase venular tone, the extent to which this shift in function acts to increase perfusion resistance across the microcirculation is unclear at this time and will require additional investigation. However, given the observation of an increased leukocyte adhesion to the venular endothelium, this physical blockade has been previously demonstrated to increase perfusion resistance within those regions (Harris *et al.*, 1994; Harris and Skalak, 1993; Lipowsky *et al.*, 1988) through the establishment of regions of “low radius” that are no longer functionally able to effectively regulate diameter. From the perspective of mass transport and exchange, the extent to which an increase in venular tone is sufficient to elevate resistance downstream from the capillaries is unclear. From a network perspective, it is reasonable to postulate that alterations in venular function may contribute to erythrocyte distribution heterogeneity and lowered microvascular hematocrit previously reported in OZR (Butcher *et al.*, 2014).

An obvious implication for the increase in venular resistance would also be an increase in the intravascular pressure within the venular environment, leading to an increased net fluid filtration into the tissue across the microcirculation. Recent study by Scallan et al. (2015) may provide insight into this outcome as the loss of nitric oxide bioavailability in the lymphatic vessels of diabetic mice (where vascular nitric oxide levels have also been established to be impaired) results in a release on the inhibition of phosphodiesterase 3 (PDE3), compromising lymphatic integrity and increasing tissue edema. It will be intriguing to determine if this fascinating observation on fluid handling across the microcirculation in diabetes represents multiple contributing pathways involving impaired venular function as well.

In summary, with the development of the metabolic syndrome, venular function within the skeletal muscle of OZR is impaired at both the post-capillary and collecting venular segments. Along with an impaired endothelium dependent dilation, and a modest increase in adrenergic constriction, the combination of a significant elevation in TxA₂ production may act to impair functional dilator and hyperemic responses at the venular level, and may contribute to the impaired function at the adjacent arteriolar level as well (Hester and Hammer,

2002). The implications of this shift in skeletal muscle venular function with the development of the metabolic syndrome on issues such as aggregate microvascular perfusion resistance, mass transport and exchange within with capillary networks, and fluid handling across the microcirculation are compelling avenues for future interrogation.

Additional Information: This study was supported by the American Heart Association (IRG 14330015, EIA 0740129N), the National Institutes of Health (RR 2865AR; P20 RR 016477, R01 DK64668, R01 DK67582), the Canadian Natural Sciences and Engineering Research Council (NSERC R4081A03, R4218A03). The authors declare no competing interests.

Author Contribution: Conception or design of the work (RWB, DG, DNJ, JCF); acquisition, analysis or interpretation of data for the work (KAL, ZF, RWB, CDS, DG, DNJ, JCF); drafting the work or revising it critically for important intellectual content (KAL, ZF, RWB, CDS, DG, DNJ, JCF). All authors have approved submission of the manuscript.

2.6 Literature Cited

1. American Heart Association Condition Pages:
https://www.heart.org/HEARTORG/Conditions/More/MetabolicSyndrome/Metabolic-Syndrome_UCM_002080_SubHomePage.jsp; accessed March 2, 2017.
2. Baker M & Wayland H (1974). On-line volume-flow rates and velocity profile measurements for blood in microvessels. *Microvasc Res* 7, 131-143.
3. Butcher JT, Stanley SC, Brooks SD, Chantler PD, Wu F & Frisbee JC (2014). Impact of increased intramuscular perfusion heterogeneity on skeletal muscle microvascular hematocrit in the metabolic syndrome. *Microcirculation* 21, 677-687.
4. Butcher JT, Goodwill AG, Stanley SC & Frisbee JC (2013). Blunted temporal activity of microvascular perfusion heterogeneity in metabolic syndrome: a new attractor for peripheral vascular disease? *Am J Physiol Heart Circ Physiol* 304, H547-H558.
5. Catella F, Healy D, Lawson JA & FitzGerald GA (1986). 11-Dehydrothromboxane B₂: a quantitative index of thromboxane A₂ formation in the human circulation. *Proc Natl Acad Sci USA*. 83, 5861-5865.
6. Clough GF (2015). Developmental conditioning of the vasculature. *Compr Physiol* 5, 397-438.
7. Davis MJ (1987). Determination of volumetric flow in capillary tubes using an optical Doppler velocimeter. *Microvasc Res* 34, 223-230.
8. Estado V, Nascimento A, Antunes B, Gomes F, Coelho L, Rangel R, Garzoni L, Daliry A, Bousquet P & Tibiriçá E (2017). Cerebral Microvascular Dysfunction and Inflammation Are Improved by Centrally Acting Antihypertensive Drugs in Metabolic Syndrome. *Metab Syndr Relat Disord* 15, 26-35.
9. Frisbee JC & Delp MD (2006). Vascular function in the metabolic syndrome and the effects on skeletal muscle perfusion: lessons from the obese Zucker rat. *Essays Biochem* 42, 145-161.
10. Frisbee JC, Goodwill AG, Frisbee SJ, Butcher JT, Brock RW, Olfert IM, DeVallance ER & Chantler PD (2014). Distinct temporal phases of microvascular rarefaction in skeletal muscle of obese Zucker rats. *Am J Physiol Heart Circ Physiol* 307, H1714-H1728.

11. Frisbee JC, Butcher JT, Frisbee SJ, Olfert IM, Chantler PD, Tabone LE, d'Audiffret AC, Shrader CD, Goodwill AG, Stapleton PA, Brooks SD, Brock RW & Lombard JH (2016). Increased peripheral vascular disease risk progressively constrains perfusion adaptability in the skeletal muscle microcirculation. *Am J Physiol Heart Circ Physiol* 310, H488-H504.
12. Gilbert RE (2013). Endothelial loss and repair in the vascular complications of diabetes: pathogenetic mechanisms and therapeutic implications. *Circ J* 77, 849-856.
13. Global Burden of Metabolic Risk Factors for Chronic Diseases Collaboration. Cardiovascular disease, chronic kidney disease, and diabetes mortality burden of cardiometabolic risk factors from 1980 to 2010: a comparative risk assessment (2014). *Lancet Diabetes Endocrinol* 2, 634-647.
14. Goodwill AG & Frisbee JC (2012). Oxidant stress and skeletal muscle microvasculopathy in the metabolic syndrome. *Vascul Pharmacol* 57, 150-159.
15. Goodwill AG, James ME & Frisbee JC (2008). Increased vascular thromboxane generation impairs dilation of skeletal muscle arterioles of obese Zucker rats with reduced oxygen tension. *Am J Physiol Heart Circ Physiol* 295, H1522-H1528.
16. Greene AS, Lombard JH, Cowley AW Jr & Hansen-Smith FM (1990). Microvessel changes in hypertension measured by Griffonia simplicifolia I lectin. *Hypertension* 15, 779-783.
17. Harris AG, Skalak TC & Hatchell DL (1994). Leukocyte-capillary plugging and network resistance are increased in skeletal muscle of rats with streptozotocin-induced hyperglycemia. *Int J Microcirc Clin Exp* 14, 159-166.
18. Harris AG & Skalak TC (1993). Effects of leukocyte activation on capillary hemodynamics in skeletal muscle. *Am J Physiol* 264, H909-H916.
19. Hester RL & Hammer LW (2002). Venular-arteriolar communication in the regulation of blood flow. *Am J Physiol Regul Integr Comp Physiol* 282, R1280-R1285.
20. Huxley VH & Scallan J (2011). Lymphatic fluid: exchange mechanisms and regulation. *J Physiol* 589, 2935-2943.

21. Iba T, Aihara K, Kawasaki S, Yanagawa Y, Niwa K & Ohsaka A (2012). Formation of the venous thrombus after venous occlusion in the experimental mouse model of metabolic syndrome. *Thromb Res* 129, e246-e250.
22. Lammert A, Hasenberg T, Kräupner C, Schnülle P & Hammes HP (2012). Improved arteriole-to-venule ratio of retinal vessels resulting from bariatric surgery. *Obesity (Silver Spring)* 20, 2262-2267.
23. Lemaster K, Jackson D, Goldman D & Frisbee JC (2017). Insidious incrementalism: The silent failure of the microcirculation with increasing peripheral vascular disease risk. *Microcirculation* 24, doi: 10.1111/micc.12332.
24. Lipowsky HH, House SD & Firrell JC (1988). Leukocyte endothelium adhesion and microvascular hemodynamics. *Adv Exp Med Biol* 242, 85-93.
25. Liu Y, Fredricks KT, Roman RJ & Lombard JH (1997). Response of resistance arteries to reduced PO₂ and vasodilators during hypertension and elevated salt intake. *Am J Physiol* 273, H869-H877.
26. Luu TN, Chester AH, O'Neil GS, Tadjkarimi S & Yacoub MH (1992). Effects of vasoactive neuropeptides on human saphenous vein. *Br Heart J* 67, 474-477.
27. Mameli C, Zuccotti GV, Carnovale C, Galli E, Nannini P, Cervia D & Perrotta C (2017). An update on the assessment and management of metabolic syndrome, a growing medical emergency in paediatric populations. *Pharmacol Res* 119, 99-117.
28. McKay MK, Gardner AL, Boyd D & Hester RL (1998). Influence of venular prostaglandin release on arteriolar diameter during functional hyperemia. *Hypertension* 31, 213-217.
29. Mellander S & Lewis DH (1963). Effect of hemorrhagic shock on the reactivity of resistance and capacitance vessels and on capillary filtration transfer in cat skeletal muscle. *Circ Res* 13, 105-118.
30. Morris T, Stables M, Hobbs A, de Souza P, Colville-Nash P, Warner T, Newson J, Bellingan G & Gilroy DW (2009). Effects of low-dose aspirin on acute inflammatory responses in humans. *J Immunol* 183, 2089-2096.
31. Mrázková O, Grim M & Carlson BM (1986). Enzymatic heterogeneity of the capillary bed of rat skeletal muscles. *Am J Anat* 177, 141-148.

32. Nies AS (1986). Prostaglandins and the control of the circulation. *Clin Pharmacol Ther* 39:481-488.
33. Pongor E, Ledó N, Altdorfer K, Lengyel G & Fehér E (2010). Distribution and possible origin of neuropeptide-containing nerve elements in the mammalian liver. *Acta Vet Hung* 58, 177-187.
34. Rothe CF (1983). Venous system: physiology of the capacitance vessels. In *The Cardiovascular System, Section 2, Vol III, Handbook of Physiology* pp. 394-452, American Physiological Society, Bethesda.
35. Saito Y, Eraslan A, Lockard V & Hester RL (1994). Role of venular endothelium in control of arteriolar diameter during functional hyperemia. *Am J Physiol* 267, H1227-H1231.
36. Scallan JP, Hill MA & Davis MJ (2015). Lymphatic vascular integrity is disrupted in type 2 diabetes due to impaired nitric oxide signaling. *Cardiovasc Res* 107, 89-97.
37. Shamseddeen H, Getty JZ, Hamdallah IN & Ali MR (2011). Epidemiology and economic impact of obesity and type 2 diabetes. *Surg Clin North Am.* 91, 1163-1172.
38. Singer G, Stokes KY, Terao S & Granger DN (2009). Sepsis-induced intestinal microvascular and inflammatory responses in obese mice. *Shock* 31, 275-279.
39. Tabrizchi R & Pang CC (1992). Effects of drugs on body venous tone, as reflected by mean circulatory filling pressure. *Cardiovasc Res* 26, 443-448.
40. Tole S, Durkan AM, Huang YW, Liu GY, Leung A, Jones LL, Taylor JA & Robinson LA (2010). Thromboxane prostanoid receptor stimulation induces shedding of the transmembrane chemokine CX3CL1 yet enhances CX3CL1-dependent leukocyte adhesion. *Am J Physiol Cell Physiol* 298, C1469-C1480.
41. Totani L, Dell'Elba G, Martelli N, Di Santo A, Piccoli A, Amore C & Evangelista V (2012). Prasugrel inhibits platelet-leukocyte interaction and reduces inflammatory markers in a model of endotoxic shock in the mouse. *Thromb Haemost* 107, 1130-1140.
42. Trasande L & Elbel B (2012). The economic burden placed on healthcare systems by childhood obesity. *Expert Rev Pharmacoecon Outcomes Res* 12, 39-45.

43. Tune JD, Goodwill AG, Sassoon DJ & Mather KJ (2017). Cardiovascular consequences of metabolic syndrome. *Transl Res* 183, 57-70.
44. Tyml K & Budreau CH (1991). A new preparation of rat extensor digitorum longus muscle for intravital investigation of the microcirculation. *Int J Microcirc Clin Exp* 10, 335-343.
45. van Brummelen P, Jie K. & van Zwieten PA (1986). Alpha-adrenergic receptors in human blood vessels. *Br J Clin Pharmacol* 21, 33S-39S.
46. Vassallo P, Driver SL & Stone NJ (2016). Metabolic syndrome: an evolving clinical construct. *Prog Cardiovasc Dis* 59, 172-177.
47. Wong TY, Duncan BB, Golden SH, Klein R, Couper DJ, Klein BE, Hubbard LD, Sharrett AR & Schmidt MI (2004). Associations between the metabolic syndrome and retinal microvascular signs: the Atherosclerosis Risk in Communities study. *Invest Ophthalmol Vis Sci* 45, 2949-2954.
48. Xiang L, Naik JS, Hodnett BL & Hester RL (2006). Altered arachidonic acid metabolism impairs functional vasodilation in metabolic syndrome. *Am J Physiol Regul Integr Comp Physiol* 290, R134-R138.
49. Zeintl H, Sack FU, Intaglietta M & Messmer K (1989). Computer assisted leukocyte adhesion measurement in intravital microscopy. *Int J Microcirc Clin Exp* 8, 293-302.
50. Zhao Y, Yang K, Wang F, Liang Y, Peng Y, Shen R, Wong T & Wang N (2012). Associations between metabolic syndrome and syndrome components and retinal microvascular signs in a rural Chinese population: the Handan Eye Study. *Graefes Arch Clin Exp Ophthalmol* 250, 1755-63.
51. Zou MH (2007). Peroxynitrite and protein tyrosine nitration of prostacyclin synthase. *Prostaglandins Other Lipid Mediat* 82, 119-127.

Chapter 3

3 Altered Distribution of Adrenergic Constrictor Responses Contributes to Skeletal Muscle Perfusion Abnormalities in Metabolic Syndrome

Kent Lemaster¹, Dwayne Jackson¹, Donald G. Welsh¹, Steven D. Brooks³,
Paul D. Chantler⁴, Jefferson C. Frisbee²

Department of Medical Biophysics¹, Department of Physiology and Pharmacology²,
Schulich School of Medicine and Dentistry, University of Western Ontario, London,
Ontario

Department of Physiology and Pharmacology³, Division of Exercise Physiology⁴, West
Virginia University Health Sciences Center, Morgantown, West Virginia

Running Head: Metabolic syndrome, adrenergic vascular responses and blood flow

Send Correspondence to:

Jefferson C. Frisbee, Ph.D.
Department of Medical Biophysics; MSB 407
Schulich School of Medicine and Dentistry
University of Western Ontario
London, ON, Canada N6A 5C1
Email: jfrisbee@uwo.ca
Phone: (519) 661-2111 x86552

3.1 Abstract

Purpose: Although studies suggest elevated adrenergic activity paralleling metabolic syndrome in obese Zucker rats (OZR), the moderate hypertension and modest impact on organ perfusion questions the multi-scale validity of these data. **Methods:** To understand how adrenergic function contributes to vascular reactivity in OZR, we utilized a multi-scale approach to investigate pressure responses, skeletal muscle blood flow and vascular reactivity following adrenergic challenge. **Results:** For OZR, adrenergic challenge resulted in increased pressor responses vs. lean Zucker rats (LZR); mediated via α_1 receptors, with minimal contribution by either ROS or NO bioavailability. *In situ* gastrocnemius muscle of OZR exhibited blunted functional hyperemia, partially restored with α_1 inhibition, although improved muscle performance and VO_2 required combined treatment with TEMPOL. Within OZR *in situ* cremaster muscle, proximal arterioles exhibited a more heterogeneous constriction to adrenergic challenge, biased toward hyperresponsiveness, vs. LZR. This increasingly heterogeneous pattern was mirrored in *ex vivo* arterioles, mediated via α_1 receptors, with roles for ROS and NO bioavailability evident in hyperresponsive vessels only. **Conclusions:** These results support the central role of the α_1 adrenoceptor for augmented pressor responses and elevations in vascular resistance but identify an increased heterogeneity of constrictor reactivity in OZR that is presently of unclear purpose.

List of Abbreviations

LZR: lean Zucker rat

OZR: obese Zucker rat

PRZ: prazosin

PHT: phentolamine

YOH: yohimbine

ROS: reactive oxygen species

NO: nitric oxide

PVD: peripheral vascular disease

TEMPOL: 4-hydroxy-2,2,6,6-tetramethylpiperidin-1 -oxyl

L-NAME: L-N^G-Nitroarginine methyl ester

PSS: physiological salt solution

VO₂: oxygen uptake

Q: muscle blood flow

C_aO₂: arterial oxygen content

C_vO₂: venous oxygen content

3.2 Introduction

As has been well established, the development of peripheral vascular disease (PVD) risk factors of sufficient severity can lead to profound alterations in the ability of resistance vessels to regulate their degree of tone, and thus the levels of perfusion to and within the tissues and organs they serve (17). Multiple previous studies across laboratories have implicated alterations to vascular nitric oxide (NO) bioavailability and effectiveness (3), altered arachidonic acid metabolism and the ensuing impacts on vascular tone (7, 15), the impacts of reactive oxygen species (ROS; 13, 19), myogenic activation (16, 23, 28) and alterations mediated via adrenergic signaling and vascular reactivity (1, 6, 21). However, it is unclear that conclusions from previous studies on the impact of altered adrenergic signaling/responses represent an accurate reflection of the true alterations to the integrated system of microvascular perfusion and control within the setting of elevated PVD risk.

The metabolic syndrome is a multi-pathology state represented by the combined presentation of multiple risk factors for PVD, including obesity, impaired glycemic control, atherogenic dyslipidemia, and moderate hypertension; with the additional systemic outcomes of a pro-oxidant, pro-inflammatory and pro-thrombotic state (4, 18). Arguably the most important outcome of this condition is that it results in the impairment of perfusion (both bulk perfusion and the spatial-temporal matching of perfusion with metabolic demand) in the tissues and organs of the afflicted subject (8, 12). Previous studies have provided compelling evidence that adrenergic traffic (5), adrenergic signaling (21) and adrenergic vascular responses (9) may all be elevated within the metabolic syndrome (the setting for elevated PVD risk). Further, it can clearly be demonstrated that treatment of the moderate hypertension within metabolic syndrome in the obese Zucker rat (OZR) model with prazosin (50 $\mu\text{g}/\text{kg}$) not only abolishes the elevated blood pressure that develops within this state, it can equalize blood pressure characteristics to those determined in the control strain, the lean Zucker rat (LZR, 27). However, what is unclear at this point is how a general elevation in vascular adrenergic output with the potential for multiple contributing elements, producing significant elevations in vascular resistance, functions within the *in vivo* setting to produce the relatively mild/moderate elevations in arterial

pressure that have been determined (9, 29). Clearly, we have not arrived at an accurate understanding of adrenergic control over muscle perfusion in the OZR model.

The purpose of the present study was to employ a multi-scale approach, integrating *in vivo*, *in situ*, and *ex vivo* conditions to garner a more accurate understanding of the changes in adrenergic control that are implicit for the development of skeletal muscle microvasculopathy within the metabolic syndrome. *In vivo* approaches will incorporate whole animal pressor responses with hindlimb blood flow measurements in anesthetized animals, while *in situ* approaches will employ perfusion/muscle performance relationships for gastrocnemius muscle and direct microscopic evaluation of vascular reactivity in cremaster muscle, and *ex vivo* approaches will employ studies of isolated vascular responses under specific challenged states. Taken together, these data will allow for a more accurate understanding of adrenergic function in the control of muscle blood flow in OZR will the full manifestation of the metabolic syndrome.

3.3 Materials and Methods

Animals: Male LZR (n=27) and OZR (n=45) were delivered at 6-7 weeks of age, and after one week of acclimation to the local environment, were aged to ~17 weeks for final experiment usage. All animals were used between 16 and 18 weeks of age. Animals were fed standard chow and tap water *ad libitum* for all experiments unless otherwise noted. Animals were housed in an accredited animal care facility, and all protocols received prior IACUC approval from the West Virginia University. At ~17 weeks of age, each rat was anesthetized with injections of sodium pentobarbital (50 mg•kg⁻¹ i.p.), and all rats received tracheal intubation to facilitate maintenance of a patent airway. In all rats a carotid artery and an external jugular vein were cannulated for determination of arterial pressure and for intravenous infusion of additional substances as necessary (e.g., anesthetic, heparin, etc.). In addition, an aliquot of mixed venous blood was drawn from the jugular vein cannula for a full profiling of metabolic and endocrine biomarkers (see below).

Experimental Series #1: *In Vivo* Whole Pressor Responses: Following the initial surgical preparation (above), the femoral artery was isolated midway between the femoral triangle and the knee and a perivascular blood flow probe was placed around the vessel (Transonic 0.7V)

which was held in place via a micromanipulator. After a period of equilibration, each animal was challenged with an intravenous infusion of the α_1/α_2 -adrenoreceptor agonist norepinephrine (10 $\mu\text{g}/\text{kg}$), with pressor responses and hindlimb blood flow continuously recorded. Subsequently, rats received a bolus intravenous infusion of the α_1 adrenoreceptor antagonist prazosin (1 mg/kg), the α_2 adrenoreceptor antagonist yohimbine (5 mg/kg), or the α_1/α_2 adrenoreceptor antagonist phentolamine (10 mg/kg), each followed by 30 minutes of equilibration, in order to remove different components of adrenergic tone from the system (n=5 for each antagonist; total n=15 for each strain). After a second norepinephrine challenge with the respective antagonist present, animals were treated with bolus intravenous infusions of TEMPOL (50 mg/kg) and a final subsequent treatment with L-NAME (100 mg/kg) to assess the roles of reactive oxygen species and nitric oxide bioavailability in contributing to responses following adrenergic challenge. After treatment with TEMPOL and again after the treatment with L-NAME, a new challenge with norepinephrine was performed as described above. Alterations in mean arterial pressure and femoral artery perfusion were monitored following agonist infusion in order to determine peak responses and the restoration of baseline (pre-treatment) conditions. All infused intravenous doses of drugs were corrected for differences in circulating blood volume between LZR and OZR at this age (10, 24).

Experimental Series #2: In Situ Skeletal Muscle Perfusion: In a separate cohort of LZR and OZR (n=5 for LZR; n=15 for OZR), the left gastrocnemius muscle was isolated *in situ* as fully described previously (9). Subsequently, a perivascular flow probe (Transonic 0.5V or 0.7V) was placed around the femoral artery, immediately proximal to its entry into the muscle group, in order to measure blood flow to the gastrocnemius muscle. At the conclusion of these procedures, an angiocatheter (24 gauge) was inserted into the femoral vein to allow for sampling of venous blood from the contracting muscle to determine blood gas levels (done using a Corning Rapid Lab Blood Gas Analyzer). The preparation was covered in PSS-soaked gauze and plastic film to minimize evaporative water loss and was placed under a heat lamp to maintain temperature at 37°C. At this time, heparin (500 IU/kg) was infused via the jugular vein to prevent blood coagulation.

Upon completion of the surgical preparation, the gastrocnemius muscle was stimulated to perform (via the sciatic nerve) bouts of isometric twitch contractions (4 Hz, 0.4

ms duration, 5V) lasting for 3 minutes followed by 15 minutes of self-perfused recovery time, with arterial pressure and femoral artery blood flow continuously monitored. Following the initial contraction regimen under control conditions, rats were given an intravenous injection of either prazosin (1 mg/kg; n=5), phentolamine (5 mg/kg; n=5) or yohimbine (5 mg/kg; n=5) and the contraction regimen was repeated. Each animal was treated with only one adrenoceptor antagonist. As above, following treatment of the animal with either adrenoceptor antagonist, animals were treated with TEMPOL and L-NAME as described above and the contraction regimen was repeated with all data and blood collection also repeated as described above.

Experiment Series #3: In Situ Skeletal Muscle Arterioles: In a dedicated cohort of rats (n=7 for LZR; n=15 for OZR), the left cremaster muscle was prepared for television microscopy (9). After completion of the preparation, the cremaster muscle was superfused with PSS, equilibrated with a gas mixture containing 5% CO₂ and 95% N₂, and maintained at 35°C as it flowed over the muscle. The ionic composition of the PSS was as follows (mM): NaCl 119.0, KCl 4.7, CaCl₂ 1.6, NaH₂PO₄ 1.18, MgSO₄ 1.17, and NaHCO₃ 24.0. Arteriolar diameter was determined with an on-screen video micrometer. After an initial post-surgical equilibration period of 30 minutes, proximal (~75 μm diameter) and distal arterioles (~30 μm diameter) were selected for investigation in a clearly visible region of the muscle. Arterioles chosen for study had walls that were clearly visible, a brisk flow velocity, and active tone, as indicated by the occurrence of significant dilation in response to topical application of 10⁻⁵ M adenosine. All arterioles that were studied were located in a region of the muscle that was away from any incision.

Following an equilibration period, the responses of selected arterioles within the cremaster muscle of LZR and OZR were assessed in response to increasing concentrations of norepinephrine (10⁻¹⁰ – 10⁻⁵ M) or phentolamine (10⁻¹⁰ – 10⁻⁵ M), as described above, to establish baseline reactivity to increasing adrenergic receptor activation and inhibition, respectively. As above, following washout, the cremaster muscle was treated with TEMPOL by adding it to the superfusate (10⁻⁴ M), and the challenge with increasing concentrations of norepinephrine and phentolamine was repeated. Finally, the TEMPOL-

treated cremaster muscle was also treated with L-NAME (10^{-4} M; in the superfusate) and challenge with the adrenergic agonist and antagonist was repeated.

Experiment Series #4: Ex Vivo Isolated Skeletal Muscle Resistance Arterioles: In anesthetized rats, prior to the preparation of the cremaster muscle (above), the intramuscular continuation of the right gracilis artery was identified, its *in vivo* diameter determined using an eyepiece micrometer, and the vessel was surgically removed. In LZR, arteriolar diameter estimated using this method was 105 ± 4 μm , while in OZR, the value was reduced to 98 ± 4 μm . Arterioles were placed in a heated chamber (37°C) that allowed the vessel lumen and exterior to be perfused and superfused, respectively, with physiological salt solution (PSS; equilibrated with 21% O_2 , 5% CO_2 ; 74% N_2) from separate reservoirs. Vessels were cannulated at both ends and were secured to inflow and outflow pipettes connected to a reservoir perfusion system allowing intraluminal pressure and luminal gas concentration to be controlled. Vessel diameter was measured using television microscopy and an on-screen video micrometer. Arterioles were extended to their *in situ* length and were equilibrated at $\sim 80\%$ of the animal's mean arterial pressure (~ 80 mmHg for LZR, ~ 100 mmHg for OZR). Active tone for vessels in the present study, calculated as $(\Delta D/D_{\text{max}}) \bullet 100$, where ΔD is the diameter increase from rest in response to Ca^{2+} -free PSS, and D_{max} is the maximum diameter measured at the equilibration pressure in Ca^{2+} -free PSS, averaged $33 \pm 3\%$ in LZR and $35 \pm 3\%$ in OZR. To get a more accurate presentation of the impact of altered adrenergic function on microvascular perfusion, we elected to reduce the inclusion criteria for isolated arterioles in this study. Traditionally, three criteria are employed to assess the viability of an individual vessel: 1) active tone $>25\%$, 2) robust constrictor response to challenge with phenylephrine, 3) viable endothelial layer (dilator response to pharmacological challenge such as methacholine). However, as one of the inclusion criteria represent the key outcome variable of the present study, this has the potential to cause experimental bias in terms of which vessels get included into experiments/analyses and which vessels are omitted for failing to achieve all three criteria. For the purposes of the present study, we omitted criterion #2 and simply considered vessels with sufficient active tone and viable endothelial function as having met the inclusion requirements.

Prior to subsequent evaluation of arteriolar reactivity, the *in vivo* diameter of vessels was restored through addition of low levels of norepinephrine to the vessel chamber. This process required $\sim 3 \times 10^{-10}$ M norepinephrine in vessels from OZR. While vessels from LZR usually regained their *in vivo* diameter without treatment with norepinephrine (n=12), some vessels required a maximum norepinephrine concentration of $\sim 1 \times 10^{-10}$ M (n=3). Following an equilibration period, arteriolar constriction was assessed in response to increasing concentrations of phenylephrine (10^{-10} M – 10^{-5} M) or clonidine (10^{-10} M – 10^{-5} M) to establish baseline reactivity to α_1 - and α_2 -adrenoreceptor agonists, respectively. Subsequently, reactivity of these isolated arterioles from LZR and OZR was assessed following treatment of the vessel with TEMPOL (10^{-4} M), and following incubation with L-NAME (10^{-4} M) to the TEMPOL-treated vessel.

Data and Statistical Analyses: In all cases, $p < 0.05$ was taken to reflect statistical significance. All data are presented as mean \pm SE.

In Vivo Pressor Response Experiments: All arterial pressure, hindlimb blood flow, and calculated hindlimb vascular resistance (pressure/flow) data are presented as the change in the parameter following treatment or challenge (Δ mmHg, Δ ml/g/min, Δ mmHg/(ml/g/min), respectively).

Vascular Reactivity Experiments: Arteriolar constrictor responses following challenge with adrenergic agonists or antagonists were fit with a three-parameter logistic equation:

$$y = \min + \left[\frac{\max - \min}{1 + 10^{\log ED_{50} - x}} \right]$$

where y represents the change in arteriolar diameter, “min” and “max” represent the lower and upper bounds, respectively, of the change in arteriolar diameter with increasing agonist concentration, x is the logarithm of the agonist concentration and $\log ED_{50}$ represents the logarithm of the agonist concentration (x) at which the response (y) is halfway between the lower and upper bounds. Statistically significant differences in lower bound employed ANOVA followed by Student-Newman-Keuls-test post-hoc as appropriate. Statistically

significant differences in the distribution of adrenergic responses between LZR and OZR utilized Student's t-test for mean and variance.

For the purposes of categorizing arteriolar responses to adrenergic challenge into "high", "normal", and "low" responders, the reactivity of all vessels (both OZR and LZR) was compared to mean responses in LZR. Given the degree of heterogeneity in the responses in OZR, a value of $\pm 20\%$ was used as the threshold for inclusion into the "high" or "low" responder categories.

In Situ Gastrocnemius Muscle Experiments: Muscle blood flow data were normalized to gastrocnemius muscle mass, which did not differ between LZR (2.29 ± 0.08 g) and OZR (2.25 ± 0.09 g). Muscle oxygen uptake (VO_2) was calculated using the Fick equation:

$$VO_2 = Q \times (CaO_2 - CvO_2)$$

where Q represents blood flow, CaO_2 represents arterial oxygen content and CvO_2 represents venous oxygen content. Muscle fatigue curves were fit using a semi-logarithmic relationship and the slope (β) coefficient was determined using curve fitting techniques. Differences in muscle blood flow, O_2 extraction, VO_2 and the slope coefficient describing muscle fatigue curves of contraction were determined using ANOVA, with Student-Newman-Keuls-test post-hoc as appropriate.

3.4 Results

As summarized in Table 1, ~17 week old OZR demonstrated the full complement of the metabolic syndrome. This included obesity, impaired glycemic control, dyslipidemia and moderate hypertension. In addition, OZR also demonstrated a high level of chronic oxidant stress and inflammation, with elevated levels of nitrotyrosine and TNF- α , respectively.

Table 1. Baseline characteristics of 17-week-old LZR and OZR used in the present study. * p<0.05 versus LZR.

| | LZR | OZR |
|---|------------|------------|
| Mass (g) | 358±11 | 679±12* |
| MAP (mmHg) | 98±4 | 129±6* |
| [Glucose] _{plasma} (mg/dl) | 105±9 | 164±11* |
| [Insulin] _{plasma} (ng/ml) | 1.4±0.2 | 7.6±1.0* |
| [Cholesterol] _{plasma} (mg/dl) | 84±7 | 132±11* |
| [Triglycerides] _{plasma} (mg/dl) | 91±10 | 361±20* |
| [Nitrotyrosine] _{plasma} (ng/ml) | 11±3 | 44±6* |

Table 2 presents the initial conditions for the vascular/systemic phenotypes across the conditions of the present study. In these data, blockade of the α_1 adrenergic system was effective in blunting the development of hypertension in OZR, as well as many of the vascular diameter and perfusion responses system. Further, the impact altering the vascular NO bioavailability in OZR in terms of contributing to integrated vascular function was relatively modest compared to the impact of alterations to adrenergic function.

Table 2. Baseline hemodynamic characteristics of 17 week-old LZR and OZR used in the present study under control conditions and in response to the different interventional treatments. AMP: mean arterial pressure (mmHg); Q_{FEM} : femoral artery blood flow (ml/g/min); R_{FEM} : resistance (mmHg/[ml/g/min]); (a-v) O_2 : oxygen extraction (ml/ml blood). * p<0.05 versus LZR value.; † p<0.05 vs. strain control.

| | | MAP | Q_{FEM} | R_{FEM} | (a-v) O_2 | | MAP | Q_{FEM} | R_{FEM} | (a-v) O_2 |
|-----|----------|-------|-----------|-----------|-------------|-----|--------|------------|-----------|-------------|
| LZR | Control | 98±4 | 0.77±0.06 | 127±8 | 0.037±0.005 | OZR | 131±4* | 0.60±0.06* | 218±15* | 0.037±0.005 |
| | +PRZ | 82±5† | 0.80±0.10 | 100±9† | 0.038±0.004 | | 91±5† | 0.70±0.07 | 137±11*† | 0.037±0.005 |
| | +PRZ/TEM | 82±6† | 0.82±0.07 | 98±8† | 0.038±0.004 | | 90±5† | 0.68±0.07* | 132±10*† | 0.038±0.004 |
| | +PRZ/LNM | 88±5 | 0.78±0.06 | 113±7 | 0.041±0.005 | | 95±5† | 0.62±0.05* | 153±12*† | 0.037±0.006 |
| | +YOH | 94±5 | 0.79±0.08 | 121±10 | 0.039±0.005 | | 124±4* | 0.64±0.06* | 194±13* | 0.038±0.005 |
| | +YOH/TEM | 92±4 | 0.78±0.07 | 118±9 | 0.039±0.005 | | 124±5* | 0.65±0.07* | 185±12*† | 0.039±0.006 |
| | +YOH/LNM | 98±5 | 0.75±0.06 | 131±9 | 0.039±0.006 | | 126±4* | 0.61±0.05* | 207±14* | 0.038±0.005 |
| | +PHT | 75±4† | 0.82±0.08 | 92±9† | 0.040±0.006 | | 92±5*† | 0.65±0.06* | 145±9*† | 0.038±0.005 |
| | +PHT/TEM | 76±4† | 0.82±0.06 | 93±6† | 0.039±0.005 | | 90±5† | 0.66±0.07* | 136±10*† | 0.040±0.006 |
| | +PHT/LNM | 85±5† | 0.75±0.07 | 113±6 | 0.038±0.006 | | 95±6† | 0.62±0.05* | 157±9*† | 0.037±0.005 |

Figures 1 and 2 summarize data describing the pressor responses (Panels A), hindlimb blood flow (Panels B) and perfusion resistance (Panels C) in OZR versus LZR under control conditions and following treatment with phentolamine (Figure 1) and prazosin or yohimbine (Figure 2). Any differences between LZR and OZR in terms of blood pressure and the pressor response to intravenous infusion of norepinephrine itself were abolished by treatment with either prazosin (the α_1 blocker) or phentolamine (the α_1/α_2 blocker), with minimal impact of yohimbine (the α_2 blocker). Treatment of OZR with TEMPOL (to blunt ROS and increase NO bioavailability) or TEMPOL/L-NAME (to remove NO bioavailability from a low ROS condition) had minimal impact on systemic responses to adrenergic challenges.

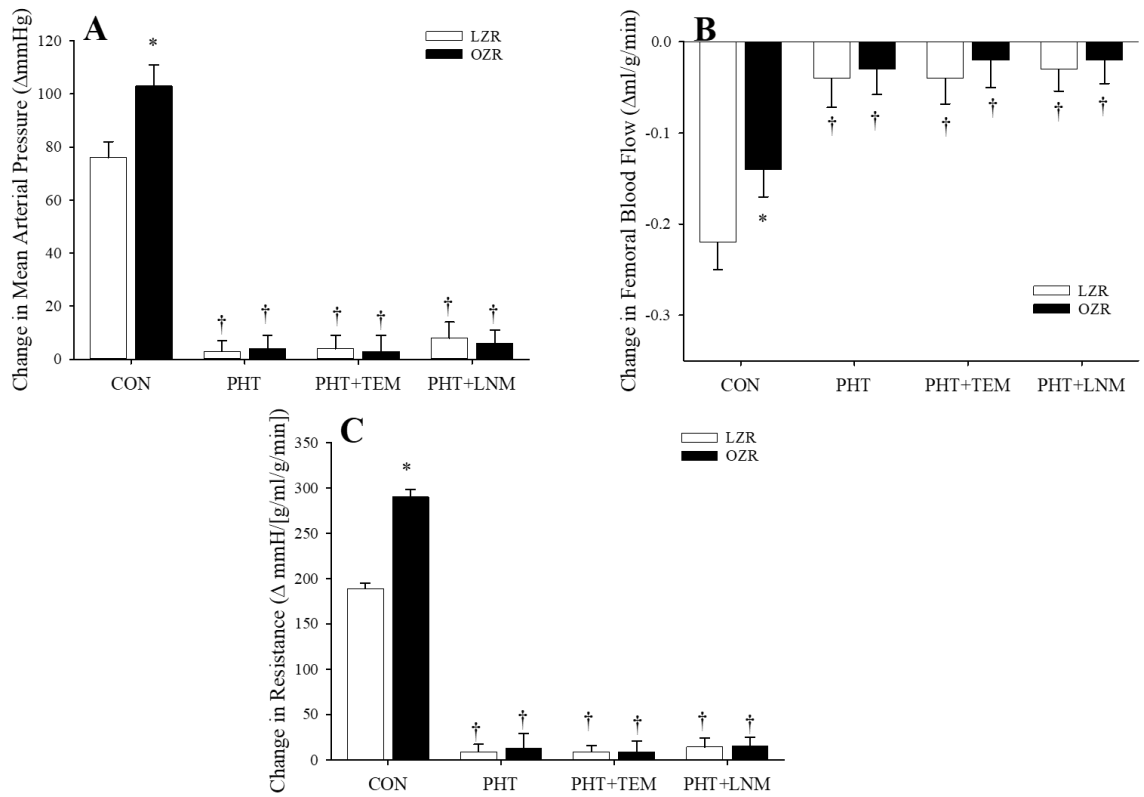


Figure 1. *In vivo* pressor responses (Panel A), *in situ* hindlimb blood flow (Panel B) and calculated vascular resistance across the hindlimb (Panel C) for LZR and OZR following intravenous infusion of 10 mg/kg norepinephrine. Data are presented as the change in the respective parameter from unstimulated, under control conditions and following pre-treatment with phentolamine (PHT), phentolamine+TEMPOL (PHT-TEM) or phentolamine+L-NAME (PHT-LNM). * p<0.05 vs. LZR in that condition; † p<0.05 vs. CON within that strain. Data are presented as mean±SE; n=5 for LZR; n=15 for OZR; please see text for details.

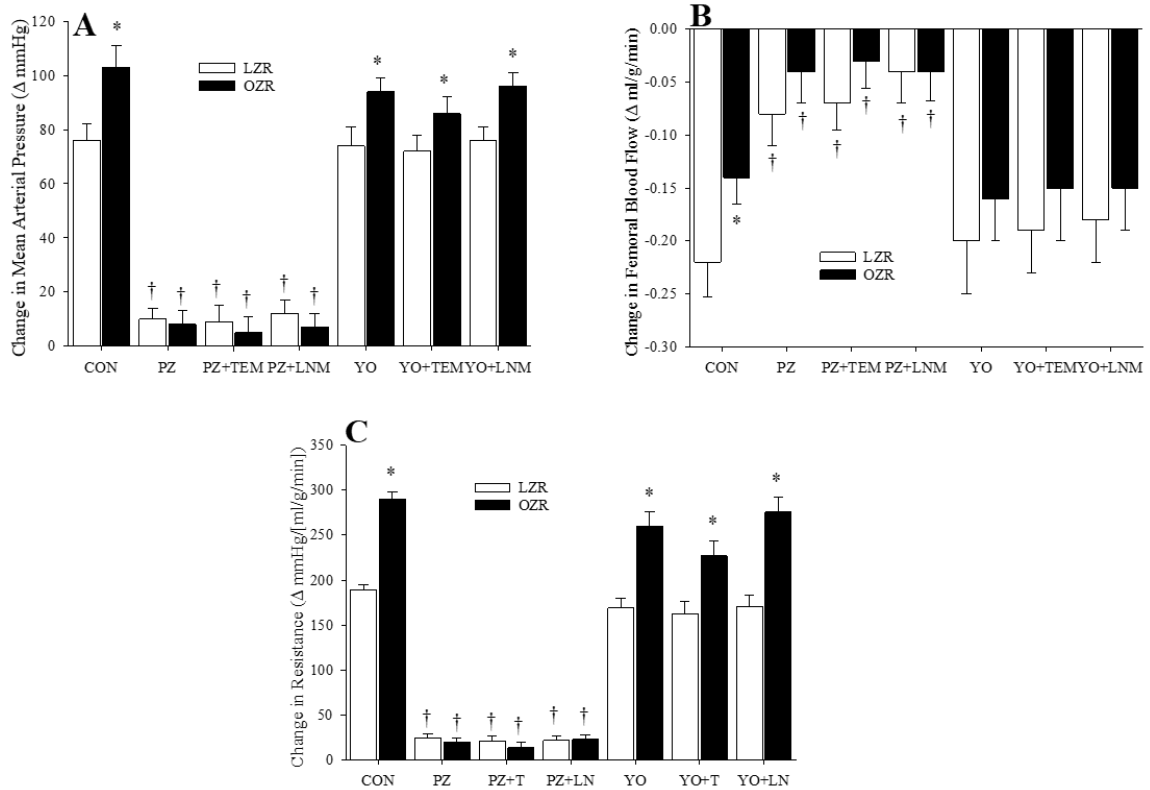


Figure 2. *In vivo* pressor responses (Panel A), *in situ* hindlimb blood flow (Panel B) and calculated vascular resistance across the hindlimb (Panel C) for LZR and OZR following intravenous infusion of 10 mg/kg norepinephrine. Data are presented as the change in the respective parameter from unstimulated, under control conditions and following pre-treatment with prazosin (PRZ), prazosin+TEMPOL (PRZ-TEM), prazosin+L-NAME (PRZ-LNM), yohimbine (YOH), yohimbine+TEMPOL (YOH-TEM) or yohimbine+L-NAME (YOH-LNM). * $p < 0.05$ vs. LZR in that condition; † $p < 0.05$ vs. CON within that strain. Data are presented as mean \pm SE; $n = 5$ for LZR; $n = 15$ for OZR; please see text for details.

Data describing the fatigue curves (Panel A), active hyperemia (Panel B), oxygen extraction (Panel C) and oxygen uptake (VO_2 ; Panel D) for *in situ* gastrocnemius muscle of LZR and OZR contracting at 4Hz (isometric twitch) under control conditions and following treatment with phentolamine are presented in Figure 3. Following three minutes of imposed elevations in metabolic demand, OZR demonstrated an increased development of muscle fatigue, co-incident with a blunted hyperemic response. While O_2 extraction was very similar between the two strains, the combination of extraction and reduced blood flow resulted in a significant reduction in VO_2 . Treatment of OZR with the combined α_1/α_2 adrenoceptor antagonist phentolamine improved hyperemic responses when given alone, with additional improvements to muscle performance and VO_2 when followed up with antioxidant (TEMPOL) treatment. Treatment of OZR with prazosin (Figure 4) mirrored the effect of phentolamine, with an improved hyperemic responses when given alone and improved

muscle performance and VO_2 when given with the antioxidant. Any beneficial impacts of TEMPOL in OZR were abolished by combined treatment with TEMPOL and L-NAME. Treatment of OZR with the α_2 -adrenoreceptor antagonist yohimbine had no consistent or significant effect from control values on muscle performance, hyperemic responses or blood gas exchange measurements (Figure 5).

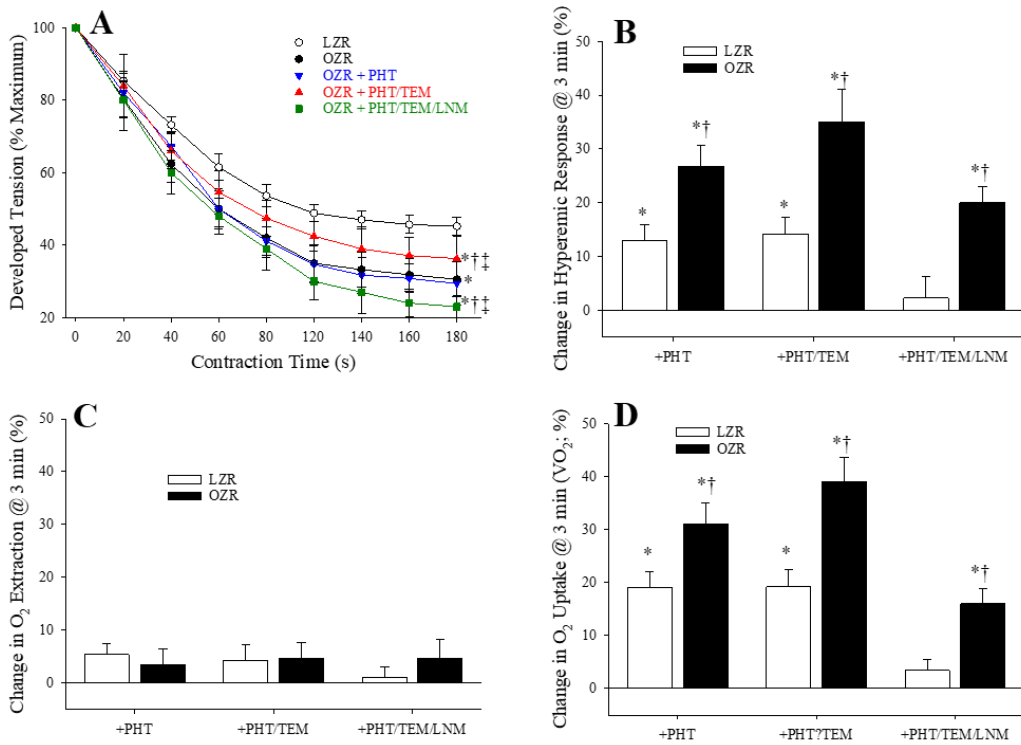


Figure 3. Data describing the performance (Panel A) and active hyperemic responses (Panel B) of *in situ* gastrocnemius muscle of LZR and OZR contracting at 4Hz (isometric twitch). Also presented are O₂ extraction (Panel C) and oxygen uptake (VO₂, Panel D) at three minutes of the contraction regimen. Data are presented under untreated control conditions and following pre-treatment with phentolamine (PHT), phentolamine+TEMPOL (PHT-TEM) or phentolamine+L-NAME (PHT-LNM). * p<0.05 vs. LZR; † p<0.05 vs. OZR; ‡ p<0.05 vs. OZR + PHT. Data are presented as mean±SE; n=5 for LZR; n=15 for OZR; please see text for details.

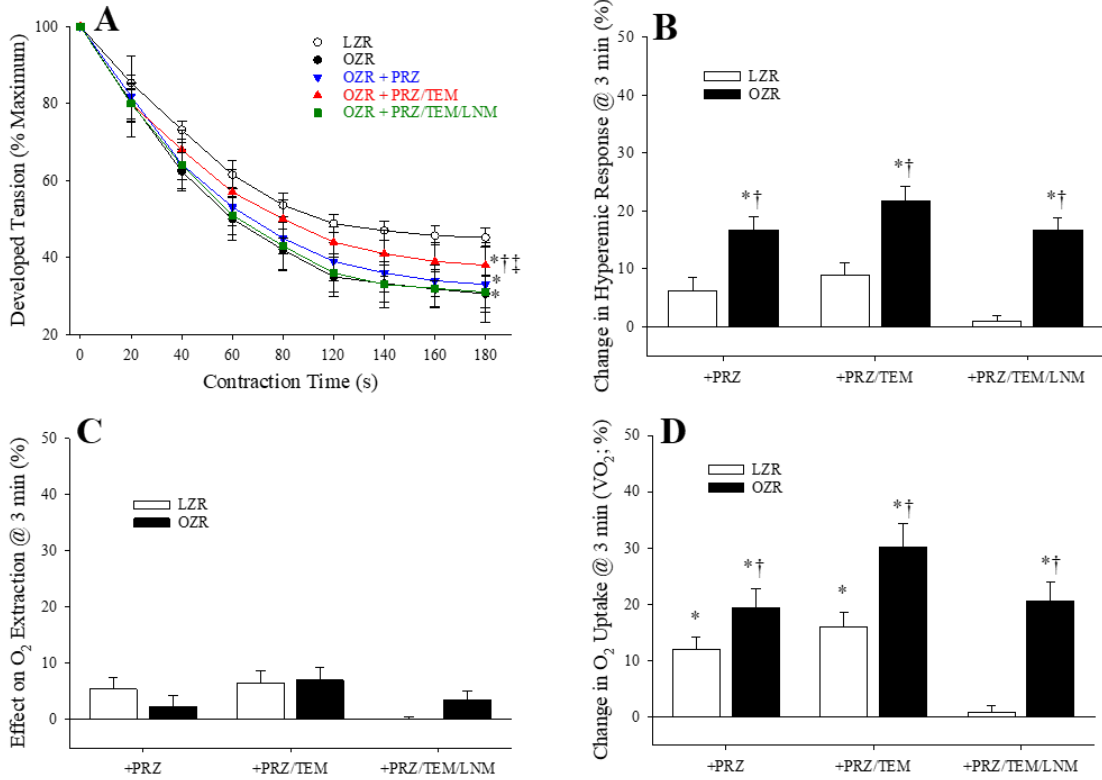


Figure 4. Data describing the performance (Panel A) and active hyperemic responses (Panel B) of *in situ* gastrocnemius muscle of LZR and OZR contracting at 4Hz (isometric twitch). Also presented are O₂ extraction (Panel C) and oxygen uptake (VO₂, Panel D) at three minutes of the contraction regimen. Data are presented under untreated control conditions and following pre-treatment with prazosin (PRZ), prazosin+TEMPOL (PRZ-TEM) or prazosin+L-NAME (PRZ-LNM). * p<0.05 vs. LZR in that condition; † p<0.05 vs. CON (100%) within that strain; ‡ p<0.05 vs. PRZ within that strain. Data are presented as mean±SE; n=5 for LZR; n=15 for OZR; please see text for details.

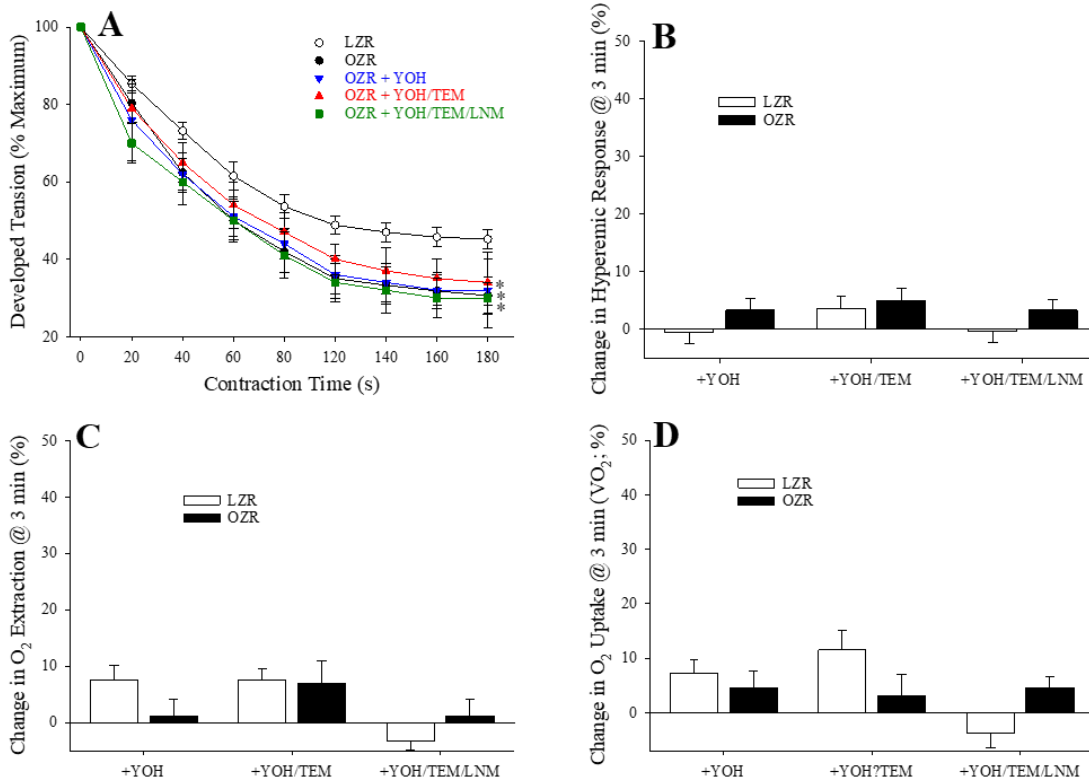


Figure 5. Data describing the performance (Panel A) and active hyperemic responses (Panel B) of *in situ* gastrocnemius muscle of LZR and OZR contracting at 4Hz (isometric twitch). Also presented are O₂ extraction (Panel C) and oxygen uptake (VO₂, Panel D) at three minutes of the contraction regimen. Data are presented under untreated control conditions and following pre-treatment with yohimbine (YOH), yohimbine+TEMPOL (YOH-TEM) or yohimbine+L-NAME (YOH-LNM). * p<0.05 vs. LZR in that condition. Data are presented as mean±SE; n=5 for LZR; n=15 for OZR; please see text for details.

Table 3 presents the baseline characteristics of *in situ* cremaster muscle proximal and distal arterioles from LZR and OZR for the experiments described in Figures 6-9. Figures 6 and 7 summarize data describing the responses of *in situ* cremaster muscle arterioles located proximally within the microvascular network to bi-directional manipulation of adrenergic stimulation. In response to increasing adrenergic stimulation (increased norepinephrine) proximal arterioles from both LZR and OZR exhibited robust constrictor responses (Figure 6). However, while arterioles from LZR exhibited a relatively consistent response, with 38/50 vessels constricting by at least 60% of their resting diameter with 10⁻⁶ M norepinephrine, there was a significant shift in the distribution of reactivity with the development of the metabolic syndrome in OZR as only 19/50 vessels demonstrated a comparable response, while 21/50 vessels exhibited a stronger degree of reactivity, with a significantly reduced ED₅₀ value, essentially closing off fully at lower concentrations of stimulation, and 10/50 vessels exhibited a significant reduction to constrictor responses, with an elevated ED₅₀. In both LZR and OZR,

treatment with either TEMPOL or L-NAME had minimal consistent impacts on adrenergic responses in either strain.

Table 3. Baseline vascular characteristics of 17 week-old LZR and OZR used in the present study under control conditions and in response to the different interventions. Data are presented for *in situ* cremaster muscle proximal (CPA) and distal arterioles (CDA) as well as *ex vivo* gracilis muscle resistance arterioles (GA). ID: internal diameter (resting; μm); MaxD: maximum diameter (μm) under 10^{-3}M adenosine + 10^{-3}M sodium nitroprusside (*in situ*) or Ca^{2+} -free conditions (*ex vivo*); AT: calculated active tone (%; please see text for detail). Despite multiple trends, no significant differences in the results below were determined.

| | | ID _{CPA} | MaxD _{CPA} | AT _{CPA} | ID _{CDA} | MaxD _{CDA} | AT _{CDA} | ID _{GA} | MaxD _{GA} | AT _{GA} |
|-----|---------|-------------------|---------------------|-------------------|-------------------|---------------------|-------------------|------------------|--------------------|------------------|
| LZR | Control | 76 \pm 4 | 118 \pm 4 | 36 \pm 5 | 34 \pm 4 | 58 \pm 5 | 41 \pm 5 | 121 \pm 3 | 186 \pm 5 | 35 \pm 4 |
| | +TEMPOL | 76 \pm 5 | ---- | 35 \pm 5 | 34 \pm 5 | ---- | 41 \pm 4 | ---- | ---- | ---- |
| | +L-NAME | 72 \pm 4 | ---- | 39 \pm 4 | 32 \pm 4 | ---- | 45 \pm 4 | ---- | ---- | ---- |
| OZR | Control | 73 \pm 4 | 110 \pm 5 | 34 \pm 4 | 31 \pm 4 | 53 \pm 5 | 42 \pm 5 | 116 \pm 4 | 175 \pm 6 | 34 \pm 5 |
| | +TEMPOL | 76 \pm 4 | ---- | 31 \pm 4 | 34 \pm 4 | ---- | 36 \pm 4 | 118 \pm 4 | ---- | 33 \pm 5 |
| | +L-NAME | 72 \pm 3 | ---- | 35 \pm 5 | 31 \pm 5 | ---- | 42 \pm 4 | 114 \pm 5 | ---- | 36 \pm 4 |

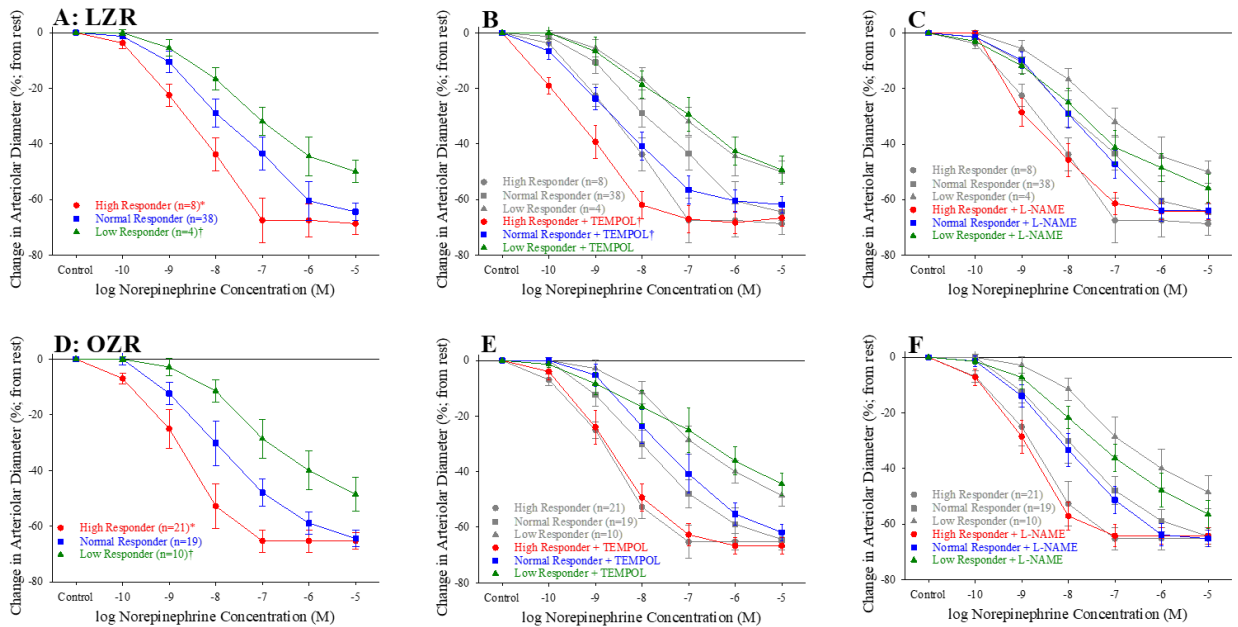


Figure 6. Constrictor responses from *in situ* cremaster muscle proximal arterioles from LZR (Panel A) and OZR (Panel D) in response to increasing concentrations of norepinephrine. In Panels A and D, different levels of reactivity are colored such that “high” responders are red, “low” responders are green and “normal” responders are blue. These colors are “greyed” in subsequent panels to facilitate comparisons. Panels B and E present the impact of TEMPOL on arteriolar constrictor responses in LZR and OZR, respectively. Panels C and F present the impact of L-NAME on arteriolar constrictor responses in LZR and OZR, respectively. * $p < 0.05$ vs. “normal” in that strain; † $p < 0.05$ vs. responses in untreated arterioles within that strain and reactivity category. Data are presented as mean \pm SE; $n=7$ for LZR; $n=15$ for OZR; please see text for details.

With increasing phentolamine treatment (Figure 7), used to simulate progressive removal of adrenergic tone to proximal arterioles of LZR and OZR, “normal” responders in both strains exhibited comparable dilation. However, arterioles in both strains that were identified as being “high” responders exhibited a very limited dilator response with increasing phentolamine concentration, while arterioles that were “low” responders to norepinephrine challenge demonstrated the greatest dilation in response to increasing concentration of phentolamine. In both strains, neither TEMPOL nor L-NAME treatment had a consistent and significant impact on the phentolamine-induced dilation in “normal” and “high” responders. However, in “low” responders of either strain, treatment of arterioles with L-NAME blunted dilator responses to phentolamine.

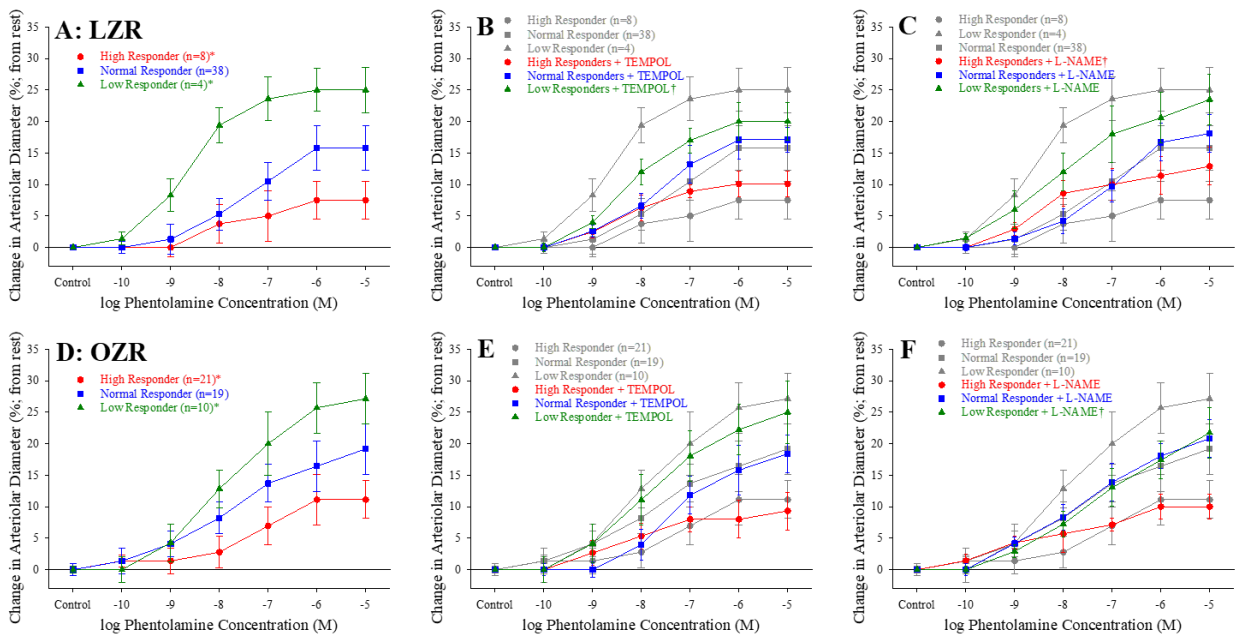


Figure 7. Dilator responses from *in situ* cremaster muscle proximal arterioles from LZR (Panel A) and OZR (Panel D) in response to increasing concentrations of phentolamine. In Panels A and D, different levels of reactivity are colored such that “high” responders are red, “low” responders are green and “normal” responders are blue (classification of responders was performed for Figure 8). These colors are “greyed” in subsequent panels to facilitate comparisons. Panels B and E present the impact of TEMPOL on arteriolar dilator responses in LZR and OZR, respectively. Panels C and F present the impact of L-NAME on arteriolar dilator responses in LZR and OZR, respectively. * $p < 0.05$ vs. “normal” in that strain; † $p < 0.05$ vs. responses in untreated arterioles within that strain and reactivity category. Data are presented as mean \pm SE; $n = 7$ for LZR; $n = 15$ for OZR; please see text for details.

Using the data presented above, Figure 8 presents the relationship between *in situ* proximal arteriolar constrictor responses to 10^{-8} M norepinephrine and the number of occurrences (out of a total $n = 50$ for each strain). These data clearly illustrate the changing distribution in constrictor responses to adrenergic challenge, where LZR exhibit a tighter

distribution of responses with lower variability than OZR, where proximal arteriolar responses to adrenergic challenge are more distributed, with a greater occurrence of constrictor responses at the “tails” of the distribution. Statistical analysis of the mean and variance between LZR and OZR demonstrated that the distributions of adrenergic responses were significantly different between the two strains.

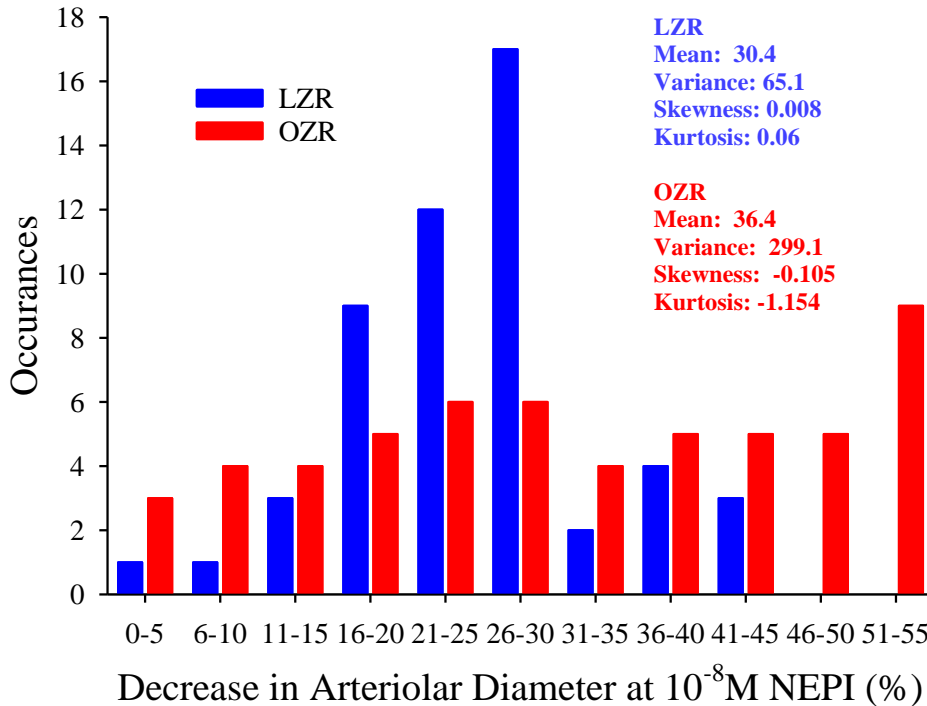


Figure 8. Distribution of constrictor responses of *in situ* cremaster muscle proximal arterioles to 10^{-8} M norepinephrine. Data are presented as the frequency of occurrence for a level of constrictor response (out of 50 occurrences) for arterioles from LZR and OZR; demonstrating the widening and flattening of the distribution in OZR as compared to that for LZR. The distribution for LZR passes the normality test ($p=0.834$), while that for OZR does not ($p=0.025$). As such, while the distributions for LZR and OZR are considered to be significantly different ($p=0.026$), they cannot both be classified as normal distributions.

Figure 9 presents the responses of distal *in situ* cremaster muscle arterioles of LZR and OZR to increasing concentrations of norepinephrine (Panels A and B) and phentolamine (Panels C and D), respectively. Under neither control conditions, nor pre-treatment conditions (TEMPOL or L-NAME) were responses of *in situ* distal arterioles significantly different between strains, nor was any evidence for an altered distribution of reactivity present (Panel E).

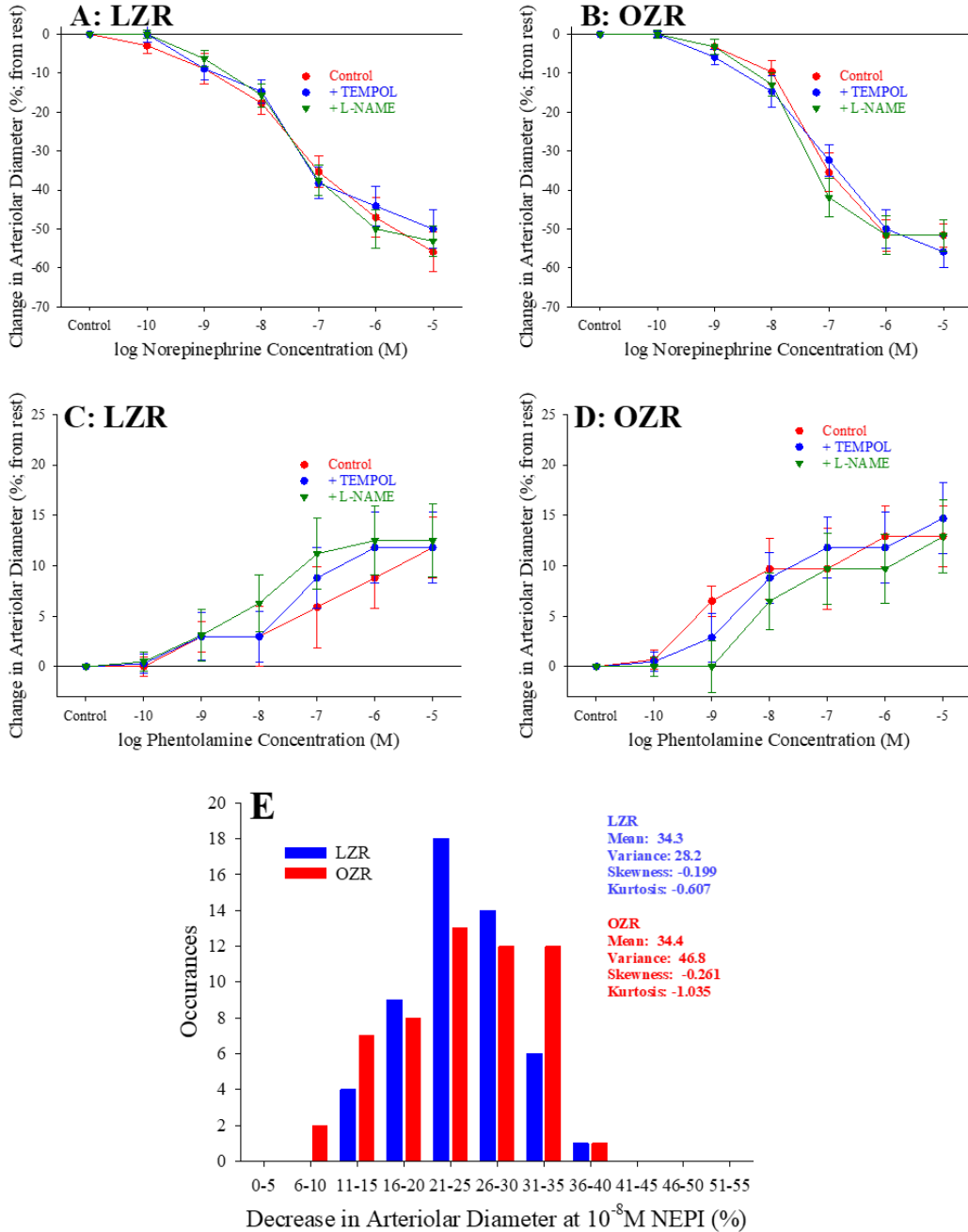


Figure 9. Mechanical responses from *in situ* cremaster muscle distal arterioles from LZR (Panel A) and OZR (Panel B) in response to increasing concentrations of norepinephrine (Panels A and B, respectively) or phentolamine (Panels C and D, respectively). Data are presented under untreated control conditions and following pre-treatment of the cremaster muscle with TEMPOL or L-NAME. Also presented is the distribution of constrictor responses of *in situ* cremaster muscle proximal arterioles to 10^{-8} M norepinephrine (Panel E). Data are presented as the frequency of occurrence for a level of constrictor response (out of 50 occurrences) for arterioles from LZR and OZR; demonstrating the lack of a difference between the distribution for LZR and OZR ($p=0.909$). Data are presented as mean \pm SE; $n=7$ for LZR; $n=15$ for OZR; please see text for details. Please see text for details.

Figure 10 presents the reactivity of *ex vivo* gracilis muscle first order resistance arterioles of LZR and OZR to increasing concentrations of the α_1 adrenoreceptor agonist phenylephrine (for data describing the baseline characteristics of *ex vivo* arterioles, please see Table 3). When the inclusion criteria of “sufficient adrenergic reactivity” was eliminated (please see above), a similar widening of constrictor responses to adrenergic challenge was determined in OZR as compared to LZR (Panel A). In “high” responders, the increased constrictor reactivity was significantly attenuated following treatment of the vessel with TEMPOL, while treatment with L-NAME was without effect (Panel B). This effect was less evident in “normal” (Panel C) and “low” (Panel D) responding arterioles from OZR, such that treatment with either TEMPOL or L-NAME resulted in minimal impact to phenylephrine-induced reactivity. Constrictor responses to increasing concentrations of the α_2 adrenoreceptor agonist clonidine did not exhibit a difference between LZR and OZR (Panel E), and this was not significantly impacted by treatment with TEMPOL or L-NAME.

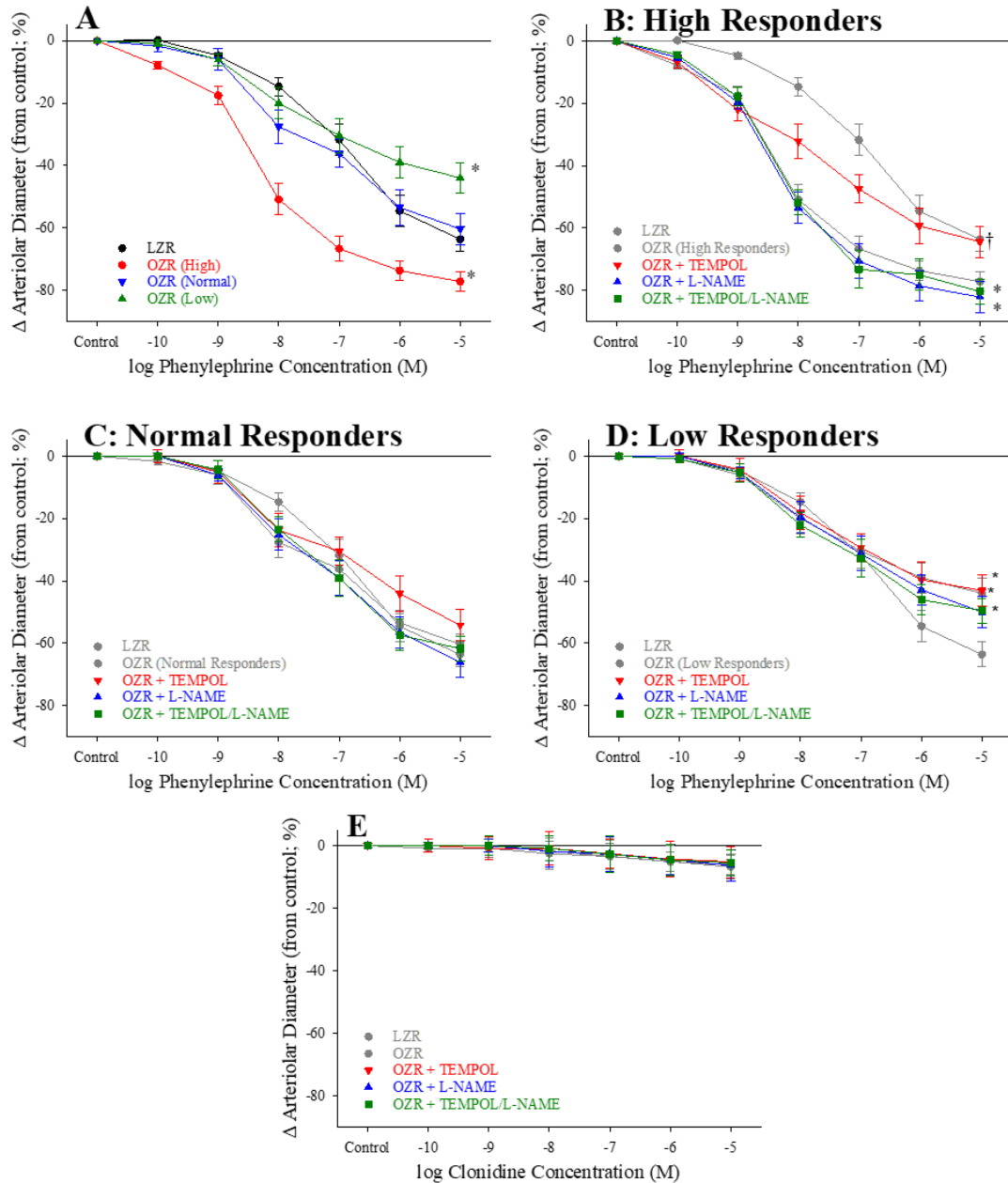


Figure 10. Constrictor responses from *ex vivo* gracilis muscle resistance arterioles from LZR and OZR in response to increasing concentrations of phenylephrine (α_1 agonist; Panels A-D) or clonidine (α_2 agonist; Panel E). Data for phenylephrine-induced constriction under control conditions are presented in Panel A, which also demonstrate the different classes of reactivity. These data are “greyed” in subsequent panels such that the impact of pre-treatment with TEMPOL, L-NAME or both are presented for vessels in the “high” (Panel B), “normal” (Panel C) and “low” responder (Panel D) categories. * $p < 0.05$ vs. “normal” in that strain; † $p < 0.05$ vs. responses in untreated arterioles within that strain and reactivity category. Data are presented as mean \pm SE; $n = 5$ for LZR; $n = 15$ for OZR; please see text for details.

3.5 Discussion

The underlying logic of the present study stemmed from a lack of clarity between the results of previous studies suggesting an increase in sympathetic activity (5), adrenergic constrictor reactivity (9, 11) and an increase in some elements of adrenergic intracellular signaling (21) in metabolic syndrome, despite the consistent observation that the development of both hypertension and any elevations in vascular resistance of adrenergic origin were relatively modest (4, 12, 16, 29). This suggests that a potential disconnect may exist between the interpretations from data collected at higher resolutions (e.g., *in situ* vascular networks, *ex vivo* resistance vessels), and responses determined under *in vivo* conditions. The present study was designed to address this discrepancy by identifying the source for this lack of clarity.

At the lowest level of spatial resolution, the *in vivo* preparation, OZR clearly exhibited an increased pressor response following adrenergic challenge as compared to responses determined in LZR, while use of adrenoreceptor antagonists demonstrated that this increased response was largely mediated via the α_1 receptors. While consistent with previous evidence (9, 11), results from the present study also provide insight into the role of vascular oxidant stress/nitric oxide bioavailability balance on the pressor response to adrenoreceptor stimulation. Despite the clearly established presence of elevated vascular oxidant stress in OZR, the current results suggest that the reduction in vascular ROS levels following TEMPOL treatment was without significant impact on the magnitude of the pressor response in OZR, nor did the subsequent L-NAME–based abolition of rescued nitric oxide bioavailability consistently impact the magnitude of the pressor responses between groups. Given the well-established relationships in question and the effectiveness of the treatment interventions in impacting ROS and NO levels, the most reasonable interpretation of these data is that, in comparison to the α_1 -mediated responses, a manipulation of vascular nitric oxide bioavailability was of insufficient significance to impact pressor responses at this level of resolution.

When taking these observations to the next higher level of resolution, the *in situ* skeletal muscle, a roughly comparable condition was evident to that for the *in vivo* setting. Specifically, the accelerated rate of muscle fatigue and blunted active hyperemia with 4Hz

twitch contraction in OZR vs. LZR were improved following α_1 receptor blockade (but only with concurrent antioxidant treatment); with no significant effect associated with α_2 receptor antagonism under any condition. This enhanced function was associated with the greatest improvements to VO_2 which also suggests that the combination of adrenoceptor antagonism and antioxidant therapy results in an overall improvement to the perfusion-based elements of mass transport and exchange beyond that for α_1 adrenoceptor antagonism alone. Further, the importance of “rescued” vascular nitric oxide bioavailability on contributing to skeletal muscle blood flow, especially during periods of elevated metabolic demand, was demonstrated following the application of L-NAME under TEMPOL-treated conditions.

These results also provide support for previous observations indicating that general blunting of adrenergic constriction can improve hyperemic responses in skeletal muscle in metabolic syndrome (8, 9, 11, 21), but are of limited effectiveness in terms of improving muscle performance unless treatments are combined with antioxidant agents to directly improve endothelial function (8). As antioxidant treatment alone was without impact on either bulk flow responses or muscle performance in the absence of α_1 adrenoceptor inhibition, these observations suggest that a conceptual division may be appropriate for the impact of the metabolic syndrome muscle performance outcomes. It may be that the modest reduction in skeletal muscle blood flow in OZR primarily reflects adrenergic constraint sufficient to hinder metabolic sympatholysis, while endothelial dysfunction (although ubiquitously present) is more important for the higher resolution matching of perfusion distribution to metabolic need within tissue.

Previous studies have suggested that there is a general increase in sympathetic traffic, intracellular signaling, and/or vascular constrictor responses to adrenergic challenge with the development of metabolic syndrome (5, 9, 21). However, as stated above, *in vivo* data do not strongly support this contention. Results from the *in situ* cremaster muscle of OZR as compared to responses in LZR may provide insight into this discrepancy, as constrictor responses of proximal resistance arterioles to increasing adrenergic stimulation exhibited a much more consistent response in LZR than in OZR, with a narrower distribution. In contrast, the responses to adrenergic challenge in OZR exhibited a larger spread in their magnitude with a greater proportion of vessels demonstrating both increased and decreased

responsiveness (although more commonly toward increased reactivity). Similarly, when treated with increasing concentrations of the α_1/α_2 adrenergic receptor antagonist phentolamine, arterioles that were classified as “high responders” exhibited the lowest degree of dilation, while the reverse was true for vessels that were “low responders”. Obviously, this somewhat skewed, but broader distribution of adrenergic constrictor responses, may contribute to the *in vivo* outcomes that have been identified in OZR, and may explain why they are more modest than would otherwise be predicted.

Based on the current data, some of this heterogeneity in reactivity may reflect variability in the initial conditions. Arterioles with increased tone under resting conditions will be unable to exhibit the full range of constriction in response to any stimulus as compared to levels from those of a greater initial diameter/reduced level of tone. Conversely, those with less tone (greater diameter) at rest have less ability to respond to the removal of adrenergic constriction as compared to those with a greater degree of tone. Given this, the greater heterogeneity of reactivity in the microcirculation of OZR vs. LZR may reflect the concept of the “optimal diameter” or “optimal wall tension” as originally described by Gore (14). In that work, the author determined that the greatest degree of reactivity was realized when vessels had the ability to constrict or dilate through a set range of optimal responsiveness and that moving the initial condition away from this range in either direction was associated with a severe decline in stimulus-induced reactivity. It may be that the more heterogeneous reactivity of proximal resistance arterioles from OZR in response to adrenergic challenge could partially reflect a loss of coordination through the sympathetic nerves that results in an increasingly heterogeneous initial “resting” condition which impacts adrenergic control over resistance at both the individual vessel and network levels. Recent work by Rachev and colleagues (22) has shed further light on this concept and provided compelling evidence of an optimal state of vascular mechanics that may result in the most efficient adaptability to changing conditions.

Interestingly, the increased variability in resistance arteriolar adrenergic reactivity in OZR following development of the metabolic syndrome in proximal arterioles, was not evident in distal arterioles. Using intravital microscopy, our group has shown that adrenergic vasoconstriction, in the rat gluteus maximus microcirculation, displays spatial-dependency.

In this work, we reported that the greatest α_{1R} and α_{2R} effects were noted in lower order (proximal) arterioles (i.e., 1A and 2A); whereas, sympathetically-mediated peptidergic and purinergic control dominated in higher order distal and terminal arterioles (2). Such spatial heterogeneity in sympathetic control provides a plausible explanation for the lack of adrenergic influences measured in distal microcirculation of OZR. Thus, future work addressing the contributions of NPY and ATP to microvascular regulation/dysregulation in the metabolic syndrome will likely reveal new mechanisms of sympathetic dysregulation in the distal microcirculation.

An important component of the present study was the removal of “robust adrenergic reactivity” as an inclusion criterion for the study of *ex vivo* resistance arterioles. When this was incorporated, a comparable pattern of divergence in adrenergic constrictor reactivity is present in the larger resistance arterioles of OZR vs. LZR to that for the proximal arterioles within the cremaster muscle. The increased variability in the adrenergic constrictor reactivity of *ex vivo* arterioles of OZR appears to reflect intrinsic vascular, and perhaps endothelial cell, function itself, as treatment of “high responders” with TEMPOL blunted the adrenergic responses, which was subsequently abolished following additional treatment with L-NAME. These effects were not observed in “normal” or “low” responders where the ability of TEMPOL and/or L-NAME to impact adrenergic constriction was severely attenuated. As a result of a relaxed inclusion criteria, the magnitude of the net increase in adrenergic constriction in large resistance arterioles of OZR was elevated as compared to LZR, but to a far less extent than previously estimated.

The results of the present study are important for several reasons. Foremost, these data provide evidence for the role of altered adrenoreceptor reactivity in the metabolic syndrome on integrated vascular function from a multi-scale perspective. Clearly, the increased pressor response to adrenergic challenge largely reflects activity mediated through the α_1 receptor and does not appear to be substantially impacted by treatment against elevated oxidant stress or a potential loss in vascular nitric oxide bioavailability. While responses from the hindlimb preparation suggested that hyperemic responses of OZR skeletal muscle can be improved by α_1 adrenoreceptor inhibition, additional antioxidant treatment of OZR was required to improve muscle performance, suggesting divergent roles for adrenergic constraint

on bulk flow and endothelial function for higher resolution perfusion:demand matching. Finally, results at the highest levels of spatial resolution, the *in situ* cremaster muscle and *ex vivo* microvessel revealed an increased diversity of vascular reactivity in OZR following adrenergic challenge. The immediate question from these results is why an increased diversity of adrenergic constrictor reactivity develops in OZR with progression of metabolic syndrome.

There does not appear to be evidence that a compensatory change in constrictor reactivity for the shifts in adrenergic responses develops in OZR, as there is no evidence that changes in myogenic activation between strains or within an individual animal that would match with increased adrenergic reactivity heterogeneity exists (i.e., vessels with low adrenergic reactivity having elevated myogenic responses, etc.). Additionally, there is no prior evidence to which the authors are aware that constrictor responses to other agents (e.g., endothelin, angiotensin II, serotonin) are significantly altered in OZR (27). However, there is evidence from some investigators that pressor reflexes may be blunted in OZR, although the mechanism underlying this and its generalizability for the model remain unclear (25). As such, one is left with speculation. Do vessels with “low” adrenergic constriction help the networks maintain an appropriate active hyperemic response, or at least largely maintain it? In an animal model that has been established as suffering from a profound loss of the microvascular network flexibility necessary to respond to imposed stressors (8), does the increased heterogeneity of adrenergic responses help to maintain system flexibility?

Perhaps even more importantly for clinical/population health outcomes, alterations in adrenergic tone and function have been previously implicated as contributing to the regulation of microvessel density, and chronic α_1 adrenoreceptor inhibition with prazosin is an established systemic model of angiogenesis (30). Of greatest relevance to the present study, may be recent work from the Haas group, where chronic prazosin treatment blunted the development of microvessel rarefaction in chronic corticosterone-treated rats (20). Given the presence of high cortisol/corticosterone levels in OZR, it may be that tissue regions containing resistance arterioles with elevated adrenergic reactivity may be associated with earlier or more severe levels of microvascular rarefaction (12). At this point, answers to the above questions are unknown. However, the challenge that the metabolic syndrome and PVD risk pose for public health outcomes (26), combined with the clear potential for improving microvascular

network function and perfusion with appropriate intervention, make this a compelling avenue for future investigation.

Acknowledgements

This study was supported by the American Heart Association (IRG 14330015, PRE 16850005, EIA 0740129N), and the National Institutes of Health (RR 2865AR; P20 RR 016477, R01 DK64668).

3.6 Literature Cited

1. Addison S, Stas S, Hayden MR, Sowers JR. Insulin resistance and blood pressure. *Curr Hypertens Rep.* 2008 Aug;10(4):319-25.
2. Al-Khazraji BK, Saleem A, Goldman D, Jackson DN. From one generation to the next: a comprehensive account of sympathetic receptor control in branching arteriolar trees. *J Physiol.* 2015 Jul 5;593(14):3093-108.
3. Allen JD, Giordano T, Kevil CG. Nitrite and nitric oxide metabolism in peripheral artery disease. *Nitric Oxide.* 2012 May 15;26(4):217-22.
4. Bonora E. The metabolic syndrome and cardiovascular disease. *Ann Med.* 2006;38(1):64-80.
5. Carlson SH, Shelton J, White CR, Wyss JM. Elevated sympathetic activity contributes to hypertension and salt sensitivity in diabetic obese Zucker rats. *Hypertension.* 2000 Jan;35(1 Pt 2):403-8.
6. Charkoudian N, Rabbitts JA. Sympathetic neural mechanisms in human cardiovascular health and disease. *Mayo Clin Proc.* 2009 Sep;84(9):822-30.
7. Coccheri S. Antiplatelet drugs--do we need new options? With a reappraisal of direct thromboxane inhibitors. *Drugs.* 2010 May 7;70(7):887-908.
8. Frisbee JC, Butcher JT, Frisbee SJ, Olfert IM, Chantler PD, Tabone LE, d'Audiffret AC, Shrader CD, Goodwill AG, Stapleton PA, Brooks SD, Brock RW, Lombard JH. Increased peripheral vascular disease risk progressively constrains perfusion adaptability in the skeletal muscle microcirculation. *Am J Physiol Heart Circ Physiol.* 2016 Feb 15;310(4):H488-504.

9. Frisbee JC. Enhanced arteriolar alpha-adrenergic constriction impairs dilator responses and skeletal muscle perfusion in obese Zucker rats. *J Appl Physiol* (1985). 2004 Aug;97(2):764-72.
10. Frisbee JC. Impaired hemorrhage tolerance in the obese Zucker rat model of metabolic syndrome. *J Appl Physiol* (1985). 2006 Feb;100(2):465-73.
11. Frisbee JC. Vascular adrenergic tone and structural narrowing constrain reactive hyperemia in skeletal muscle of obese Zucker rats. *Am J Physiol Heart Circ Physiol*. 2006 May;290(5):H2066-74.
12. Frisbee JC, Delp MD. Vascular function in the metabolic syndrome and the effects on skeletal muscle perfusion: lessons from the obese Zucker rat. *Essays Biochem*. 2006;42:145-61.
13. Gliemann L, Nyberg M, Hellsten Y. Nitric oxide and reactive oxygen species in limb vascular function: what is the effect of physical activity? *Free Radic Res*. 2014 Jan;48(1):71-83.
14. Gore RW. Wall stress: a determinant of regional differences in response of frog microvessels to norepinephrine. *Am J Physiol*. 1972 Jan;222(1):82-91.
15. Hackam DG, Eikelboom JW. Antithrombotic treatment for peripheral arterial disease. *Heart*. 2007 Mar;93(3):303-8.
16. Hodnett BL, Hester RL. Regulation of muscle blood flow in obesity. *Microcirculation*. 2007 Jun-Jul;14(4-5):273-88.
17. http://www.heart.org/HEARTORG/Conditions/HEARTORG/Conditions/VascularHealth/Vascular-Health_UCM_488109_SubHomePage.jsp
18. http://www.heart.org/HEARTORG/Conditions/More/MetabolicSyndrome/Metabolic-Syndrome_UCM_002080_SubHomePage.jsp
19. Lee MY, Griendling KK. Redox signaling, vascular function, and hypertension. *Antioxid Redox Signal*. 2008 Jun;10(6):1045-59.
20. Mandel ER, Dunford EC, Trifonova A, Abdifarkosh G, Teich T, Riddell MC, Haas TL. Prazosin Can Prevent Glucocorticoid Mediated Capillary Rarefaction. *PLoS One*. 2016 Nov 18;11(11):e0166899.

21. Naik JS, Xiang L, Hester RL. Enhanced role for RhoA-associated kinase in adrenergic-mediated vasoconstriction in gracilis arteries from obese Zucker rats. *Am J Physiol Regul Integr Comp Physiol*. 2006 Jan;290(1):R154-61.
22. Rachev A, Greenwald S, Shazly T. Are geometrical and structural variations along the length of the aorta governed by a principle of "optimal mechanical operation"? *J Biomech Eng*. 2013 Aug;135(8):81006.
23. Rossi M, Carpi A, Galetta F, Franzoni F, Santoro G. The investigation of skin blood flowmotion: a new approach to study the microcirculatory impairment in vascular diseases? *Biomed Pharmacother*. 2006 Sep;60(8):437-42.
24. Schreihofe AM, Hair CD, Stepp DW. Reduced plasma volume and mesenteric vascular reactivity in obese Zucker rats. *Am J Physiol Regul Integr Comp Physiol*. 2005 Jan;288(1):R253-61.
25. Schreihofe AM, Mandel DA, Mobley SC, Stepp DW. Impairment of sympathetic baroreceptor reflexes in obese Zucker rats. *Am J Physiol Heart Circ Physiol*. 2007 Oct;293(4):H2543-9.
26. Sperling LS, Mechanick JI, Neeland IJ, Herrick CJ, Després JP, Ndumele CE, Vijayaraghavan K, Handelsman Y, Puckrein GA, Araneta MR, Blum QK, Collins KK, Cook S, Dhurandhar NV, Dixon DL, Egan BM, Ferdinand DP, Herman LM, Hessen SE, Jacobson TA, Pate RR, Ratner RE, Brinton EA, Forker AD, Ritzenthaler LL, Grundy SM. The CardioMetabolic Health Alliance: Working Toward a New Care Model for the Metabolic Syndrome. *J Am Coll Cardiol*. 2015 Sep 1;66(9):1050-67.
27. Stepp DW, Frisbee JC. Augmented adrenergic vasoconstriction in hypertensive diabetic obese Zucker rats. *Am J Physiol Heart Circ Physiol*. 2002 Mar;282(3):H816-20.
28. Tano JY, Schleifenbaum J, Gollasch M. Perivascular adipose tissue, potassium channels, and vascular dysfunction. *Arterioscler Thromb Vasc Biol*. 2014 Sep;34(9):1827-30.
29. Tofovic SP, Jackson EK. Rat models of the metabolic syndrome. *Methods Mol Med*. 2003;86:29-46.

30. Zhou A, Egginton S, Hudlická O, Brown MD. Internal division of capillaries in rat skeletal muscle in response to chronic vasodilator treatment with alpha1-antagonist prazosin. *Cell Tissue Res.* 1998 Aug;293(2):293-303.

Chapter 4

4 Chronic Atorvastatin and Exercise can Partially Reverse Established Skeletal Muscle Microvasculopathy in Metabolic Syndrome

Kent A. Lemaster¹, Stephanie J. Frisbee², Luc Dubois³, Nikolaos Tzemos⁴, Fan Wu⁵,
Matthew T. Lewis⁶, Robert W. Wiseman⁶ and Jefferson C. Frisbee¹

Departments of Medical Biophysics¹, Pathology and Laboratory Medicine², Divisions of
Vascular Surgery³ and Cardiology⁴, University of Western Ontario, London, Ontario
DMPK, Nonclinical Development, Celgene Corporation, Summit, New Jersey⁵
Department of Physiology, Michigan State University, East Lansing, Michigan⁶

Running Head: Reversal of microvascular dysfunction

Send Correspondence to:

Jefferson C. Frisbee, Ph.D.
Department of Medical Biophysics; MSB 407
Schulich School of Medicine & Dentistry
University of Western Ontario
London, Ontario, Canada, N6A 5C1
Phone: (519) 661-2111 x8552
Email: jfrisbee@uwo.ca

4.1 Abstract

It has been long known that chronic metabolic disease is associated with a parallel increase in the risk for developing peripheral vascular disease. Although more clinically relevant, our understanding about reversing established vasculopathy is limited in comparison to our understanding of the mechanisms and development of impaired vascular structure/function under these conditions. Using the 13-week old obese Zucker rat (OZR) model of the metabolic syndrome, where microvascular dysfunction is sufficiently established to contribute to impaired skeletal muscle function, we imposed a 7-week intervention of chronic atorvastatin (ATOR) treatment, chronic treadmill exercise (EXER), or both. By 20 weeks of age, untreated OZR manifested a diverse vasculopathy that was a central contributor to poor muscle performance, perfusion and impaired O₂ exchange. ATOR or EXER, with the combination being most effective, improved skeletal muscle vascular metabolite profiles (i.e., nitric oxide, PGI₂ and TxA₂ bioavailability), reactivity and perfusion distribution at both individual bifurcations and within the entire microvascular network versus responses in untreated OZR. However, improvements to microvascular structure (i.e., wall mechanics and microvascular density) were less robust. The combination of the above improvements to vascular function with interventions resulted in an improved muscle performance and O₂ transport and exchange versus untreated OZR, especially at moderate metabolic rates (3Hz twitch contraction). These results suggest that specific interventions can improve specific indices of function from established vasculopathy, but this process was either incomplete after 7 weeks duration or that measures of vascular structure are either resistant to reversal or require better targeted interventions.

Key Words: vascular dysfunction, rodent models of the metabolic syndrome, regulation of blood flow, peripheral vascular disease, microvascular dysfunction, reversing vascular disease

New and Noteworthy

We used atorvastatin and/or chronic exercise to reverse established microvasculopathy in skeletal muscle of rats with metabolic syndrome. With established vasculopathy, atorvastatin or exercise had moderate abilities to reverse dysfunction, combined application of both was more effective at restoring function. However, increased vascular wall stiffness and reduced microvessel density were more resistant to reversal.

List of Abbreviations

ANOVA: analysis of variance
AT: active tone
ATOR: atorvastatin
C_aO₂: arterial oxygen content
C_vO₂: venous oxygen content
EIA: enzyme immune assay
EXER: exercise
GS-1: *Griffonia simplicifolia*-1 lectin
ID: internal diameter
IL-10: interleukin 10
IL-1 β : interleukin 1 beta
IL-6: interleukin 6
L-NAME: L-N^G-Nitroarginine methyl ester
LZR: lean Zucker rat
MAP: mean arterial pressure
MCP-1: monocyte chemoattractant protein-1
MTT: maximal twitch tension
MVD: microvessel density
NO: nitric oxide
OZR: obese Zucker rat
PSS: physiological salt solution
PVD: peripheral vascular disease
Q: muscle blood flow
ROS: reactive oxygen species
TEMPOL: 4-hydroxy-2,2,6,6-tetramethylpiperidin-1 -oxyl
TNF- α : tumor necrosis factor-alpha
TxA₂: thromboxane A₂
VO₂: oxygen uptake
WT: wall thickness

4.2 Introduction

One of the major contributors to the functional or clinical manifestations of peripheral vascular disease is the progressive loss of microvessel and microvascular network structure and function which is tightly coupled to developing metabolic disease in afflicted animals (9, 15) or humans (20, 25). This compromised function within the microcirculation can take multiple forms, including impairments to arteriolar reactivity, mechanical changes to the microvessel wall, and a progressive lowering of microvessel density (rarefaction) within the skeletal muscle (14, 26). Taken together, these impede effective mass transport and exchange, and the regulation of blood flow to, and perfusion within, skeletal muscle (9, 23). In addition, while the functional impact of these impairments may be modest under resting or low-metabolic demand conditions, their cumulative impact becomes more severe as muscle activity increases (6, 13, 28). Given the insidious nature of the development of peripheral vascular diseases (PVD), and the very real clinical challenge of reversing the development of established vasculopathy in affected patients (rather than blunting its subsequent development from an otherwise “healthy” condition), investigation into if/how a compromised microvascular network can be restored to a more normal level of structure and integrated function represents an important area of investigation. Arterial reconstructive surgery for symptomatic PVD can restore macrovascular perfusion but its effects on microvascular dysfunction are unclear. Persistent microvascular dysfunction following successful macrovascular reperfusion may explain why arterial reconstruction does not always lead to wound healing or amelioration of symptoms in patients with PVD (12)

Previous studies in our laboratory (13, 14) and from others (9, 31-34) have clearly established that the loss of normal microvascular structure and function parallels the development of metabolic disease. Of particular relevance to the present study, we have recently demonstrated that rarefaction in the skeletal muscle of the obese Zucker rat (OZR) appears to develop in stages, where an early reduction of microvessel density is well predicted by an oxidant stress- and inflammation-dependent shift in arachidonic acid metabolism toward increasing levels of thromboxane A₂ (TxA₂), with a later stage of rarefaction that is associated with a loss in vascular nitric oxide bioavailability (14).

However, any interventions that have been employed to improve these vascular outcomes have been relevant for blunting the severity of the vasculopathy that ultimately develops, rather than reversing an established compromised condition once it has already developed (16, 18).

The OZR (*fa/fa*) represents a model of the metabolic syndrome that is fundamentally grounded in a mutation in the leptin receptor leading to severe leptin resistance, chronic hyperphagia and the ensuing development of severe obesity (2, 11). Tracking with the severe obesity is a steadily worsening glycemic control, a progressive dyslipidemia and a moderate hypertension, with the additional co-morbidities of a growing pro-oxidant, pro-inflammation, and pro-thrombotic state (22). OZR exhibit high translational relevance to the metabolic syndrome condition in humans (29) and manifest a progressively worsening skeletal muscle microvascular structure and function that parallels that determined in affected humans.

The purpose of the present study was to utilize two clinically-relevant interventions against the further development of established PVD – increased physical activity/exercise and chronic ingestion of the HMG CoA-reductase inhibitor atorvastatin – to determine if an established impairment to skeletal muscle arteriolar and microvascular structure and function can be reversed toward normal prior to reaching its maximum severity. For this study, “reversibility” is defined as the effectiveness of the imposed intervention in OZR to restore the normal level of measured parameter (e.g., nitric oxide bioavailability) to that determined in untreated LZR. This study tested the hypothesis that, once developed, skeletal muscle microvascular impairments in the OZR model of the metabolic syndrome cannot be reversed, as the environment within the microvasculature cannot be modified sufficiently to generate a condition that allows for reversibility. We propose that a deeper understanding of the reversibility of skeletal muscle microvasculopathy that occurs in metabolic disease will provide greater insight into the clinical challenge of most direct relevance to human subjects.

4.3 Materials and Methods

Animals: Male lean (LZR) and OZR (Harlan) were fed standard chow and drinking water *ad libitum*, unless otherwise indicated, were housed in an accredited animal care facility at either the West Virginia University Health Sciences Center (all experimental procedures) or at the University of Western Ontario (*ex vivo* vascular experiments only) and all protocols received prior IACUC approval. Animals were used for terminal experiments at 13 (initial condition) or 20 (following intervention) weeks of age. At 13 weeks of age, LZR and OZR (n=6 for each) were either used for terminal experiments (to establish the initial condition within the microcirculation) or were placed into one of four groups:

1. Time control (n=6; rats were housed without intervention and aged to ~20 weeks)
2. Atorvastatin (n=6; 25 mg•kg⁻¹•day⁻¹; mixed with food; Ref.18)
3. Treadmill exercise (n=6; 20 m/min, 5% incline, 60 minutes/day, 6 days/week; Ref. 16)
4. A combination of atorvastatin treatment and treadmill exercise as described above, to ~20 weeks of age; n=6.

At the time of final usage, after an overnight fast, rats were anesthetized with injections of sodium pentobarbital (50 mg/kg, i.p.), and received tracheal intubation to facilitate maintenance of a patent airway. In all rats, a carotid artery and an external jugular vein were cannulated for determination of arterial pressure and for infusion of supplemental anesthetic or pharmacological agents, as necessary. Blood samples were drawn from the venous cannula within approximately 20 minutes following implantation for determination of insulin concentrations (Cayman Chemical Company, Ann Arbor, MI), plasma nitrotyrosine levels and markers of inflammation using commercially available EIA systems (Luminex 100 PS; EMD Millipore, Billerica, MA). While glucose levels were determined at the time of the blood draw (Freestyle, Abbott Diabetes Care, Inc, Alameda, CA), all other samples were spun to remove the plasma, which was snap frozen in liquid N₂ until they could be analyzed as groups.

Preparation of Isolated Skeletal Muscle Resistance Arterioles: In anesthetized rats, prior to the preparation of the cremaster muscle (below), the intramuscular continuation of the right gracilis artery was identified, the *in vivo* length and diameter estimated using an

eyepiece micrometer, and the vessel was surgically removed and doubly-cannulated (7). Within each arteriole, vessel reactivity was evaluated in response to application of acetylcholine (10^{-9} M – 10^{-6} M) or hypoxia (reduction in PO_2 from ~135 mmHg to ~50 mmHg). Subsequently, vessels were treated with TEMPOL (10^{-4} M) to assess the contribution of vascular oxidant stress to these mechanical responses.

At the conclusion of all procedures described above, vessel diameter was determined under Ca^{2+} -free conditions over a range of intraluminal pressures spanning 0 mmHg to 160 mmHg (in 20 mmHg increments) for the subsequent calculation of wall mechanics. For these procedures, 5 mmHg was used as the “zero pressure” condition to prevent vessel collapse and to eliminate the potential for creating a vacuum within the vessel.

Preparation of In Situ Cremaster Muscle: In each rat, the left cremaster muscle was prepared for television microscopy (24). After completion of the preparation, the muscle was superfused with PSS, equilibrated with a gas mixture containing 5% CO_2 and 95% N_2 , and maintained at 35°C as it flowed over the muscle at a rate of 2.5 – 3.0 ml/min. The ionic composition of the PSS was as follows (mM): NaCl 119.0, KCl 4.7, $CaCl_2$ 1.6, NaH_2PO_4 1.18, $MgSO_4$ 1.17, $NaHCO_3$ 24.0, and disodium EDTA 0.03. After an initial post-surgical equilibration period of 30 minutes, two sets of arterioles and their bifurcations were selected. Proximal (~75 μ m diameter) and distal (~40 μ m) parent arterioles and their immediate daughter branches were selected for investigation in a clearly visible region of the muscle (please see reference 17 for a full description). All arterioles chosen for study had walls that were clearly visible, a brisk flow velocity, and active tone, as indicated by the occurrence of significant dilation in response to topical application of 10^{-5} M adenosine. All arterioles that were studied were located in a region of the muscle that was away from any incision.

Initial evaluations of *in situ* arteriolar reactivity were assessed by determining mechanical responses (using on-screen videomicroscopy) to increasing concentrations of acetylcholine (10^{-9} - 10^{-6} M) and norepinephrine (10^{-10} - 10^{-7} M). Subsequently, the diameter and perfusion (using optical Doppler velocimetry) responses of both the ‘parent’ and ‘daughter’ arterioles at either level of the microcirculation were assessed under resting conditions within the

cremaster muscle of each rat. All procedures were then repeated following treatment of the *in situ* cremaster muscle with the anti-oxidant TEMPOL (10^{-3} M; within the superfusate; for a minimum of 40 minutes prior to any subsequent data collection).

Measurement of Vascular NO Bioavailability: From each rat, the abdominal aorta was removed and vascular NO production was assessed using amperometric sensors (World Precision Instruments, Sarasota, FL). Briefly, aortae were isolated, sectioned longitudinally, pinned in a silastic coated dish and superfused with warmed (37°C) PSS equilibrated with 95% O_2 and 5% CO_2 . An NO sensor (ISO-NOPF 100) was placed in close apposition to the endothelial surface and a baseline level of current was obtained. Subsequently, increasing concentrations of methacholine (10^{-10} – 10^{-6} M) were added to the bath and the changes in current were determined. To verify that responses represented NO release, these procedures were repeated following pre-treatment of the aortic strip with L-NAME (10^{-4} M).

Determination of Vascular Metabolites of Arachidonic Acid: Vascular production of 6-keto-prostaglandin $\text{F}_{1\alpha}$ (6-keto-PGF $_{1\alpha}$; the stable breakdown product of PGI $_2$; Ref. 27), and 11-dehydro-thromboxane B_2 (11-dehydro-TxB $_2$; the stable plasma breakdown product of TxA $_2$; Ref. 8) was assessed in response to challenge with reduced PO_2 using pooled arteries (femoral, saphenous, iliac) from LZR and OZR. Pooled arteries from each animal were incubated in microcentrifuge tubes in 1 ml of PSS for 30 minutes under control conditions (21% O_2). After this time, the superfusate was removed, stored in a new microcentrifuge tube and frozen in liquid N_2 , while a new aliquot of PSS was added to the vessels and the equilibration gas was switched to 0% O_2 for the subsequent 30 minutes. After the second 30-minute period, this new PSS was transferred to a fresh tube, frozen in liquid N_2 and stored at -80°C . Metabolite release by the vessels was determined using commercially available EIA kits for 6-keto-PGF $_{1\alpha}$ and 11-dehydro-TxB $_2$ (Cayman).

Histological Determination of Microvessel Density: From each rat, the gastrocnemius muscle from the left leg was removed, rinsed in PSS and fixed in 0.25% formalin. Muscles were embedded in paraffin and cut into 5 μm cross sections. Sections were incubated with *Griffonia simplicifolia* I lectin (GS-1) for subsequent determination of microvessel density.

GS-1 is a general stain that labels all microvessels <20 μm in diameter (19). Gastrocnemius muscle microvessel density was determined using fluorescence microscopy) as described previously (14).

Preparation of In Situ Blood Perfused Gastrocnemius: In a separate set of age-matched LZR and OZR under the conditions outlined above, the left gastrocnemius of each animal was isolated *in situ* (13). Heparin (500 IU/kg) was infused via the jugular vein to prevent blood coagulation. Subsequently, an angiocatheter was inserted into the femoral artery, proximal to the origin of the gastrocnemius muscle to allow for bolus tracer injection. Additionally, a small shunt was placed in the femoral vein draining the gastrocnemius muscle that allowed for diversion of flow into a port which facilitated sampling of the venous effluent. Finally, a microcirculation flow probe (Transonic; 0.5/0.7 PS) was placed on the femoral artery to monitor muscle perfusion.

Following completion of the surgical preparation and 30 minutes of self-perfused rest, the muscle was stimulated via the sciatic nerve to contract for 3 minutes at either 3 or 5 Hz isometric twitch contractions, separated by 15 minutes of self-perfused rest. Muscle tension development and blood flow were monitored continuously, and arterial and venous blood aliquots were taken within the final 30 seconds for the determination of blood gas content.

Upon completion of the contraction protocols, the gastrocnemius muscle was allowed at least 20 minutes of rest for full recovery. At this point, 20 μl of ^{125}I -albumin (10 μCi ; Perkin-Elmer, Shelton, CT) was injected as a spike bolus (injection time <0.5 s) into the arterial angiocatheter and venous effluent samples were collected at a rate of 1/s for the subsequent 35 seconds. Venous effluent samples were then immediately transferred into silicate tubes and placed into a gamma counter for activity determination. In order to assess the potential for leakage of the labeled albumin from the intravascular space as a source for error, the gastrocnemius muscle was cleared by perfusion with PSS following euthanasia. Subsequent to a determination of mass, the muscle was placed in the counter for determination of residual activity. Residual activity within the gastrocnemius muscle did not exceed 200 cpm/animal, a level that was far lower than those determined in the venous blood aliquots.

Mathematical Analyses of Results: Arteriolar perfusion in both parent and daughter vessels within *in situ* cremaster muscle of LZR and OZR was calculated as:

$$Q = (V \times 1.6^{-1})(\pi r^2)(0.001) \quad \text{Equation 1}$$

where Q represents arteriolar perfusion ($\text{nl} \cdot \text{s}^{-1}$), V represents the measured red cell velocity from the optical Doppler velocimeter ($\text{mm} \cdot \text{s}^{-1}$; with $V/1.6$ representing an estimated average velocity assuming a parabolic flow profile; Ref. 10), and r represents arteriolar radius (μm ; Ref. 3).

The total volume perfusion in the daughter arterioles was determined as the sum of the individual perfusion rates, and the proportion of flow within each was determined as the quotient of the individual branch divided by the total. γ is defined as the ratio of the greater of the two flows in the daughter vessel to the total flow in the parent vessel. As an example, if flow distribution was homogeneous between daughters, γ for that bifurcation would be 0.5 in both daughter arterioles, while if the proportion of flow in one daughter arteriole was 60%, γ for that bifurcation would be 0.6, with flow distribution being 0.6 in the ‘high perfusion’ arteriole and 0.4 in the ‘low perfusion’ arteriole (13). For the present study, following the initial determination of γ (described above) we determined the changes in γ every 20 seconds over the subsequent 5-minute period.

The dilator or constrictor responses of *ex vivo* microvessels or aortic rings following agonist challenge were fit with the three-parameter logistic equation:

$$y = \min + \left[\frac{\max - \min}{1 + 10^{\log ED_{50} - x}} \right] \quad \text{Equation 2}$$

where y represents the change in arteriolar diameter, “min” and “max” represent the lower and upper bounds, respectively, of the change in diameter or tension with increasing agonist concentration, x is the logarithm of the agonist concentration, and $\log ED_{50}$ represents the logarithm of the agonist concentration (x) at which the response (y) is halfway between the lower and upper bounds.

Vascular NO bioavailability measurements were fit with a linear regression equation:

$$y = \alpha_0 + \beta_1 x \quad \text{Equation 3}$$

where y represents the NO concentration, α_0 represents an intercept term, β_1 represents the slope of the relationship, and x represents the log molar concentration of methacholine.

The determination of passive arteriolar wall mechanics (used as indicators of structural alterations to the individual microvessel) are based on those used previously (5), with minor modification. For the calculation of circumferential stress, intraluminal pressure was converted from mmHg to N/m², where 1 mmHg=1.334×10² N/m².

Circumferential stress (σ) was then calculated as:

$$\sigma = \frac{(P_{IL} \times ID)}{(2WT)} \quad \text{Equation 4}$$

where ID represents arteriolar inner diameter (μm), and WT represents wall thickness (μm) at that intraluminal pressure (P_{IL}). Circumferential strain (ε) was calculated as:

$$\varepsilon = \frac{(ID - ID_5)}{ID_5} \quad \text{Equation 5}$$

where ID_5 represents the internal arteriolar diameter at the lowest intraluminal pressure (i.e., 5 mmHg).

The stress versus strain relationship from each vessel was fit (ordinary least squares analyses, $r^2 > 0.85$) with the following exponential equation:

$$\sigma = \sigma_5 e^{\beta \varepsilon} \quad \text{Equation 6}$$

where σ_5 represents circumferential stress at ID_5 and β is the slope coefficient describing arterial stiffness. Higher levels of β are indicative of increasing arterial stiffness (i.e., requiring a greater degree of distending pressure to achieve a given level of wall

deformation).

In specific experiments, 200 µl blood samples were drawn from the carotid artery cannula and femoral vein angiocatheter immediately prior to and following completion of, the muscle contraction periods. Samples were stored on ice until they were processed for blood gas pressures, percent oxygen saturation and hemoglobin concentration using a Corning Rapidlab 248 blood gas analyzer. Muscle perfusion, arterial pressure, and bulk blood flow through the femoral artery were monitored for one minute prior to muscle contractions and throughout the contraction period using a Biopac MP150 with Acqknowledge data acquisition software at a 50Hz sampling frequency. Muscle perfusion and performance data after three minutes of contraction were normalized to gastrocnemius mass, which was not different between LZR (2.18±0.09 g) and OZR (2.06±0.10 g). Oxygen content within the blood samples was determined using the following standard equation:

$$C_xO_2 = (1.39 \times [Hb] \times \% SatO_2) + (0.003 \times P_xO_2) \quad \text{Equation 7}$$

Where C_xO_2 and P_xO_2 represent the total content (ml/dL) or partial pressure of oxygen (mmHg), respectively, of arterial or venous blood (denoted simply as 'x'). $[Hb]$ represents hemoglobin concentration within the blood sample (g/dL); %O₂Sat represents the percentage oxygen saturation of the hemoglobin and 1.39 and 0.003 represent constants describing the amounts of bound and dissolved oxygen in blood. Oxygen uptake across the gastrocnemius muscle was calculated using the Fick equation:

$$VO_2 = Q \times (CaO_2 - CvO_2) \quad \text{Equation 8}$$

where VO_2 represents oxygen uptake by the gastrocnemius muscle, Q represents femoral artery blood flow (ml/g/min), and CaO_2 and CvO_2 represent arterial and venous oxygen content, respectively.

Analyses of Tracer Washout Curves: For the ¹²⁵I-albumin washout, four standard parameters describing characteristics of tracer washout curves, including mean transit time (\bar{t}), relative dispersion (RD), skewness (β_1), and kurtosis (β_2), were computed as functions of the transport function $h(t)$ (4). As described in our recent study (17), the tails

of the tracer washout curves were extrapolated in the form of single exponential time course to allow for computing the four parameters by the integration for sufficiently long time for convergence (21). In this study, experimentally-measured time courses are extrapolated to 100 seconds, at which $C(t)$ is estimated to be less than 10^{-9} of the maximum washout tracer activity. The transport function $h(t)$ is estimated from

$$h(t) = C(t) / \int_0^{\infty} C(t) dt \quad \text{Equation 9}$$

where $C(t)$ is the time course of activity of intravascular tracer in outlet flow exiting the collecting tube. The mean transit time \bar{t} is calculated from experimentally measured washout curves according to:

$$\bar{t} = \int_0^{\infty} t \cdot h(t) dt \quad \text{Equation 10}$$

The *RD* of $h(t)$ is a measure of the relative temporal spread of $h(t)$ and computed as the ratio of standard deviation of $h(t)$ to the mean transit time from:

$$RD = \left(\int_0^{\infty} (t - \bar{t})^2 \cdot h(t) dt \right)^{1/2} / \bar{t} \quad \text{Equation 11}$$

The skewness (β_1) is a measure of asymmetry of $h(t)$ and computed from:

$$\beta_1 = \int_0^{\infty} (t - \bar{t})^3 \cdot h(t) dt / \left(\int_0^{\infty} (t - \bar{t})^2 \cdot h(t) dt \right)^{3/2} \quad \text{Equation 12}$$

Skewness is a measure of the asymmetry of the perfusion distribution. In other words, it is a measure of the extent to which the perfusion distribution is skewed (as opposed to simply being shifted) to higher or lower values of perfusion. The kurtosis (β_2) is a measure of deviation of $h(t)$ from a normal distribution and computed from:

$$\beta_2 = \int_0^{\infty} (t - \bar{t})^4 \cdot h(t) dt / \left(\int_0^{\infty} (t - \bar{t})^2 \cdot h(t) dt \right)^{4/2} - 3 \quad \text{Equation 13}$$

Kurtosis is a measure of the “sharpness of the peak” of the perfusion distribution. The familiar Gaussian bell-shaped curve has $\beta_2 = 0$; positive values of β_2 indicate a sharper peak than a Gaussian. The four parameters are estimated based on the above equations for each animal in each experimental group.

Determining the Effectiveness of Interventions: The effectiveness of the chronic interventions at improving specific biological outcomes (e.g., biomarkers, vascular function, behavioral scores, etc.) were calculated as:

$$\left[\frac{ABS(OZR_{Intervention} - OZR_{Control})}{ABS(OZR_{Control} - LZR_{Control})} \right] \times 100 \quad \text{Equation 14}$$

where $LZR_{Control}$ and $OZR_{Control}$ represent the values of the measured parameter under untreated control conditions and $OZR_{Intervention}$ represents the values of the measured parameter as a result of chronic imposition of a given intervention under age-matched conditions. This determines the % recovery in a parameter from the control condition in OZR, back to that in control LZR, as a result of the specific intervention.

Statistical Analyses of Results: All data are presented as mean \pm SE. Statistically significant differences in measured physiological parameters (e.g., arterial pressure, blood flow, microvessel density), calculated physiological parameters (e.g., slope coefficients, upper or lower bounds), measurements of plasma biomarkers, were determined using analysis of variance (ANOVA). In all cases, Student-Newman-Keuls post hoc test was used when appropriate and $p < 0.05$ was taken to reflect statistical significance.

4.4 Results

Table 1 presents data describing the baseline and systemic characteristics of the animal groups used in the present study. By 13 weeks of age, OZR were already manifesting multiple elements of the metabolic syndrome as compared to LZR, including significant elevations in body mass, plasma insulin and glucose levels, dyslipidemia and markers of oxidant stress and inflammation. These differences between LZR and OZR were exacerbated by 20 weeks of age, with a significant elevation in blood pressure as well. While single treatment with either atorvastatin or exercise was able to improve specific markers of the metabolic syndrome over the duration of the treatment, simultaneous imposition of both treatments was of greater effectiveness in terms of restoring the metabolic profile to that presented in control LZR.

Table 1. Data (mean±SE) describing the baseline conditions of the animals under the conditions of the present study. The data in the parentheses represents the extent to which the relevant intervention restored the normal level of the parameter. Please see text for details. * p<0.05 vs. LZR at that age; † p<0.05 vs. OZR at that age.

| | 13 Week | | 20 Week | | | | |
|------------------------|-----------|-----------------|-----------|-----------------|---------------------------|---------------------------|--------------------------|
| | LZR (n=6) | OZR (n=6) | LZR (n=6) | OZR (n=6) | OZR+ATOR (n=6) | OZR+EXER (n=6) | OZR+Both (n=6) |
| MAP (mmHg) | 106±5 | 114±6* | 104±4 | 130±5* | 129±6* (3.8±1.5%) | 120±5* (38.5±5.4%) | 112±5† (69.2±5.9%) |
| Glucose (mg/dl) | 88±6 | 120±7* | 94±5 | 184±8* | 172±6* (13.0±4.8%) | 145±8*† (43.6±6.8%) | 142±7*† (46.8±5.9%) |
| Insulin (ng/ml) | 1.2±0.3 | 4.1±0.8* | 1.3±0.3 | 7.9±1.0* | 6.8±0.7* (16.9±4.8%) | 5.2±0.6* (41.2±6.9%) | 4.8±0.6*† (46.9±6.4%) |
| Cholesterol (mg/dl) | 81±5 | 98±6* | 90±6 | 128±8* | 106±7*† (58.5±4.9%) | 119±6* (24.6±5.8%) | 104±6† (63.0±6.4%) |
| N-tyrosine (ng/ml) | 15±2 | 26±4* | 18±4 | 58±6* | 37±5*† (53.0±6.5%) | 35±6*† (58.2±5.1%) | 32±5*† (66.1±6.8%) |
| TNF-α (pg/ml) | 1.0±0.2 | 2.9±0.4* | 1.4±0.4 | 7.4±0.8* | 4.2±0.5*† (54.1±6.2%) | 4.9±0.6*† (42.1±4.9%) | 3.9±0.6*† (58.5±6.4%) |
| MCP-1 (pg/ml) | 38.5±4.2 | 102.6±11.5 * | 42.4±8.7 | 125.9±10.8 * | 70.5±6.9*† (66.5±7.1%) | 85.7±7.9*† (48.5±5.8%) | 66.0±8.4† (72.1±6.8%) |
| IL-1β (pg/ml) | 10.1±1.8 | 19.8±3.4* | 11.8±1.8 | 26.8±4.2* | 20.8±2.6* (40.5±4.9%) | 21.2±3.2* (37.8±5.8%) | 20.1±2.6* (45.1±4.9%) |

(Table 1 continued)

| | 13 Week | | 20 Week | | | | |
|-----------------------------------|-------------|-------------|-------------|--------------|---------------------------|----------------------------|-----------------------------|
| | LZR | OZR | LZR | OZR | OZR+ATOR | OZR+EXER | OZR+Both |
| IL-6 (pg/ml) | 40.2±5.1 | 70.8±6.4* | 45.4±5.8 | 84.8±5.8* | 74.0±5.4* (27.4±5.2%) | 72.5±5.9* (31.3±6.2%) | 68.9±6.4*† (40.2±5.9%) |
| IL-10 (pg/ml) | 19.2±3.9 | 82.9±10.6* | 24.5±5.0 | 126.7±12.4* | 102.6±7.4* (23.5±4.9%) | 96.8±6.8* (29.5±5.1%) | 90.8±10.8*† (35.1±4.9%) |
| AT (<i>ex vivo</i> ; %) | 41±4 | 43±3 | 38±3 | 42±3 | 40±3 | 41±4 | 40±4 |
| AT (<i>in situ</i> ; %) | 35±3 | 36±3 | 28±2 | 32±3 | 33±2 | 35±3 | 34±4 |
| Q _{Rest} (ml/g/min) | 0.12±0.02 | 0.11±0.03 | 0.13±0.02 | 0.09±0.01 | 0.10±0.02 | 0.11±0.02 | 0.11±0.02 |
| MIT (g/g) | 354±19 | 345±17 | 388±20 | 376±19 | 380±16 | 374±20 | 384±22 |
| (a-v) _{O2} (ml/ml) | 0.052±0.003 | 0.049±0.004 | 0.051±0.005 | 0.041±0.003 | 0.048±0.004 (0.0±4.8%) | 0.047±0.005 (33.3±6.7%) | 0.049±0.003* (33.3±7.2%) |
| VO _{2Rest} (ml/g/min) | 0.006±0.001 | 0.005±0.001 | 0.007±0.001 | 0.004±0.001* | 0.005±0.001 | 0.005±0.001 | 0.005±0.001 |

Figure 1 summarizes the data describing the dilator reactivity of *ex vivo* gracilis muscle resistance arterioles in response to increasing concentrations of acetylcholine in the present study. As compared to responses in LZR, dilator reactivity in arterioles of OZR at 13 weeks to acetylcholine was significantly reduced (Panel A). Acute treatment of the vessels with TEMPOL had minimal impact on responses in LZR, but improved reactivity in OZR arterioles. By 20 weeks of age, the difference in acetylcholine-induced reactivity was pronounced between LZR and OZR (Panel B). While chronic treatment with ATOR or EXER improved responses to acetylcholine in OZR; the combination of the two treatments resulted in the greatest restoration of dilator responses. Panel C presents data describing the impact of acute treatment with TEMPOL on the acetylcholine-induced gracilis arteriolar dilation in all groups of rats at 20 weeks. While TEMPOL had negligible impact on responses in vessels from LZR, and the greatest impact on dilator responses in vessels from OZR, the impact on responses in arterioles from OZR that had been treated with ATOR, EXER or both were blunted as compared to that in untreated OZR. The ability of the chronic interventions to restore normal dilator reactivity (determined in LZR) from the maximum impairment (determined in OZR) are presented in Panel D. While both ATOR and EXER resulted in a significant restoration of normal function in OZR, with a significant additive benefit of acute TEMPOL treatment, the combination of both interventions resulted in the greatest degree of recovery in acetylcholine-induced responses with the smallest additional benefit from an acute treatment with the antioxidant.

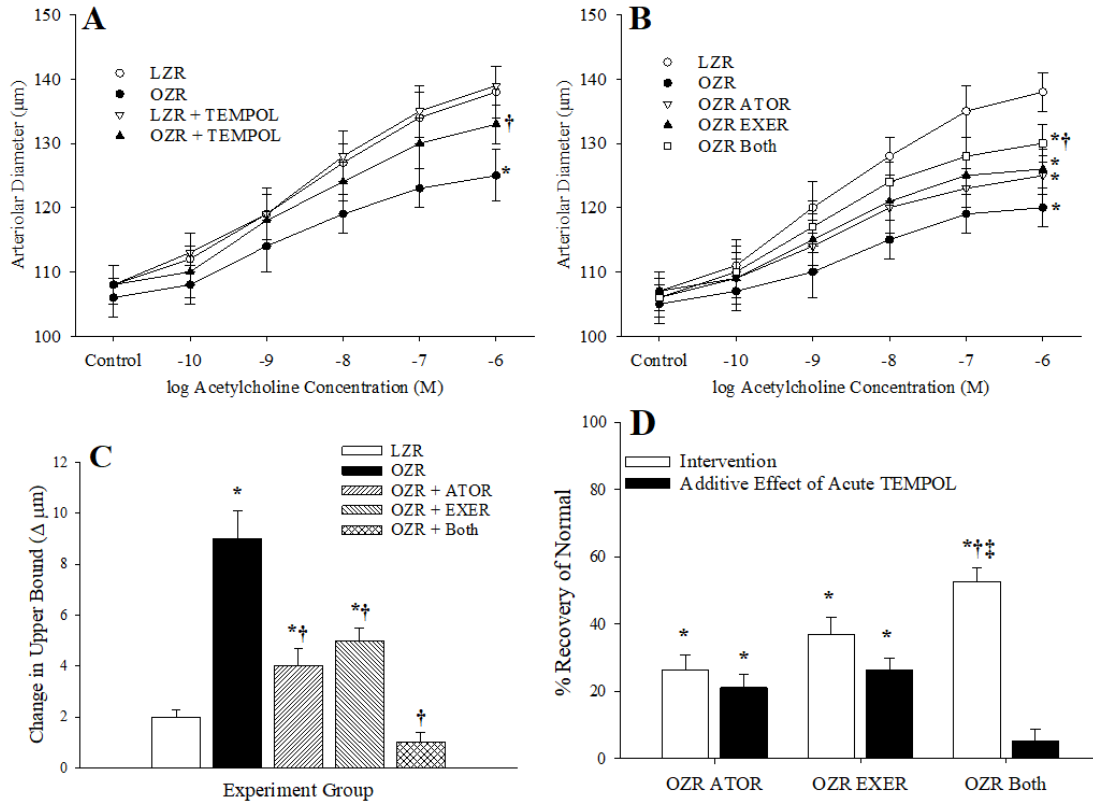


Figure 1. Data (mean±SE) describing the dilator reactivity of *ex vivo* gracilis muscle resistance arterioles in response to increasing concentrations of acetylcholine. *Panel A:* data from LZR and OZR at 13 weeks of age under untreated conditions and following acute treatment with the antioxidant TEMPOL. *Panel B:* data from LZR and OZR at 20 weeks of age under control conditions and following 7 weeks of intervention with atorvastatin (ATOR), exercise (EXER) or both concurrently. *Panel C:* the change in the upper bound of the logistic equation fit to the curves in Panel B following acute treatment with the antioxidant TEMPOL. *Panel D:* the extent to which the different interventions restored normal function, and the additive benefit of acute treatment with TEMPOL. n=6 for all groups. For Panels A-C: * p<0.05 vs. LZR; † p<0.05 vs. OZR, For Panel D: * p<0.05 vs. no change; ‡ p<0.05 vs. OZR EXER. Please see text for details.

Dilator responses of gracilis arterioles in response to hypoxia from LZR and OZR at 13 weeks are summarized in Figure 2, Panel A. Hypoxic dilation in vessels from OZR was significantly reduced as compared to that in LZR, although acute treatment of the vessel with TEMPOL improved responses in vessels from OZR only. By 20 weeks, the impaired hypoxic dilation in arterioles from OZR was exacerbated, and chronic treatments with EXER or ATOR+EXER resulted in significant improvements (ATOR alone did not significantly improve responses; Panel B). Acute treatment of gracilis arterioles from the groups of rats at 20 weeks of age with TEMPOL had a significant impact on hypoxic dilation in untreated OZR and in OZR treated with chronic ATOR or EXER only (Panel C), while the effectiveness of the interventions on restoring normal function was similar between ATOR and EXER, with the combination of both being most effective, the

additional benefit of acute TEMPOL treatment was lowest in the ATOR+EXER group (Panel D).

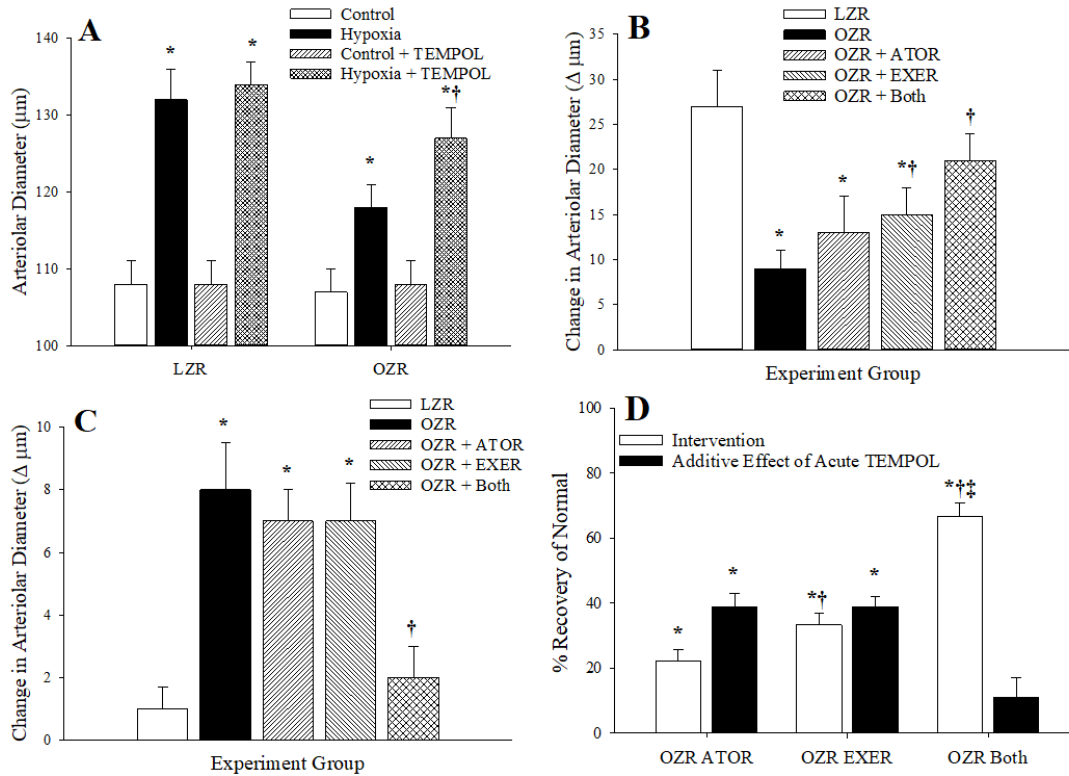


Figure 2. Data (mean±SE) describing the dilator reactivity of *ex vivo* gracilis muscle resistance arterioles in response to reduced PO₂ in the chamber (hypoxia). *Panel A:* data from LZR and OZR at 13 weeks of age under untreated conditions and following acute treatment with the antioxidant TEMPOL. *Panel B:* data from LZR and OZR at 20 weeks of age under control conditions and following 7 weeks of intervention with atorvastatin (ATOR), exercise (EXER) or both concurrently. *Panel C:* the change in the dilator response in Panel B following acute treatment with the antioxidant TEMPOL. *Panel D:* the extent to which the different interventions restored normal function, and the additive benefit of acute treatment with TEMPOL. n=6 for all groups. For Panels A-C: * p<0.05 vs. LZR; † p<0.05 vs. OZR, For Panel D: * p<0.05 vs. no change; † p<0.05 vs. OZR ATOR; ‡ p<0.05 vs. OZR EXER. Please see text for details.

The constriction of *ex vivo* skeletal muscle resistance arterioles in 13-week old LZR and OZR following in response to increasing concentrations of norepinephrine is presented in Figure 3, Panel A. At this age, there was no difference in vasoconstriction to increasing concentrations of the adrenergic agonist between groups. However, by 20 weeks of age (Panel B), constrictor responses to norepinephrine were significantly greater in OZR vs. LZR, and this difference in reactivity was nearly abolished by chronic treatment with ATOR, EXER or both. Acute treatment of these groups with TEMPOL improved responses in untreated OZR but had minimal impact on constrictor reactivity of gracilis arterioles from all other groups (Panel C). The extent to which chronic ATOR, EXER or

both interventions restored normal norepinephrine-induced reactivity is summarized in Panel D. As compared to OZR at 20 weeks, chronic imposition of all three interventions resulted in an excellent recovery to normal constriction to norepinephrine, with minimal added benefit from acute treatment with TEMPOL.

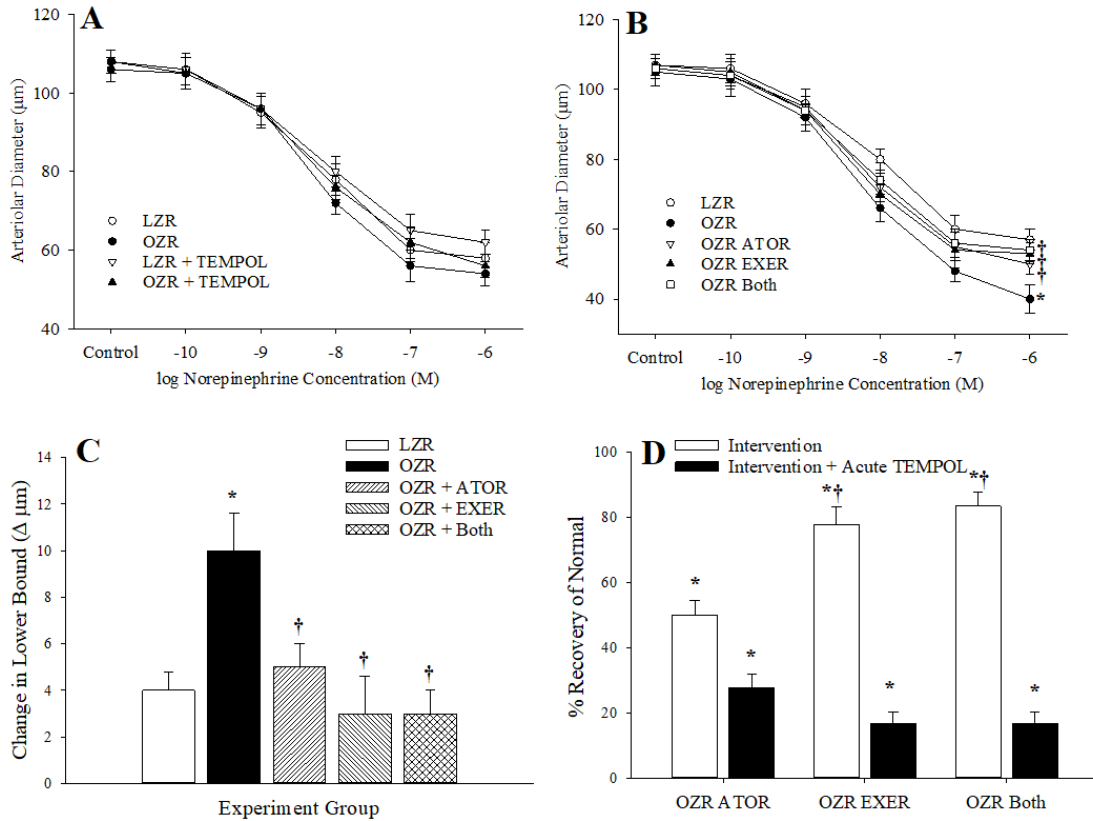


Figure 3. Data (mean±SE) describing the constrictor reactivity of *ex vivo* gracilis muscle resistance arterioles in response to increasing concentrations of norepinephrine. *Panel A:* data from LZR and OZR at 13 weeks of age under untreated conditions and following acute treatment with the antioxidant TEMPOL. *Panel B:* data from LZR and OZR at 20 weeks of age under control conditions and following 7 weeks of intervention with atorvastatin (ATOR), exercise (EXER) or both concurrently. *Panel C:* the change in the lower bound of the logistic equation fit to the curves in Panel B following acute treatment with the antioxidant TEMPOL. *Panel D:* the extent to which the different interventions restored normal function, and the additive benefit of acute treatment with TEMPOL. n=6 for all groups. For Panels A-C: * p<0.05 vs. LZR; † p<0.05 vs. OZR, For Panel D: * p<0.05 vs. no change; ‡ p<0.05 vs. OZR EXER. Please see text for details.

The dilator response of proximal *in situ* cremasteric arterioles to increasing concentrations of acetylcholine in LZR and OZR at 13 weeks of age are presented in Figure 4, Panel A, where responses were significantly reduced in vessels in OZR, and this difference was largely abolished following treatment of the cremaster muscle with TEMPOL. In OZR at 20 weeks, while the differences in acetylcholine-induced dilation with LZR were increased, chronic imposition of ATOR, EXER or both significantly

improved responses (Panel B) and reduced the beneficial impact of acute TEMPOL treatment on dilator reactivity (Panel C). Additionally, chronic imposition of ATOR, EXER or both from 13 weeks of age (with ‘both’ being most effective), significantly restored normal vascular reactivity to increasing concentrations of acetylcholine (Panel D). For distal arterioles of *in situ* cremaster muscle, the patterns in the data were extremely similar to those for proximal arterioles (data not shown).

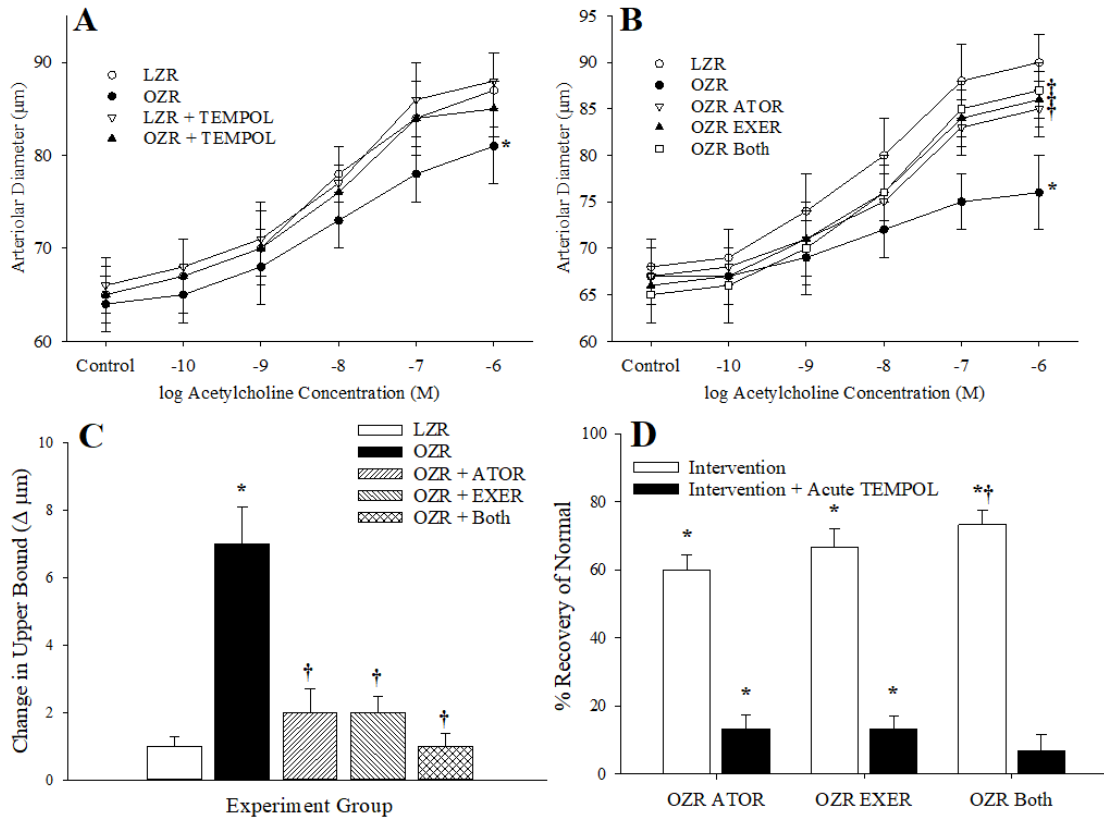


Figure 4. Data (mean±SE) describing the dilator reactivity of *in situ* cremaster muscle resistance arterioles in response to increasing concentrations of acetylcholine. *Panel A:* data from LZR and OZR at 13 weeks of age under untreated conditions and following acute treatment with the antioxidant TEMPOL. *Panel B:* data from LZR and OZR at 20 weeks of age under control conditions and following 7 weeks of intervention with atorvastatin (ATOR), exercise (EXER) or both concurrently. *Panel C:* the change in the upper bound of the logistic equation fit to the curves in Panel B following acute treatment with the antioxidant TEMPOL. *Panel D:* the extent to which the different interventions restored normal function, and the additive benefit of acute treatment with TEMPOL. n=6 for all groups. For Panels A-C: * p<0.05 vs. LZR; † p<0.05 vs. OZR, For Panel D: * p<0.05 vs. no change; † p<0.05 vs. OZR ATOR; ‡ p<0.05 vs. OZR EXER. Please see text for details.

Figure 5 presents the data describing the changes in constrictor responses to increasing concentrations of norepinephrine for *in situ* cremasteric arterioles. While there were minimal differences in responses at 13 weeks of age between strains (Panel A), the differences at 20 weeks of age were somewhat more extensive, there were no differences

in reactivity that were demonstrated to be consistently statistically significant (Panel B). As above, for distal arterioles of *in situ* cremaster muscle, the norepinephrine-induced constriction, while potent, did not demonstrate statistically significant differences between LZR and OZR at either age range as such, have not been formally presented (data not shown).

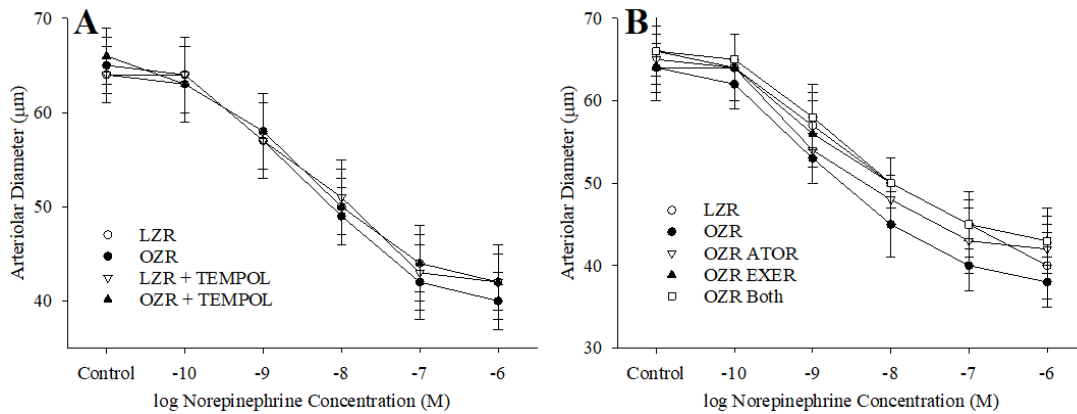


Figure 5. Data (mean±SE) describing the constrictor reactivity of *in situ* cremaster muscle resistance arterioles in response to increasing concentrations of norepinephrine. *Panel A:* data from LZR and OZR at 13 weeks of age under untreated conditions and following acute treatment with the antioxidant TEMPOL. *Panel B:* data from LZR and OZR at 20 weeks of age under control conditions and following 7 weeks of intervention with atorvastatin (ATOR), exercise (EXER) or both concurrently. n=6 for all groups.

The impact of chronic interventions on the reversibility of altered wall mechanics in LZR and OZR gracilis arterioles are summarized in Figure 6. At 13 weeks of age, there were no significant differences in the inner diameter of gracilis arterioles (Panel A), their incremental distensibility (Panel C) or the slope (β) coefficient from their stress versus strain relationship (Panel E). By 20 weeks of age, arterioles from OZR exhibited a reduced passive inner diameter as compared to those from LZR (Panel B), with a reduced incremental distensibility (Panel D) and a significant left-shifting of the stress versus strain relationship (Panel F). Chronic interventions with ATOR and EXER, alone or in combination, were largely ineffective at blunting this effect (Panel G).

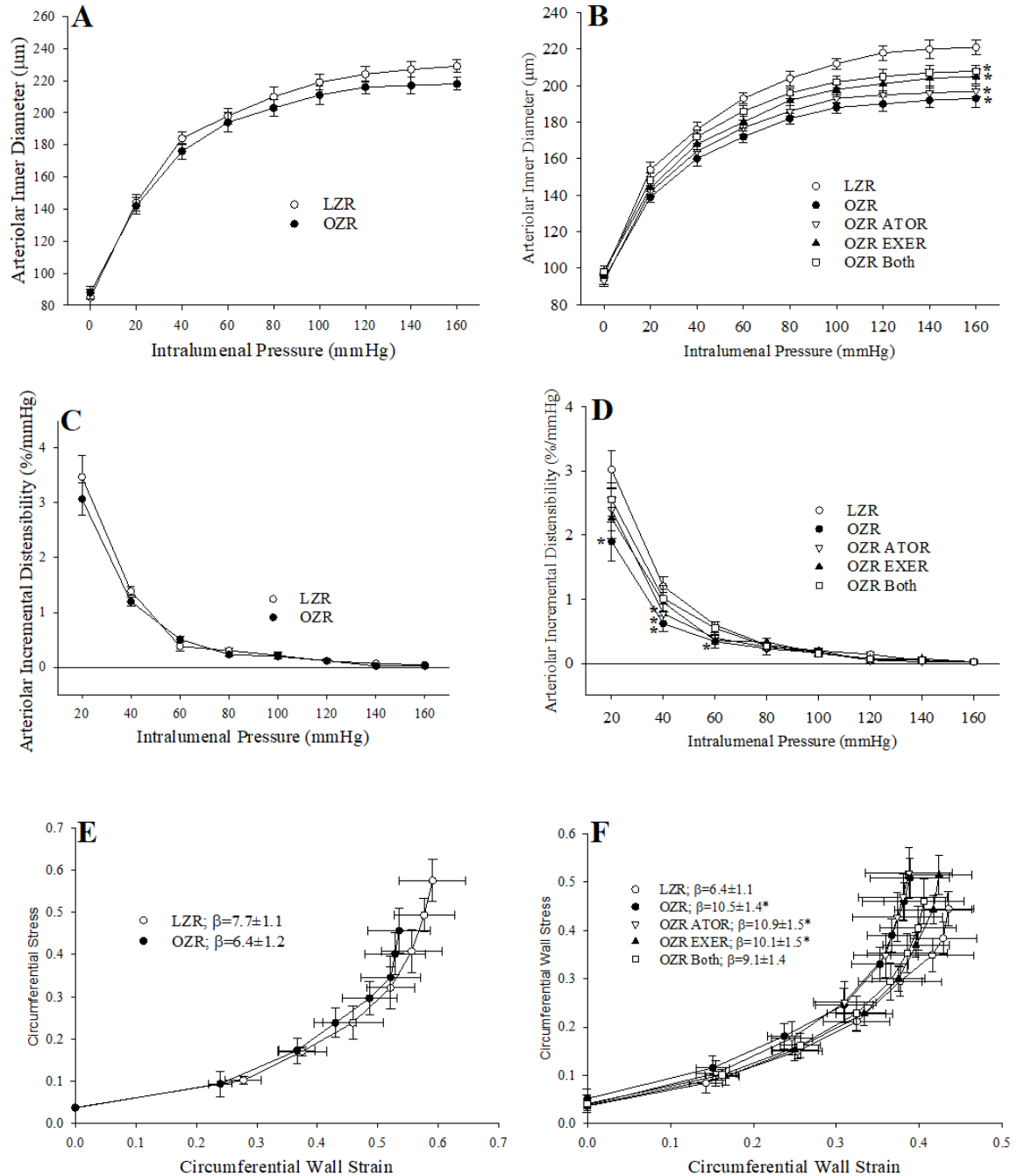


Figure 6. The mechanics of the wall of ex vivo gracilis muscle resistance arterioles under Ca^{2+} -free conditions with increasing intraluminal pressure. Data are presented as mean \pm SE. Panel A: inner diameter of gracilis muscle resistance arterioles from LZR and OZR at 13 weeks. Panel B: inner diameter of gracilis muscle resistance arterioles from LZR and OZR at 20 weeks under control conditions and in response to 7 weeks of intervention with atorvastatin (ATOR), exercise (EXER) or both concurrently. Panel C: incremental distensibility of gracilis arterioles from LZR and OZR at 13 weeks. Panel D: incremental distensibility of gracilis arterioles from LZR and OZR at 20 weeks under control conditions and in response to 7 weeks of intervention with ATOR, EXER or both. Panel E: circumferential stress versus strain relationship between gracilis arterioles from LZR and OZR at 13 weeks with the determination of the slope (\square) coefficient. Panel F: stress versus strain relationship between gracilis arterioles from LZR and OZR at 20 weeks under control conditions and in response to 7 weeks of intervention with ATOR, EXER or both with the determination of the slope (\square) coefficient. $n=6$ for all groups. * $p < 0.05$ vs. LZR; $\dagger p < 0.05$ vs. OZR. Please see text for details.

Figure 7 presents data describing the gastrocnemius muscle microvessel density (Panel A) and the extent of recovery in MVD as a result of the chronic interventions (Panel B) in LZR and OZR. At 13 weeks of age, there was a reduction in MVD between LZR and OZR, which became much more pronounced by 20 weeks of age. This difference was largely unaffected by chronic treatment with ATOR and only marginally affected by chronic EXER from 13 weeks of age in OZR. However, combined imposition of both interventions resulted in a significant improvement in skeletal muscle MVD in OZR.

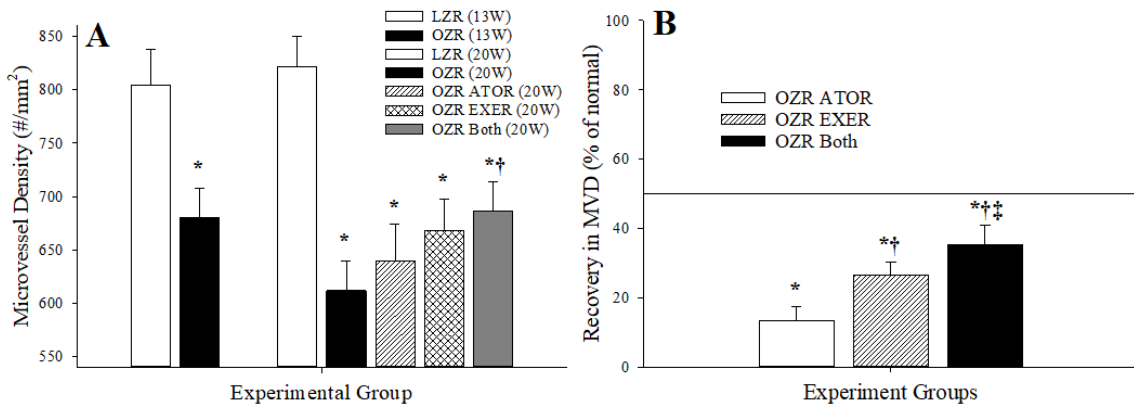


Figure 7. Microvessel density within gastrocnemius muscle of LZR and OZR under the conditions of the present study. Data (mean±SE) are presented for animals at 13 weeks of age and at 20 weeks of age under control (untreated) conditions and in response to 7 weeks of ATOR, EXER or both interventions imposed concurrently (Panel A). Panel B presents the extent to which the different chronic interventions restored normal levels of microvessel density in OZR. n=6 for all groups. Panel A: * p<0.05 vs. LZR; † p<0.05 vs. OZR. Panel B: * p<0.05 vs. no change; † p<0.05 vs. OZR ATOR; ‡ p<0.05 vs. OZR EXER. Please see text for details.

Data describing the perfusion distribution coefficient (γ), in both the proximal (Panel A) and distal (Panel B) cremasteric microcirculation are summarized in Figure 8. These data suggest that there were minimal differences in the average magnitude of γ between LZR and OZR at 13 weeks of age, although the temporal variability in γ over the data collection window was reduced in OZR. In contrast, γ was increased, and its variability reduced, in OZR at 20 weeks of age versus LZR, and chronic imposition of ATOR, EXER or both from 13 weeks of age resulted in improvements to γ and a greater degree of variability as compared to responses in untreated OZR. These results were consistent in both proximal (Panel A) and distal (Panel B) arteriolar bifurcations within the cremasteric microcirculation.

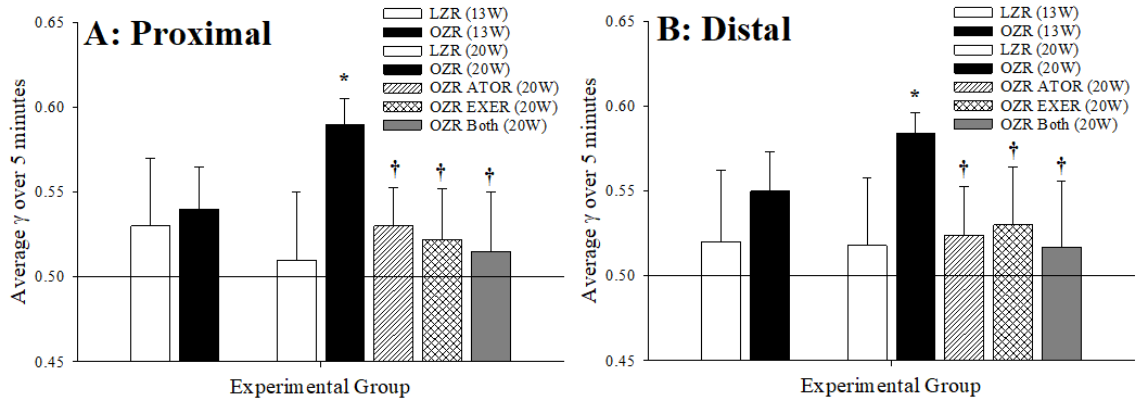


Figure 8. Perfusion heterogeneity (γ) at proximal ($\sim 70 \mu\text{m}$ diameter; Panel A) and distal ($\sim 30 \mu\text{m}$ diameter; Panel B) arteriolar bifurcations within *in situ* cremaster muscle of LZR and OZR under the conditions of the present study. Data (mean \pm SE) are presented for animals at 13 weeks of age and at 20 weeks of age under control (untreated) conditions and in response to 7 weeks of ATOR, EXER or both interventions imposed concurrently (Panel A). $n=6$ for all groups. * $p<0.05$ between variability in group vs. LZR variability; † $p<0.05$ between variability in this group vs. OZR variability. Please see text for details.

Figure 9 summarizes the bioavailability of vasoactive metabolites that have been previously demonstrated to play a contributing role in the vascular phenotypes discussed above. Vascular nitric oxide bioavailability (Panel A) was reduced in arteries of OZR as compared to that in LZR at 13 weeks, and this was exacerbated by 20 weeks. Chronic intervention with ATOR, EXER or both resulted in a significant improvement in levels of NO bioavailability at 20 weeks of age in OZR. Vascular hydrogen peroxide levels, elevated in arteries of OZR versus LZR at 20 weeks of age (Panel B), demonstrated a higher degree of variability and, although presenting a mirrored trend as compared to NO, did not produce a consistently significant outcome subsequent to the interventions. A similar pattern to that for NO was determined for PGI_2 bioavailability (Panel C), although the ability of the interventions to restore normal levels was less robust. Conversely, TxA_2 bioavailability (Panel D) was significantly increased by 13 weeks of age in arteries of OZR as compared to that in LZR, and this elevation was only reduced at 20 weeks following combined imposition of ATOR and EXER from 13 weeks of age in OZR.

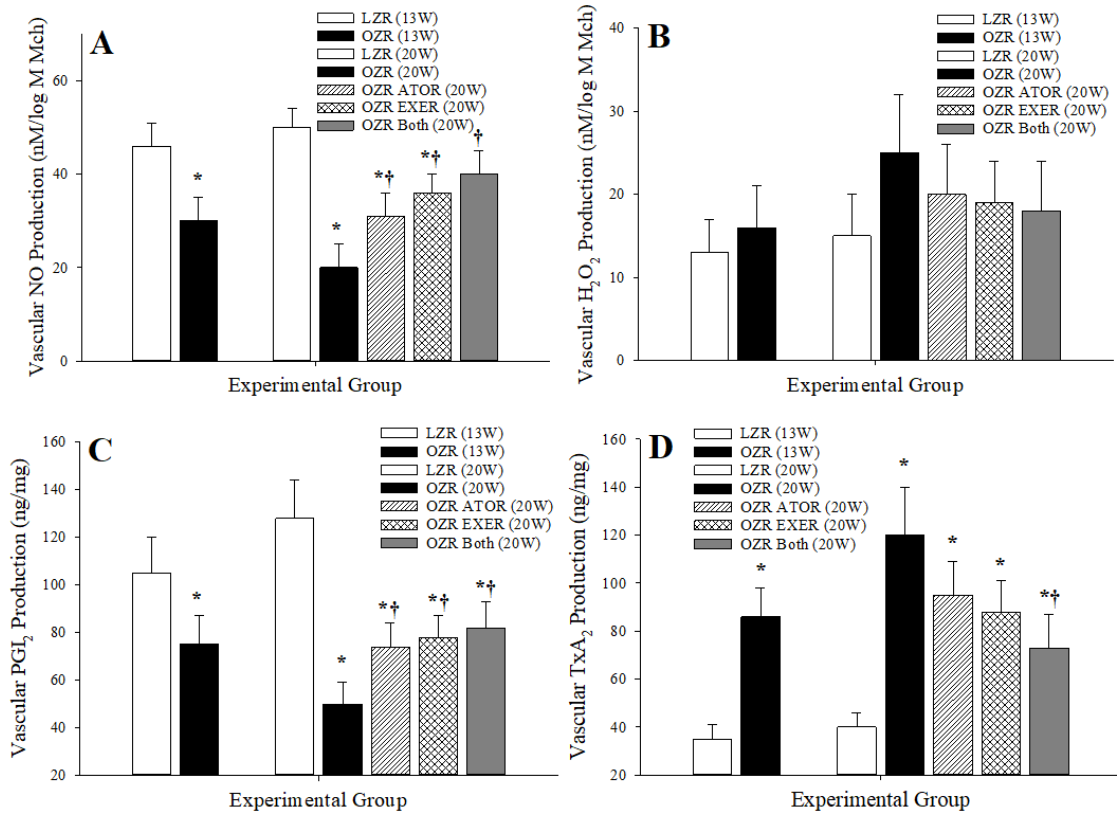


Figure 9. Data describing the bioavailability of signaling molecules associated with healthy and impaired vascular function. Data (mean±SE) are presented for the bioavailability of nitric oxide (NO, Panel A), hydrogen peroxide (H₂O₂, Panel B), prostacyclin (PGI₂, Panel C) and thromboxane A₂ (TxA₂, Panel D). n=6 for all groups. * p<0.05 vs. LZR; † p<0.05 vs. OZR. Please see text for details.

The results of the *in-situ* gastrocnemius muscle performance experiments are summarized in Figure 10. At 13 weeks of age OZR demonstrated an accelerated muscle fatigue rate as compared to LZR after 3 minutes of contraction at both 3Hz and 5Hz (isometric twitches), with the difference being exacerbated at 5Hz (Panel A). This impaired muscle performance was increased at 20 weeks of age, and was not significantly impacted by ATOR or EXER, but only in response to the combination intervention. The functional hyperemic response to muscle contraction was similar between LZR and OZR at 13 weeks but was attenuated by 20 weeks for both 3Hz and 5Hz contractions (Panel B). All three interventions were successful at significantly improving the bulk hyperemic response to both levels of increased metabolic demand following chronic intervention from 13 weeks. Oxygen extraction (Panel C) and VO₂ (Panel D) across the muscle, while comparable in LZR and OZR at 13 weeks, were reduced by 20 weeks of age. While ATOR and EXER alone resulted in mild improvements that were not statistically significant for

extraction of VO_2 , the combination of the two interventions restored both parameters to levels that were not significantly different from that in LZR (at 3Hz only).

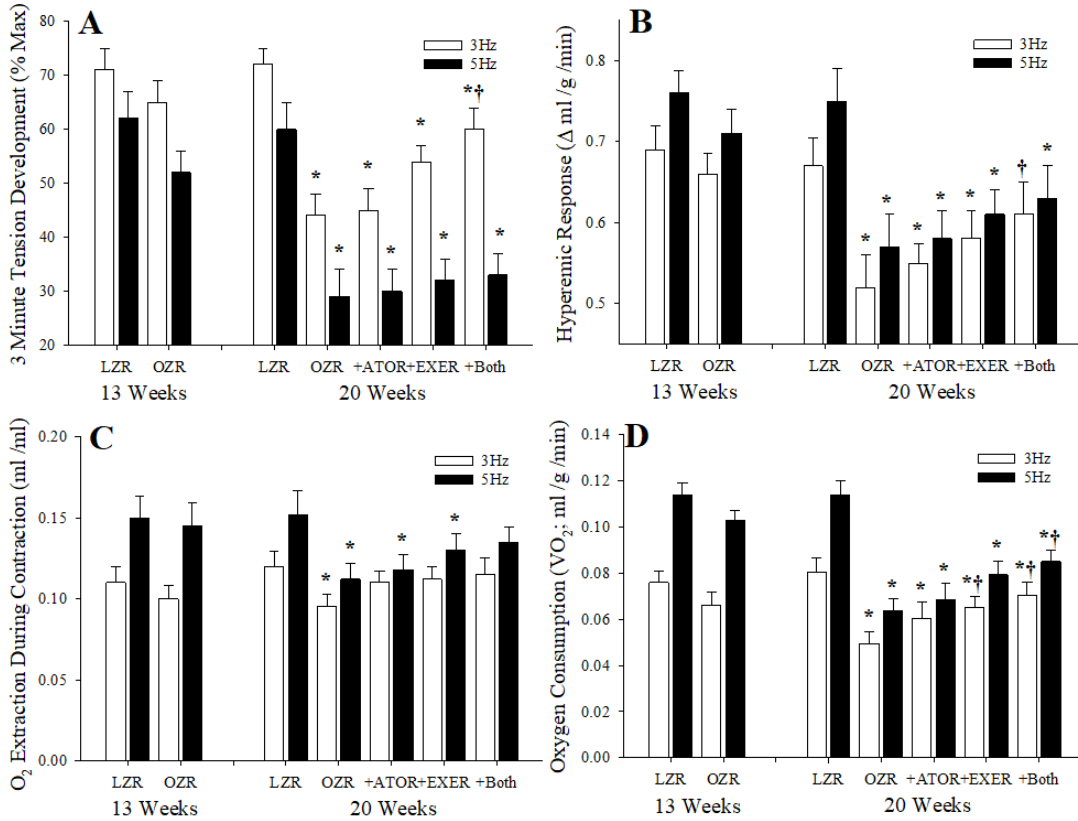


Figure 10. Vascular responses and contractile performance of *in situ* skeletal muscle of LZR and OZR at 13 weeks of age and at 20 weeks of age under control (untreated) conditions and in response to 7 weeks of intervention with atorvastatin (ATOR), treadmill exercise (EXER) or both concurrently. Data (mean±SE) are presented from the animal groups in response to three minutes of muscle contraction at 3 or 5Hz (isometric twitch). Data are presented for the percentage of the peak force development after three minutes of the contraction bout (Panel A), the hyperemic responses to muscle contraction (Panel B), oxygen extraction across the gastrocnemius muscle (Panel C), and oxygen consumption across the gastrocnemius muscle (Panel D). n=6 for all groups. * p<0.05 vs. LZR; † p<0.05 vs. OZR. Please see text for details.

Figure 11 presents data describing the average tracer washout from the *in situ* gastrocnemius preparation under rest conditions across the different experiment groups of the present study. The appearance of ^{125}I -albumin in the venous effluent draining the gastrocnemius muscle in all groups in the present study is represented in Panel A. Figure 12 summarizes data describing the aggregate washout curves. Mean transit time of the tracer across the gastrocnemius was very similar across all groups, suggesting that the relationship between bulk blood flow to the gastrocnemius muscle and vascular volume in

the different groups was not significantly different in the present study (Panel A). The relative dispersion of tracer across the muscle (RD; Panel B) was elevated in untreated OZR at 20 weeks of age as compared to all other groups, suggestive of an increased perfusion heterogeneity throughout the microcirculation of the gastrocnemius muscle. While treatment with ATOR was ineffective at restoring RD, chronic exercise, alone or in combination with ATOR, was superior at restoring RD toward levels determined in age-matched LZR. Both the skewness (Panel C) and the kurtosis (Panel D) of the tracer washout curves were reduced in OZR as compared to age-matched LZR, and these shifts in the washout patterns were improved toward that determined in LZR as a result of either ATOR, EXER or both interventions imposed concurrently.

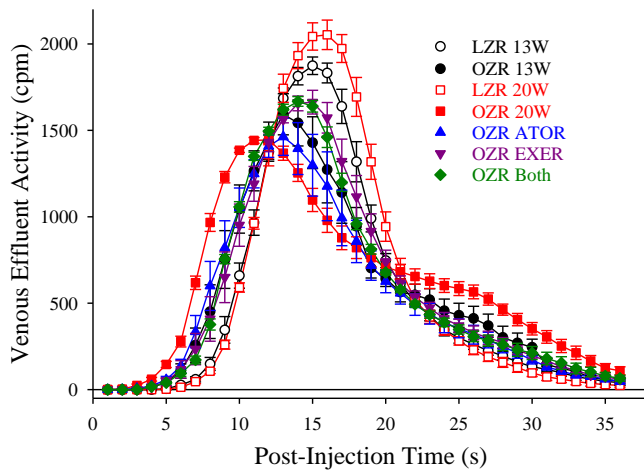


Figure 11. Data describing the tracer washout of ^{125}I -albumin from the *in situ* gastrocnemius muscle of LZR and OZR under the conditions of the present study. Data (mean \pm SE) are presented for LZR and OZR at 13 weeks of age and at 20 weeks of age under control (untreated) conditions and in response to 7 weeks of intervention with atorvastatin (ATOR), treadmill exercise (EXER) or both concurrently. Please see text for details; n=5 for each group.

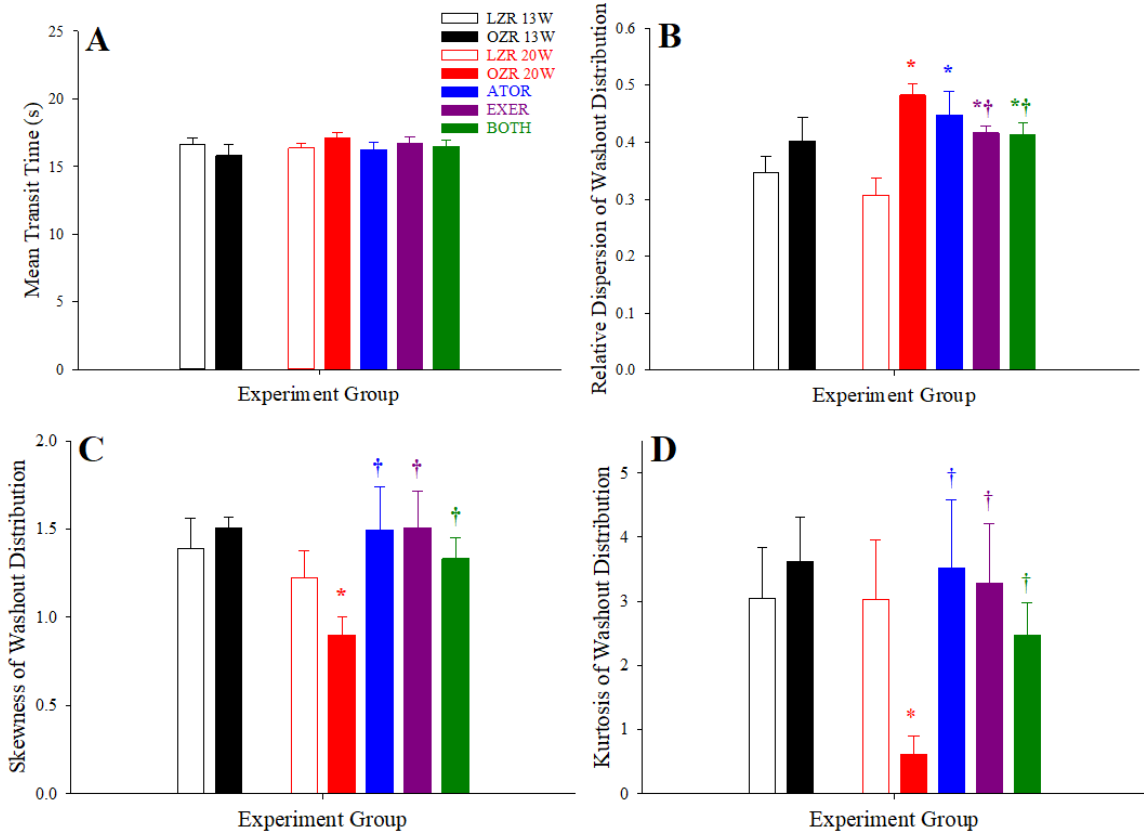


Figure 12. Data (presented as mean±SE) describing the four moments of the washout of ^{125}I -albumin from the *in situ* gastrocnemius muscle for LZR and OZR at 13 weeks of age and at 20 weeks of age under control (untreated) conditions and in response to 7 weeks of intervention with atorvastatin (ATOR), treadmill exercise (EXER) or both concurrently. Data are shown for the mean transit time of the washout (Panel A), the relative dispersion of the washout (RD; Panel B), the distribution skewness (Panel C) and kurtosis (Panel D). Please see text for details; n=5 for each. * p<0.05 vs. LZR; † p<0.05 vs. OZR.

4.5 Discussion

The powerful association between chronic metabolic disease and the increased risk for the development of PVD has been well known for many years. While there have been many studies seeking to understand the mechanisms underlying the compromised vascular function under these conditions, or how interventional strategies could serve to blunt the development of the poor vascular outcomes (please see Ref. 33 for a recent review), an understanding of the outright reversibility of established vasculopathy in translationally relevant models has been more elusive. This is particularly troubling, as it is this challenge which is most clinically relevant, where patients present themselves in a clinical setting only once they have already experienced the manifestations of PVD (e.g., rapid muscle fatigue, pain upon exertion, etc.). The purpose of this study was to use the OZR model of the metabolic syndrome, at an age where impairments to skeletal muscle microvascular structure and function have already been established, and where impairments to hyperemic responses and muscle performance are still mild, to determine the extent to which clinically-relevant interventions could improve not only microvascular reactivity and structure, but also muscle fatigue and hyperemia with increased metabolic demand.

At 13 weeks of age, the presence of the metabolic disease in OZR was associated with impaired endothelial function, reduced microvessel density and initial evidence of impaired muscle performance and active hyperemic responses. As severity of the metabolic syndrome progressed, impairments to microvascular structure and function increased to include an increased stiffening of the arteriolar wall, an increasing (and increasingly stable) heterogeneity of perfusion at arteriolar bifurcations and a worsening of skeletal muscle perfusion and oxygen exchange. While this is not novel information and has been described previously, it does set the appropriate context for the present study: the vasculopathy associated with the metabolic syndrome at 13 weeks of age was present, was sufficient to impact skeletal muscle performance, and continued to evolve naturally over the subsequent 7 weeks to further compromise muscle blood flow and performance.

Chronic ingestion of atorvastatin from 13 weeks of age or chronic imposition of treadmill exercise demonstrated some effectiveness at improving vascular, and by extension muscle blood flow and performance, outcomes in OZR as compared to no

intervention, but even the combination of the two had clear limits on effectiveness. Under all three interventions, with the combination of both atorvastatin and exercise being most effective, the improvement to the vasoactive metabolite profile – associated with the improvement in oxidant stress and inflammation levels – was critical for improving vascular reactivity to acetylcholine, hypoxia and norepinephrine. In addition, there were some improvements to microvessel density, although the extent of the rarefaction even with the combined interventions remained considerable in the OZR despite 7 weeks of aggressive treatment. Further, there was very little change in the progression of altered wall mechanics in the arterioles of OZR, regardless of intervention.

While the structure of the microvascular networks was resistant to improvement following intervention, there was an improvement in both the magnitude and in the variability of γ throughout the microcirculation of OZR with chronic atorvastatin, exercise or both. This was evident in both the direct observations of the microvascular networks in the cremaster or using the tracer washout curve analyses for the labeled albumin. These results suggest that the increased heterogeneity of perfusion distribution that accompanies progressive metabolic disease in OZR can be partially reversed with aggressive intervention, even with established dysfunction. The combination of these improvements to reactivity, and especially to perfusion distribution, was associated with improvements to muscle performance, hyperemic responses and oxygen exchange for skeletal muscle in OZR. However, as recovery was most clearly evident at 3Hz contraction, as it seemed that 5Hz contraction frequency have been too severe a challenge for any significant recovery to have been evident.

A study of this scope and focus immediately lends itself to a wide array of provocative questions, some of which we will attempt to address or clarify in the succeeding paragraphs. Obviously, one question that immediately comes to mind is the timing of the intervention and its duration. We elected to use 13 weeks of age for two major reasons. First, the vasculopathy was established at this age and was beginning to impact muscle blood flow and performance, so this was considered to be the earliest time point that was relevant for “reversing” rather than for “blunting development” of vascular dysfunction. Secondly, in preliminary studies, 15 weeks of age was also considered as an

option for the initiation of intervention due to the greater establishment of vasculopathy. However, it was rapidly determined that the exercise intervention was not feasible as OZR at that age were not able to consistently exercise without invoking a level of attrition that made the experiments unrealistic.

The use of the 7 weeks of intervention was selected for two reasons as well. First, using a 4-week intervention, which would bring animals to the ~17-week age range we have employed historically, was not considered to of sufficient duration to determine any meaningful outcome. Second, using a 7-week intervention duration brings us to a 20-week old OZR, which we have determined is the maximum age we have been able to employ before changes to skeletal muscle function (e.g., Ca^{2+} handling, half relaxation time, maximal twitch tension, fiber type distribution) become too great to allow for an accurate interpretation of the data.

The failure of arteriolar wall mechanics to demonstrate any significant improvement with intervention or, given its lack of presence at 13 weeks of age in OZR, could actually be considered as an appearance of the dysfunction despite the interventions, was a particularly striking observation of the present study. While the mechanisms underlying the progressive reduction in vascular wall distensibility with metabolic disease (in OZR and in other models) are a continuing area of active investigation, it may be that the combination of atorvastatin and exercise are simply “off target” for preventing vascular wall remodeling. In our previous studies, the increased stiffness of the arteriolar wall in OZR was associated more with the development of hypertension rather than with impaired glycemic control or dyslipidemia (18), and previous studies using interventions specifically targeted at reducing blood pressure have been more effective at moderating the changes to vascular wall structure and mechanics (30).

The relatively modest responses at improving microvessel density are also intriguing, as previous studies have clearly demonstrated that chronic atorvastatin treatment and/or exercise from a relatively young age and severity of the metabolic syndrome was effective at blunting rarefaction severity in skeletal muscle of OZR (14). However, it seems plausible that the use of the 13 week age for the start of intervention,

while justifiable from the perspective of translational relevance, may have missed the window when the extent of rarefaction is most modifiable. In a recent study examining the temporal nature and mechanistic bases of rarefaction in skeletal muscle of OZR, it was evident that the initial phase of rarefaction occurs prior to 10-12 weeks of age in OZR and was most closely predicted by the severity of both inflammation and vascular production of TxA₂ (14). For maximal effectiveness, it was proposed that interventions against rarefaction should be initiated prior to 10 weeks of age in OZR, although this is somewhat problematic as there is no functional phenotype associated with these early changes to microvessel density that has been identified. Regardless, it seems likely that the optimal window for intervening against microvessel loss in skeletal muscle rarefaction in OZR may have been missed with interventions starting only after 13 weeks of age. However, it must be emphasized that we have only used a 7-week intervention duration. Whether a longer duration of atorvastatin treatment, exercise regimen or both (or some other intervention), would result in a greater degree of reversibility of the skeletal muscle microvascular impairments will require dedicated study.

An additional issue that requires some comment is the observation that, while there were significant improvements to the reactivity of arterioles from the gracilis muscle, muted improvements to the microvessel density of the gastrocnemius muscle, and improvements to the performance, blood flow, oxygen handling and tracer washout kinetics indicative of a less heterogeneous perfusion distribution within the *in situ* gastrocnemius muscle of OZR, this study also presents data describing the improvement to the hemodynamic control of perfusion distribution in the *in situ* cremaster muscle – a tissue that is not involved in the exercise training regimen and that does not directly benefit from the effects of the chronic exercise (with or without concurrent atorvastatin therapy). This provides strong support that the improved systemic effects of chronic exercise therapy in OZR, which can include an improved endocrine, oxidant stress and pro-inflammation status, can be highly effective in terms of improving vascular function and may work in combination with direct effects in the exercising muscles of interest to produce a system-wide improvement to vascular health under conditions of the metabolic syndrome. However, caution must be employed when interpreting some of the results of the present study. The measurement of vascular metabolites that can impact the regulation of tone

used larger arteries and not resistance arterioles. While this allowed us to reduce animal number and provide insight into “within animal” comparisons, it must be remembered that vascular environments are different between larger arteries and resistance arterioles, with the potential for introducing inaccuracy in terms of assessing the importance of the metabolites to tone regulation.

Given the results of the present study, it may be appropriate to speculate on not just the effect of the interventions on the potential for reversibility of established vasculopathy (or potential mechanisms), but also on whether the effects of these interventions can be additive or potentially synergistic. It has been well established that both ATOR and EXER can improve anti-inflammatory and anti-oxidant capacity, thereby improving vascular function and health outcomes through those mechanistic pathways. However, results from the present study suggest that this effect is more diverse than a single issue, such as improved nitric oxide bioavailability and may also include a partial restoration of vascular arachidonic acid metabolism. This beneficial effect appears to be localized primarily to the endothelial cell as responses vascular smooth muscle-dependent stimuli were largely unaffected. Further, over the time course of the present study, the impacts of the interventions did not significantly reverse vascular structure, either at the individual vessel or whole network levels of resolution. While it is possible that a longer duration intervention might improve the structural characteristics of the vasculature, we may simply have intervened outside of the most appropriate window of time to elicit a beneficial outcome (14). Regardless, although the design of the current study does not allow for a rigorous assessment of whether the interventions were additive or synergistic at this time, it is clear that the combination therapy is sufficiently robust that it helps to restore not just hyperemic responses and muscle fatigue rates, but also perfusion distribution, and thus O₂ delivery, patterns within the skeletal muscle.

In summary, the results of the present study provide compelling evidence that the imposition of two clinically-relevant interventions (atorvastatin and chronic exercise), alone or in combination to an OZR with a pre-existing established vasculopathy can result in improvements to specific indices of vascular reactivity, hemodynamics, blood flow, oxygen handling and muscle performance. Further, these improvements appear to be

clearly tied to the effects of both interventions on enhancing oxidant stress and pro-inflammation severity system-wide. The use of statins has been shown to result in improved patency and limb salvage rates in patients undergoing revascularization for limb ischemia (1). The specific mechanisms underlying this effect remain unclear. Perhaps these improvements in microvascular dysfunction observed in this animal model help to explain this clinical association in humans. Indices of altered vascular structure, both at the individual vessel and whole network levels of resolution were more resistant to reversibility with the selected interventions and their duration, although determining if this represents specific procedural issues with the present study or simply processes that are more difficult to reverse will require further investigation. Regardless, the results of the present study provide compelling insight and provocative direction for future study into the reversibility of established vasculopathies under condition of chronic metabolic disease and may have implications for primary and secondary prevention of PVD.

Acknowledgements

This work was the result of many individuals working over the period of years, each contributing in their own way to the dataset. We would like to acknowledge the contributions of Drs. Adam Goodwill, Phoebe Stapleton, Joshua Butcher, Steven Brooks and Ms. Milinda James to this study as well as multiple other student trainees within the laboratory over many years. This study was supported by the American Heart Association (IRG 14330015, EIA 0740129N), the National Institutes of Health (RR 2865AR; R01 DK 64668), support from the Center for Cardiovascular and Respiratory Sciences at West Virginia University and the Schulich School of Medicine & Dentistry at the University of Western Ontario.

4.6 Literature Cited

1. Aiello FA, Khan AA, Meltzer AJ, Gallagher KA, McKinsey JF, Schneider DB. Statin therapy is associated with superior clinical outcomes after endovascular treatment for critical limb ischemia. *J Vasc Surg* 2012;55:371-380
2. Alexandre de Artiñano A, Miguel Castro M. Experimental rat models to study the metabolic syndrome. *Br J Nutr.* 2009 Nov;102(9):1246-53.
3. Baker M, Wayland H. On-line volume-flow rates and velocity profile measurements for blood in microvessels. *Microvasc. Res.* 7:131-143, 1974.
4. Bassingthwaite JB, Goresky CA. Modeling in the analysis of solute and water exchange in the microvasculature. In: *Handbook of Physiology. The Cardiovascular System. Microcirculation.* Bethesda, MD: Am. Physiol. Soc., 1984, sect. 2, vol. IV, pt. 1, chapt. 13, p. 549–626
5. Baumbach GL, Hajdu MA. Mechanics and composition of cerebral arterioles in renal and spontaneously hypertensive rats. *Hypertension.* 1993 Jun;21(6 Pt 1):816-26.
6. Behnke BJ, Kindig CA, McDonough P, Poole DC, Sexton WL. Dynamics of microvascular oxygen pressure during rest-contraction transition in skeletal muscle of diabetic rats. *Am J Physiol Heart Circ Physiol.* 2002 Sep;283(3):H926-32.
7. Butcher JT, Goodwill AG, Frisbee JC. The ex vivo isolated skeletal microvessel preparation for investigation of vascular reactivity. *J Vis Exp.* 2012 Apr 28;(62). pii: 3674. doi: 10.3791/3674.
8. Catella F, Healy D, Lawson JA, FitzGerald GA. 11-Dehydrothromboxane B₂: a quantitative index of thromboxane A₂ formation in the human circulation. *Proc Natl Acad Sci U S A.* 83:5861-5865, 1986.
9. Clough GF, Kuliga KZ, Chipperfield AJ. Flow motion dynamics of microvascular blood flow and oxygenation: Evidence of adaptive changes in obesity and type 2

- diabetes mellitus/insulin resistance. *Microcirculation*. 2017 Feb;24(2). doi: 10.1111/micc.12331.
10. Davis MJ. Determination of volumetric flow in capillary tubes using an optical Doppler velocimeter. *Microvasc Res* 34:223-30, 1987.
 11. Fellmann L, Nascimento AR, Tibiriça E, Bousquet P. Murine models for pharmacological studies of the metabolic syndrome. *Pharmacol Ther*. 2013 Mar;137(3):331-40.
 12. Forsythe RO, Brownrigg J, Hinchliffe RJ. Peripheral arterial disease and revascularization of the diabetic foot. *Diabetes Obes Metab*. 2015;17(5):435-444.
 13. Frisbee JC, Butcher JT, Frisbee SJ, Olfert IM, Chantler PD, Tabone LE, d'Audiffret AC, Shrader CD, Goodwill AG, Stapleton PA, Brooks SD, Brock RW, Lombard JH. Increased peripheral vascular disease risk progressively constrains perfusion adaptability in the skeletal muscle microcirculation. *Am J Physiol Heart Circ Physiol*. 2016 Feb 15;310(4):H488-504.
 14. Frisbee JC, Goodwill AG, Frisbee SJ, Butcher JT, Brock RW, Olfert IM, DeVallance ER, Chantler PD. Distinct temporal phases of microvascular rarefaction in skeletal muscle of obese Zucker rats. *Am J Physiol Heart Circ Physiol*. 2014 Dec 15;307(12):H1714-28.
 15. Frisbee JC, Goodwill AG, Frisbee SJ, Butcher JT, Wu F, Chantler PD. Microvascular perfusion heterogeneity contributes to peripheral vascular disease in metabolic syndrome. *J Physiol*. 2016 Apr 15;594(8):2233-43. doi: 10.1113/jphysiol.2014.285247.
 16. Frisbee JC, Samora JB, Peterson J, Bryner R. Exercise training blunts microvascular rarefaction in the metabolic syndrome. *Am J Physiol Heart Circ Physiol*. 2006 Nov;291(5):H2483-92.
 17. Frisbee JC, Wu F, Goodwill AG, Butcher JT, Beard DA. Spatial heterogeneity in skeletal muscle microvascular blood flow distribution is increased in the metabolic syndrome. *Am J Physiol Regul Integr Comp Physiol*. 2011 Oct;301(4):R975-86.
 18. Goodwill AG, Frisbee SJ, Stapleton PA, James ME, Frisbee JC. Impact of chronic anticholesterol therapy on development of microvascular rarefaction in the metabolic syndrome. *Microcirculation*. 2009 Nov;16(8):667-84.

19. Greene AS, Lombard JH, Cowley AW Jr, Hansen-Smith FM. Microvessel changes in hypertension measured by Griffonia simplicifolia I lectin. *Hypertension*. 1990 Jun;15(6 Pt 2):779-83.
20. Gutterman DD, Chabowski DS, Kadlec AO, Durand MJ, Freed JK, Ait-Aissa K, Beyer AM. The Human Microcirculation: Regulation of Flow and Beyond. *Circ Res*. 2016 Jan 8;118(1):157-72.
21. Hamilton WF, Moore JW, Kinsman JM, Spurling RG. Studies on the circulation IV. Further analysis of the injection method, and of changes in hemodynamics under physiological and pathological conditions. *Am J Physiol* 99: 534–551, 1932
22. Henriksen EJ, Diamond-Stanic MK, Marchionne EM. Oxidative stress and the etiology of insulin resistance and type 2 diabetes. *Free Radic Biol Med*. 2011 Sep 1;51(5):993-9.
23. Keske MA, Premilovac D, Bradley EA, Dwyer RM, Richards SM, Rattigan S. Muscle microvascular blood flow responses in insulin resistance and ageing. *J Physiol*. 2016 Apr 15;594(8):2223-31.
24. Kunert MP, Liard JF, Abraham DJ, Lombard JH. Low-affinity hemoglobin increases tissue PO₂ and decreases arteriolar diameter and flow in the rat cremaster muscle. *Microvasc Res*. 1996 Jul;52(1):58-68.
25. Loader J, Montero D, Lorenzen C, Watts R, Méziat C, Reboul C, Stewart S, Walther G. Acute Hyperglycemia Impairs Vascular Function in Healthy and Cardiometabolic Diseased Subjects: Systematic Review and Meta-Analysis. *Arterioscler Thromb Vasc Biol*. 2015 Sep;35(9):2060-72.
26. Machado MV, Martins RL, Borges J, Antunes BR, Estado V, Vieira AB, Tibiriçá E. Exercise Training Reverses Structural Microvascular Rarefaction and Improves Endothelium-Dependent Microvascular Reactivity in Rats with Diabetes. *Metab Syndr Relat Disord*. 2016 Aug;14(6):298-304.
27. Nies AS. Prostaglandins and the control of the circulation. *Clin Pharmacol Ther*. 39:481-488, 1986.
28. Padilla DJ, McDonough P, Behnke BJ, Kano Y, Hageman KS, Musch TI, Poole DC. Effects of Type II diabetes on capillary hemodynamics in skeletal muscle. *Am J Physiol Heart Circ Physiol*. 2006 Nov;291(5):H2439-44.

29. Rosenthal T, Younis F, Alter A. Combating Combination of Hypertension and Diabetes in Different Rat Models. *Pharmaceuticals (Basel)*. 2010 Mar 26;3(4):916-939.
30. Schriffin EL. Mechanisms of remodelling of small arteries, antihypertensive therapy and the immune system in hypertension. *Clin Invest Med*. 2015 Dec 4;38(6):E394-402.
31. Sebai M, Lu S, Xiang L, Hester RL. Improved functional vasodilation in obese Zucker rats following exercise training. *Am J Physiol Heart Circ Physiol*. 2011 Sep;301(3):H1090-6.
32. Tigno XT, Hansen BC, Nawang S, Shamekh R, Albano AM. Vasomotion becomes less random as diabetes progresses in monkeys. *Microcirculation*. 2011 Aug;18(6):429-39. doi: 10.1111/j.1549-8719.2011.00103.x.
33. Tune JD, Goodwill AG, Sassoon DJ, Mather KJ. Cardiovascular consequences of metabolic syndrome. *Transl Res*. 2017 May;183:57-70. doi: 10.1016/j.trsl.2017.01.001.
34. Xiang L, Dearman J, Abram SR, Carter C, Hester RL. Insulin resistance and impaired functional vasodilation in obese Zucker rats. *Am J Physiol Heart Circ Physiol*. 2008 Apr;294(4):H1658-66.

Chapter 5

5 Thesis Conclusion

Approximately 20% of the adult population is afflicted with Metabolic Syndrome (METS; Riediger & Clara, 2011) which is the presentation of obesity, dyslipidemia, hypertension, and insulin resistance. METS increases the risk of cardiovascular disease (CVD) by 2.6-fold and type 2 diabetes mellitus (T2DB) by 5-fold (Lakka, 2002). Additionally, almost 40% of adults with METS over the age of 40 are afflicted with peripheral vascular disease (PVD), the presentation of poor skeletal muscle blood perfusion with increases in metabolic demand (Sumner et al., 2012). Thus, this perfusion-demand mismatch typically gives rise to increases in muscle fatigue and pain during times of increased physical activity (Abdulhannan et al., 2012). The purpose of this dissertation is to generate novel insights for both venular and arteriolar micro-vasculopathies using the translational animal model for METS, the obese Zucker rat (OZR), and to investigate the potential reversibility of established PVD using exercise and atorvastatin.

Chapter 1: Altered Postcapillary and Collecting Venular Reactivity in Skeletal Muscle with Metabolic Syndrome

Retinal microcirculation studies have provided insight to alterations in venular function with METS and how the control of venular diameter and venular network structure can be significantly impacted (Lammert et al., 2012). While there are some studies dedicated to venular function in the context of leukocyte interactions within the venular walls in inflammation (Iba et al., 2012), there is limited information pertaining to these dysfunctions in relevant animal models for METS and PVD. These experiments sought to identify any alterations in postcapillary and collecting venule function in the OZR compared to healthy controls.

The OZR presented with impaired dilator reactivity in both postcapillary and collecting venules which was attributed to elevations in reactive oxygen species and its negative effects on venular nitric oxide and prostacyclin bioavailability. Further,

elevation in adrenergic and thromboxane A₂ constrictor responses may contribute to the impaired dilator responses. Taken together, these disparities indicated an altered microvascular reactivity at the venular level of skeletal muscle, thereby providing insight to an area of METS vasculopathy which has received little investment. Where this fits in the context of METS microcirculatory research, as a whole, is a starting point for potential, compelling avenues of future research. Previous studies have shown some of the earlier, measurable changes to the microcirculation occur on the venular side (with respect to leukocyte rolling and adhesion) in METS. The current study shows apparent differences in vascular reactivities, with METS risk factors, which favor that of a more vasoconstrictive state. While it is known that venules and veins do not necessarily change resistance to restrict blood flow, but rather compliance to facilitate it (Rothe, 1983). Therefore, the speculation can be made that the observable differences may be either an adaptation to the existing microvasculopathies or a potential contributor to their severity. Nevertheless, the changes are apparent and additional, dedicated studies are required to further investigate these changes with respect to identifying the nature of their existence.

Chapter 2: Altered Distribution of Adrenergic Constrictor Responses Contributes to Skeletal Muscle Perfusion Abnormalities in Metabolic Syndrome

Adrenergic traffic, signaling, and vascular responses may be elevated with METS risk factors (Carlson et al., 2000; Naik et al, 2006; Frisbee 2004). Treatment with α -adrenoreceptor antagonists equalizes the elevated blood pressure of the OZR to levels comparable to healthy controls. However, it is unclear how general elevations in vascular adrenergic output, which produces significant elevations in resistance, functions in vivo to produce mild/moderate elevations in blood pressure observed in OZR (Tofovic et al., 1998; Frisbee, 2004). Therefore, these experiments sought to reveal potential contributors of this disconnect using a multi-scale/resolution approach, thus garnering a greater understanding of the impaired adrenergic control for PVD within METS.

The OZR experienced an increased α ₁ adrenoreceptor mediated, whole-animal pressor response compared to healthy controls, independent of reactive oxygen species or nitric oxide bioavailability. However, the blunted in situ hyperemic response in the OZR

was mediated, in part, by reactive oxygen species (ROS) as the combination of TEMPOL (ROS scavenger) and $\alpha 1$ -adrenoreceptor inhibition elicited the greatest improvements in muscle performance and volume of oxygen consumption. With a minor adjustment of the classically used inclusion criteria for experiments of this nature, high resolution interrogations of the *in-situ* cremaster muscle arterioles and *ex vivo* gracilis muscle artery revealed an $\alpha 1$ -adrenoreceptor mediated hyperresponsiveness with OZR vessels, contributed to by ROS and nitric oxide bioavailability. Lastly, OZR arteriolar responses to an $\alpha 1$ adrenoreceptor challenge revealed a more heterogeneous, constrictor response compared to healthy controls. While these results support $\alpha 1$ adrenoreceptor as a key contributor to the elevated pressor responses and vascular resistance in the OZR, the purpose of a more heterogeneous response is unclear.

In the context of METS microvasculopathy research, it is well established α -adrenoreceptor stimulated vasoconstrictor responses are elevated for subjects with METS associated vascular dysfunction. Therefore, the current adrenergic literature emphasizes investigation on biochemical signaling pathways and secondary messengers that may contribute to the differences in response for the OZR versus healthy controls. While the pathways are essential to understanding the underlying pathologies, it is critical we continue to interrogate the functional outcomes of these pathologies as there are important questions which remain unanswered. The current study, in part, provides insight for the discrepancies of *in vivo* blood pressure responses and *ex vivo* vascular responses observed with the OZR model. In doing so, changes in variance and frequency distributions were coupled to these apparent differences in vascular response giving rise to further questions. A speculative purpose for this phenomenon may include that of a shift in initial tangential stresses due to changes in pressure and wall thickness in the OZR vessels, thereby influencing vascular responses (described by Gore et al., 1972). However, additional studies are necessary to explore this potential phenomenon.

Chapter 3: Chronic Atorvastatin and Exercise can Partially Reverse Established Skeletal Muscle Microvasculopathy in Metabolic Syndrome

The final set of experiments are dedicated to reversing established METS associated vasculopathies of the skeletal muscle. Previous studies demonstrate a loss in microvascular density (rarefaction) and function in parallel to the development of metabolic syndrome (Machado et al., 2016). While there are interventional strategies to decrease the severity of these vasculopathies, there is limited research on the restoration or reversibility of vascular health following the onset of these vasculopathies. Consequently, these experiments sought to determine the potential for reversibility or restoration of established PVD using the chronic ingestion of an HMG-CoA inhibitor, atorvastatin (ATOR), and/or the implementation of regular exercise (EXER).

In the current study, following the establishment of PVD at 13 weeks of age, a 7-week intervention was implemented in which the ATOR group and EXER group experienced significant improvements compared to time control OZR while the combination group of ATOR and EXER elicited the greatest degree of reversibility, in certain criteria. There were favorable changes to vasoactive metabolite bioavailability, reactivity, and perfusion distributions, thereby resulting in better muscle performance and oxygen transport during stimulated muscle contractions compared to the time control OZR group. With respect to the stated definition of reversibility, these improvements were more comparable to the measured values of the healthy controls, indicating a potential for reversibility of established PVD, within specific parameters.

While improvements to microvascular density were modest and there were no significant improvements in wall mechanics, microvascular densities of the intervention OZR groups did improve compared to the 20-week OZR time control. Those improvements were comparable to the 13-week OZR time controls. This may be interpreted as a blunting effect rather than restorable indicating a low potential for reversibility. A lack of significant structural improvements may have resulted from missing the appropriate interventional window (Frisbee et al., 2014) or potentially the short duration of the intervention as Orr et al. reported improvements in the vessel mechanics in humans following a 12-week ATOR intervention. However, the current study using the OZR model is restricted to a narrow interventional window for an

accurate assessment of established PVD (details in chapter 4 discussion; Orr et al., 2009). Nevertheless, ATOR and EXER can significantly reverse specific indices of microvascular function following established vasculopathy in the OZR thus representing an effective avenue for interventions aimed at reversing microvasculopathies.

It is well established both forms of intervention possess anti-inflammatory and anti-oxidant properties which can improve vascular health. Previous literature utilizing both ATOR and EXER as primary and secondary (respectively) forms of treatment have been shown to improve blood flow in health and with cardiovascular disease in humans. Exercise has been shown to improve blood flow via mechanisms including increases in eNOS expression, improved anti-oxidant systems, and decreases in NADPH oxidase generated reactive oxygen species (Machado et al., 2016; Rush et al., 2003). Although the mechanisms are unclear, ATOR has been shown to improve vascular outcomes for inflammation related diseases by means of decreasing the expression of IL-6 and TNF- α , decreasing CRP production, and upregulation of anti-oxidant systems (Rabkin et al., 2013; Sodha et al., 2015). While speculation that a combination of these two treatment methods elicit the greatest potential for PVD reversibility can be made, it is not known if the improvements are synergistic or additive in a model for METS. Although the existence of synergy between the two treatment methods has been shown in atherosclerotic mice (Moustardas et al, 2014), the current study's design does not allow for such an assessment. Due to this, additional studies are required to garner a greater understanding of the synergistic capacities for EXER and ATOR.

5.1 Literature Cited

- 1) Abdulhannan, P., Russell, D. A., & Homer-Vanniasinkam, S. (2012). Peripheral arterial disease: A literature review. *British Medical Bulletin*, 104(1), 21–39.

- 2) Carlson SH, Shelton J, White CR, Wyss JM. (2000). Elevated sympathetic activity contributes to hypertension and salt sensitivity in diabetic obese Zucker rats. *Hypertension*. Jan;35(1 Pt 2):403-8.
- 3) Frisbee JC. (2004). Enhanced arteriolar alpha-adrenergic constriction impairs dilator responses and skeletal muscle perfusion in obese Zucker rats. *J Appl Physiol* (1985). Aug;97(2):764-72.
- 4) Frisbee, J. C., Goodwill, A. G., Frisbee, S. J., Butcher, J. T., Brock, R. W., Olfert, I. M., ... Chantler, P. D. (2014). Distinct temporal phases of microvascular rarefaction in skeletal muscle of obese Zucker rats. *American Journal of Physiology-Heart and Circulatory Physiology*, 307(12), H1714–H1728.
- 5) Gore RW. Wall stress: a determinant of regional differences in response of frog microvessels to norepinephrine. *Am J Physiol*. 1972 Jan;222(1):82-91.
- 6) Hamdy, O., Ledbury, S., Mullooly, C., Jarema, C., Porter, S., Ovalle, K., ... Horton, E. S. (2003). Lifestyle modification improves endothelial function in obese subjects with the insulin resistance syndrome. *Diabetes Care*, 26(7), 2119–2125.
- 7) Haslinger-Löffler, B. (2008). Multiple effects of HMG-CoA reductase inhibitors (statins) besides their lipid-lowering function. *Kidney International*, 74(5), 553–555.
- 8) Iba T, Aihara K, Kawasaki S, Yanagawa Y, Niwa K & Ohsaka A (2012). Formation of the venous thrombus after venous occlusion in the experimental mouse model of metabolic syndrome. *Thromb Res* 129, e246-e250.
- 9) Lakka, H.-M. (2002). The Metabolic Syndrome and Total and Cardiovascular Disease Mortality in Middle-aged Men. *Jama*, 288(21), 2709.
- 10) Lammert A, Hasenberg T, Kräupner C, Schnülle P & Hammes HP (2012). Improved arteriole-to-venule ratio of retinal vessels resulting from bariatric surgery. *Obesity (Silver Spring)* 20, 2262-2267.
- 11) Machado MV, Martins RL, Borges J, Antunes BR, Estado V, Vieira AB, Tibiriçá E. (2016). Exercise Training Reverses Structural Microvascular Rarefaction and Improves Endothelium-Dependent Microvascular Reactivity in Rats with Diabetes. *Metab Syndr Relat Disord*. Aug;14(6):298-304.

- 12) Moustardas, P., Kadoglou, N. P. E., Katsimpoulas, M., Kapelouzou, A., Kostomitsopoulos, N., Karayannacos, P. E., ... Liapis, C. D. (2014). The complementary effects of atorvastatin and exercise treatment on the composition and stability of the atherosclerotic plaques in apoE knockout mice. *PLoS ONE*, 9(9).
- 13) Naik JS, Xiang L, Hester RL. (2006). Enhanced role for RhoA-associated kinase in adrenergic-mediated vasoconstriction in gracilis arteries from obese Zucker rats. *Am J Physiol Regul Integr Comp Physiol*. Jan;290(1):R154-61.
- 14) Orr, J. S., Dengo, A. L., Rivero, J. M., & Davy, K. P. (2009). Arterial destiffening with atorvastatin in overweight and obese middle-aged and older adults. *Hypertension*, 54(4), 763–768.
- 15) Rabkin, S. W., Langer, A., Ur, E., Calciu, C. D., & Leiter, L. A. (2013). Inflammatory biomarkers CRP, MCP-1, serum amyloid alpha and interleukin-18 in patients with HTN and dyslipidemia: Impact of diabetes mellitus on metabolic syndrome and the effect of statin therapy. *Hypertension Research*, 36(6), 550–558.
- 16) Riediger, N. D., & Clara, I. (2011). Prevalence of metabolic syndrome in the Canadian adult population. *CMAJ : Canadian Medical Association Journal*, 183(15), E1127-34
- 17) Rothe CF (1983). Venous system: physiology of the capacitance vessels. In *The Cardiovascular System, Section 2, Vol III, Handbook of Physiology* pp. 394-452, American Physiological Society, Bethesda.
- 18) Rush, J. W. E., Turk, J. R., & Laughlin, M. H. (2003). Exercise training regulates SOD-1 and oxidative stress in porcine aortic endothelium. *American Journal of Physiology-Heart and Circulatory Physiology*, 284(4), H1378–H1387.
- 19) Sodha, N. R., & Sellke, F. W. (2015). The effect of statins on perioperative inflammation in cardiac and thoracic surgery. *Journal of Thoracic and Cardiovascular Surgery*, 149(6), 1495–1501.
- 20) Sumner, A. D., Khalil, Y. K., & Reed, J. F. (2012). The Relationship of Peripheral Arterial Disease and Metabolic Syndrome Prevalence in Asymptomatic US Adults 40 Years and Older: Results From the National Health and Nutrition

Examination Survey (1999-2004). *The Journal of Clinical Hypertension*, 14(3), 144–148.

21) Tofovic SP, Jackson EK. Rat models of the metabolic syndrome. *Methods Mol Med*. 2003;86:29-46.

22) Zhou A, Egginton S, Hudlická O, Brown MD. Internal division of capillaries in rat skeletal muscle in response to chronic vasodilator treatment with alpha1-antagonist prazosin. *Cell Tissue Res*. 1998 Aug;293(2):293-303.

Condensed Curriculum Vitae

Education:

- Western University (UWO)
 - Ph.D. Candidate in Medical Biophysics (2016-Present)
- West Virginia University (WVU)
 - Ph.D. Student in Clinical Translational Science (2015-2016; Transferred)
 - M.S. in Clinical Exercise Physiology: School of Medicine (2013-2015)
 - B.S. in Exercise Physiology: School of Medicine (2008-2013)

Employment/Appointment History:

- Blue Ridge Community and Technical College: Faculty Instructor (2018-Present)
- UWO Medical Biophysics: PhD Candidate (2016-Present)
- WVU Clinical Translations Sciences: PhD Research Assistantship (2015-2016)
- WVU Exercise Physiology: MSc Research Assistantship (2014-2015)
- WVU Exercise Physiology: MSc Human Performance Lab Assistantship (2013-2014)

Scholarships and Academic Achievements:

- Ontario Graduate Scholarship (2018: \$15,000/year)
- Dr. Alfred Jay Medical Biophysics Award for Cardiovascular Research (2017: \$1000)
- Western Graduate Research Scholarship (2016-present; \$16,400/year stipend)
- Abstract featured in American Physiological Society press release (2016)
- Outstanding Master of Science Research Award (2015)
- Blaydes Award for Outstanding Clinical Care (2013; \$500)
- Davis-Michael Scholarship (2009; \$500/semester)
- Paul Ropp Memorial Scholarship (2008; \$1000)

Teaching and Leadership:

- UWO Teaching Assistant (2017)
- WVU Teaching Assistant (2014-2015)
- Lab Mentorships (2014-Present):
- WVU Human Performance Lab Undergraduate Intern Supervisor (2013-2014)

Publications:

First Author

- Published: **Kent A. Lemaster**, Daniel Goldman, Dwayne N. Jackson, Stephanie J. Frisbee, Paul D. Chantler, I. Mark Olfert, Matthew T. Lewis, Robert W. Wiseman and Jefferson C. Frisbee. Reversibility of Established Microvasculopathy in Skeletal Muscle of Obese Zucker Rats. Submitted to J Physiol.
- Published: **Lemaster, K.** Farid, Z., Brock, RW, Shrader, CD, Goldman, D, Jackson, DN, Frisbee JC. Altered post-capillary and collecting venular reactivity in skeletal muscle with metabolic syndrome. J Physiol. 2017 Aug 1;595(15):5159-5174. doi: 10.1113/JP274291. Epub 2017 Jul 5.
- Published: **Lemaster, K.** Jackson D, Welsh DG, Brooks SD, Chantler PD, Frisbee JC. Altered distribution of adrenergic constrictor responses contributes to skeletal muscle perfusion abnormalities in metabolic syndrome. Microcirculation. 2017 Feb;24(2). doi: 10.1111/micc.12349.
- Published: **Lemaster, K.**, Jackson, D., Goldman, D., & Frisbee, J. C. (2016). Insidious incrementalism: the silent failure of the microcirculation with increasing peripheral vascular disease risk. Microcirculation. 2017 Feb;24(2). doi: 10.1111/micc.12332. Review.

Co-author Publications: 8 (not listed; available upon request)

Conference Abstracts: 31 (not listed; available upon request)